Investigating post-translational modification and trafficking of Arabidopsis phosphate exporter PHOSPHATE1

Vetal Pallavi

Vetal Pallavi, 2023, Investigating post-translational modification and trafficking of Arabidopsis phosphate exporter PHOSPHATE1

Originally published at : Thesis, University of Lausanne

Posted at the University of Lausanne Open Archive http://serval.unil.ch
Document URN : urn:nbn:ch:serval-BIB_EB074FE5C96D3

UNIL | Université de Lausanne
Faculté de biologie
et de médecine

Département de Biologie Moléculaire Végétale

Investigating post-translational modification and trafficking of Arabidopsis phosphate exporter PHOSPHATE1

Thèse de doctorat ès sciences de la vie (PhD)

présentée à la

Faculté de biologie et de médecine
de l'Université de Lausanne

par

Pallavi Vetal

Master de l'Indian Institute of Science Education and Research,
Bhopal, Inde

Jury

Prof. Marc Robinson-Rechavi, Président
Prof. Yves Poirier, Directeur de these
Prof. Niko Geldner, Expert
Prof. Gregory Vert, Expert

Lausanne
(2023)

UNIL | Université de Lausanne
Faculté de biologie et de médecine

Département de Biologie Moléculaire Végétale

Investigating post-translational modification and trafficking of Arabidopsis phosphate exporter PHOSPHATE1

Thèse de doctorat ès sciences de la vie (PhD)

présentée à la

Faculté de biologie et de médecine
de l'Université de Lausanne

par

Pallavi Vetal

Master de l'Indian Institute of Science Education and Research,
Bhopal, Inde

Jury

Prof. Marc Robinson-Rechavi, Président
Prof. Yves Poirier, Directeur de these
Prof. Niko Geldner, Expert
Prof. Gregory Vert, Expert

Lausanne
(2023)

UNIL | Université de Lausanne

Faculté de biologie et de médecine

Ecole Doctorale

Doctorat ès sciences de la vie

Imprimatur

Vu le rapport présenté par le jury d'examen, composé de

Président·e	Monsieur	Prof.	Marc	**Robinson-Rechavi**
Directeur·trice de thèse	Monsieur	Prof.	Yves	**Poirier**
Expert·e·s	Monsieur	Prof.	Niko	**Geldner**
	Monsieur	Prof.	Grégory	**Vert**

le Conseil de Faculté autorise l'impression de la thèse de

Pallavi Vetal

Master - Bs-Ms in Biological sciences, Indian Institute of Science Education and Research, Bhopal, Inde

intitulée

Investigating post-translational modification and trafficking of Arabidopsis phosphate exporter PHOSPHATE1

Lausanne, le 30 juin 2023

pour le Doyen
de la Faculté de biologie et de médecine

Prof. Marc Robinson-Rechavi

Acknowledgement

I am extremely grateful to Prof. Yves Poirier for offering me the opportunity to undertake Ph.D. in his group and for believing in me. This endeavor would not have been possible without his endless support, patience, encouragement, and his trust throughout my research journey. I am truly grateful for his advice, guidance, and expertise that made this work possible.

I would also like to extend my gratitude to the members of my thesis committee, Prof. Marc Robinson-Rechavi, Prof. Niko Geldner, and Prof. Gregory Vert for taking their valuable time to read and evaluate my Ph.D. thesis and for their insights and constructive feedback during this research.

I am thankful to past and present members of Prof. Poirier's research group for their support and for creating a pleasant work atmosphere. Many thanks to Syndie Delessert, Jules Deforges, Thi Ngoc Nga Nguyen, and Yi-fang Hsieh for helping me settle in the lab and Switzerland. Many thanks to Anita Loha and Sami Bouziri for their valuable advice and discussions. Also, a big thank you to Rodrigo Reis for his critical advice and suggestions, as well as Joaquin Clua and Aime Jaskolowski for their constructive inputs throughout my PhD thesis.

I am thankful to all the members of DBMV for their scientific exchanges, technical assistance, and camaraderie. Their input and feedback have greatly contributed to the development of my research and have made my academic journey more enjoyable. I would also like to acknowledge the invaluable assistance of Debora Zoia and Laurence Cienciala for their administrative work, and Blaise Tissot for his maintenance of the plant growth room.

I would like to thank my Indian friends for making me feel at home and for cheering me up these past years. It would be very remiss of me not to mention the amazing people I played badminton with, who have brought joy to my weekends.

Words cannot express my gratitude to my friends and family back home for their constant encouragement, understanding, and emotional support. Their belief in me and my abilities have been a driving force behind my determination to complete this

thesis. Finally, I am so grateful to KK, who has always been there for me all these years with his unwavering support.

Table of contents

List of frequently used abbreviations

AP2	Adaptor protein complex 2
CCV	Clathrin coated vesicle
CHC	Clathrin heavy chain
CLC	Clathrin light chain
CME	Clathrin-mediated endocytosis
DNA	Deoxy-ribonucleic acid
EEs	Early endosomes
ER	Endoplasmic reticulum
EV	Empty vector
EXS	ERD1/XPR1/SYG1
GFP	Green fluorescent protein
LEs	Late endosomes
P	Phosphorus
PAE	Phosphate acquisition efficiency
PHO1	PHOSPHATE1
PHO2	PHOSPHATE2
Pi	Inorganic phosphate
PM	Plasma membrane
PPInsPs	Inositol pyrophosphates
PUE	Phosphate use efficiency
RNA	Ribonucleic acid
RT-qPCR	Real-Time quantitative reverse transcription polymerase chain reaction
SDM	Site directed mutagenesis
SPX	SYG1/PHO81/XPR1
TGN	trans-Golgi network
TM	Transmembrane domain
WT	Wild type

List of Figures

1. Introduction

2. Chapter 1

Supplemental figures

3. Chapter 2

4. Chapter 3

Abstract

Inorganic phosphate (Pi) homeostasis is essential for plant growth and development. Pi homeostasis in multicellular organisms is dependent on a battery of transporters involved in both Pi uptake into the cells as well as its export out of the cells for radial transport toward the vascular tissues. In roots, Pi export to the xylem apoplastic space is important for the transfer of Pi from roots to shoots. In *Arabidopsis thaliana*, PHOSPHATE1 (PHO1) is the Pi exporter known to export Pi from roots to shoots. PHO1 is primarily expressed in the root vascular tissue, where it loads Pi into the xylem apoplastic space. Arabidopsis *pho1* mutants are defective in the transfer of Pi from roots to shoots and exhibit Pi starvation-associated phenotypes like reduced shoot and root biomass and anthocynin accumulation. PHO1 protein consists of a hydrophilic SPX domain required for binding inositol pyrophosphate at the N-terminus, a hydrophobic EXS domain at the C-terminus, and four transmembrane domains (4TM) in between. Surprisingly, PHO1 is localized to the Golgi and trans-Golgi network (TGN) and the EXS domain has been shown to be essential for this localization. The presence of PHO1 at the Golgi/TGN instead of the PM raised the question of how it can mediate Pi export across the plasma membrane (PM) for the long-distance root-to-shoot transfer of Pi.

To address this question, we inhibited the most common endocytic pathway by overexpressing either *AUXILIN-LIKE 2* or *HUB1.* We found that PHO1 localizes to the PM and undergoes constitutive internalization via clathrin-mediated endocytosis (CME). We further show that the internalization of PHO1 from the PM is not dependent on the adaptor protein complex AP2, the Pi status of the plant, or the ubiquitin-conjugating E2 enzyme PHO2. The reduced root-to-shoot Pi export activity of PM-stabilized PHO1 further highlights the importance of CME for its optimal Pi export activity. Moreover, the EXS domain of PHO1 fused to GFP (SPX-4TM truncated PHO1) also stabilizes at the PM when inhibiting endocytosis, suggesting an important role of this domain in the trafficking of PHO1 to and/or from the PM. Overall, our findings provide evidence for the dynamic trafficking of PHO1 to and from the PM and demonstrate that this cycling is important to maintain plant Pi homeostasis.

Résumé

L'homéostasie du phosphate inorganique (Pi) est essentielle à la croissance et au développement des plantes. L'homéostasie du Pi dans les organismes multicellulaires dépend d'un ensemble de transporteurs impliqués à la fois dans l'absorption du Pi dans les cellules et dans son exportation hors des cellules pour le transport radial vers les tissus vasculaires. Dans les racines, l'exportation du Pi vers l'apoplasme du xylème est importante pour le transfert du Pi des racines vers les feuilles. Chez *Arabidopsis thaliana*, PHOSPHATE1 (PHO1) est le transporteur connu pour le transfert du Pi des racines vers les feuilles. PHO1 est principalement exprimé dans le tissu vasculaire de la racine, où il charge le Pi dans l'apoplasme du xylème. Les mutants *pho1* d'Arabidopsis sont défectueux dans le transfert du Pi des racines vers les feuilles et présentent des phénotypes associés à la carence en Pi, comme la réduction de la biomasse des feuilles et des racines et l'accumulation d'anthocyanines. La protéine PHO1 se compose d'un domaine SPX hydrophile à l'extrémité N-terminale, nécessaire à la liaison de l'inositol pyrophosphate, d'un domaine EXS hydrophobe à l'extrémité C-terminale et de quatre domaines trans-membranaires (4TM) entre les deux. De façon surprenante, PHO1 est localisé dans le Golgi et le réseau trans-golgien (TGN) et le domaine EXS de PHO1 s'est avéré essentiel pour cette localisation. La présence de PHO1 dans le Golgi/TGN au lieu de la membrane plasmique (MP) a soulevé la question de savoir comment PHO1 peut médier l'exportation de Pi à travers la MP pour un transfert du Pi à longue distance, des racines vers les feuilles.

Pour répondre à cette question, nous avons inhibé la voie d'endocytose la plus courante en sur-exprimant AUXILIN-LIKE 2 ou HUB1. Nous avons constaté que PHO1 se localise dans la MP et subit une internalisation constitutive par endocytose médiée par la clathrine (CME). Nous démontrons également que l'internalisation de PHO1 à partir de la MP ne dépend pas du complexe de protéines adaptatrices AP-2, du statut du Pi de la plante ou de l'enzyme PHO2 impliquée dans l'ubiquitination de PHO1. La réduction de l'activité d'exportation de Pi lorsque PHO1 est stabilisé à la MP souligne l'importance de la CME pour son activité optimale d'exportation de Pi. De plus, le domaine EXS de PHO1 fusionné à la GFP se stabilise également dans la MP lors de l'inhibition de l'endocytose, ce qui suggère un rôle important de ce domaine dans le trafic de PHO1 vers et/ou depuis la MP. Dans l'ensemble, nos résultats fournissent

des preuves du trafic dynamique de PHO1 vers et depuis la MP et démontrent que ce cycle est important pour maintenir l'homéostasie du Pi chez les plantes.

Résumé vulgarisé

Étude des modifications post-traductionnelles et du trafic du transporteur de phosphate PHO1 d'*Arabidopsis thaliana*

Le phosphate est un nutriment important pour la croissance et le développement des plantes. Les plantes possèdent des protéines spéciales appelées transporteurs qui les aident à prélever le phosphate du sol et à le déplacer à l'intérieur de la plante jusqu'à l'endroit où il est nécessaire. L'un de ces transporteurs chez *Arabidopsis thaliana* s'appelle PHOSPHATE1 (PHO1) et est responsable de l'exportation du phosphate des racines vers les feuilles.

Les scientifiques ont découvert que le transporteur PHO1 est situé dans un organite de la cellule appelé Golgi et réseau trans-golgien (TGN), au lieu de la membrane plasmique (MP), i.e. la membrane qui sépare l'intérieur de la cellule de l'environnement extérieur. Ce résultat est surprenant car PHO1 doit exporter le phosphate à travers la MP pour qu'il soit transporté des racines vers les feuilles. Pour comprendre comment cela se produit, nous avons mené des expériences pour étudier si PHO1 se localise à la MP d'une manière transitoire pour exporter le phosphate.

Nous avons découvert que PHO1 atteint la MP et en est constamment retiré par un processus appelé endocytose médié par la clathrine (CME). Le CME est un moyen pour les cellules d'absorber des substances provenant de l'extérieur et de recycler les protéines membranaires. Nous avons également découvert que la partie de PHO1 appelée domaine EXS, qui se trouve à l'extrémité carboxy-terminale de la protéine, est importante pour sa localisation dans le Golgi/TGN et joue un rôle dans le trafic de PHO1 vers et depuis la MP.

En outre, nous avons démontré que lorsque PHO1 est stabilisé au niveau de la MP en inhibant le processus de la CME, l'activité d'exportation du phosphate est réduite, ce qui indique que ce mouvement dynamique de PHO1 vers et depuis la MP est important pour sa fonction d'exportation du phosphate des racines vers les feuilles. Ces résultats fournissent des informations importantes sur la manière dont les plantes maintiennent l'homéostasie ou l'équilibre du phosphate et sur la façon dont PHO1, un important transporteur de phosphate, se déplace à travers la MP pour remplir sa fonction. D'autres recherches dans ce domaine pourraient nous aider à mieux comprendre comment les plantes utilisent efficacement les nutriments et pourraient

avoir des implications pour l'amélioration de l'absorption et de l'utilisation du phosphate dans l'agriculture.

Introduction

The importance of phosphorus in life

Phosphorus (P) is an essential macronutrient for plant growth and development. In plants, P is mostly utilized as a building block of important molecules such as DNA and RNA, which carry the genetic information, and adenosine triphosphate (ATP) that is synthesized through photosynthesis and used as an energy source in the cell. Moreover, P is one of the critical elements of phospholipids, the main component of cell membranes that separate the cytoplasm from the outside environment and create compartments in the cell. The necessity of P in energy-mediated metabolic processes and signal transduction also stresses the importance of P for plant survival.

The major source of P in soil that is available to plants for absorption is free inorganic phosphate (Pi) found mainly as $H_2PO_4^-$ or HPO_4^{-2}. However, the concentration of Pi found in soil in natural and agricultural ecosystems is very low due to its limited solubility and mobility (Holford, 1997). Adsorption of Pi to metal oxides (mostly Fe and Al), formation of complexes with calcium such as apatite ($Ca(PO_4)_3$), and loss of soluble Pi through erosion and leaching are the main reasons for the limited availability of Pi for plants (Figure 1; Fink et al., 2016; Tian et al., 2021). Pi concentration in the soil solution barely reaches 10 µM and may even drop to sub-micromolar levels at the root/soil interface, where Pi uptake by plants and root surface-colonizing microorganisms generates a zone of Pi depletion around the root surface that is maintained due to slow diffusion of Pi from regions distant to the root (Schachtman et al., 1998; Poirier and Bucher, 2002).

Excessive application of P fertilizer is widely practiced in agriculture to secure high crop yield due to its rapid growth-promoting effects coming from its readily available soluble Pi, as well as its slow-release Pi from organic sources in the soil. Unlike chemically reproduced nitrogen (N) fertilizer, P fertilizer is mainly sourced from finite and geographically restricted natural P rock reserves, which face rapid depletion due to intensive excavation to meet the agricultural demand over the past years. Depending on Pi fertilizers to increase or maintain crop yield will be challenging in the future due to the finite nonrenewable P resource and the environmental problems such as eutrophication caused by Pi overuse (Sattari et al., 2016). Eutrophication is caused by excess algal growth and results in ecological imbalances and water deoxygenation

which can lead to the death of aquatic animals. Hence, understanding how plants acquire, transport, and utilize Pi to respond to fluctuating Pi levels will be important to optimize Pi usage efficiency (PUE) to achieve a high yield with lower fertilizer input.

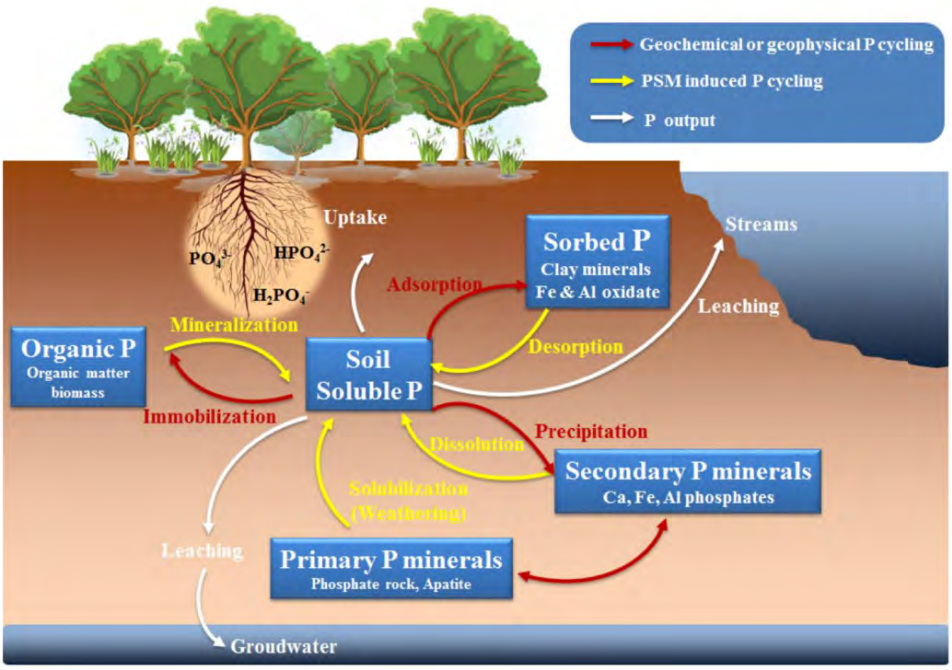

Figure 1. A schematic diagram of the phosphorus cycle in the environment. The limited availability of Pi in soil comes from the loss of soluble Pi through erosion and leaching, absorption by a functional group of iron or aluminium oxide, precipitation with cations, such as calcium to form apatites, and interaction with an organic compound. PSM- Phosphate solubilizing microorganisms. (From Tian et al., 2021).

Optimization of Pi acquisition by plants during Pi deficiency

Plants have evolved different mechanisms to cope with the limiting Pi conditions in the soil. Pi deficiency induces broad changes in gene and protein expression, leading to different developmental and metabolic adaptations to improve Pi acquisition efficiency (PAE), storage, and remobilization (Figure 2; Zhang et al., 2014; Gutiérrez-Alanís et al., 2018; Poirier et al., 2022). At the morphological level, to improve the capacity of the root system to explore and forage soil for poorly available Pi, its architecture is modified, with an increase in root/shoot ratio, increase in the length and density of root hairs (Bates and Lynch, 1996; Ma et al., 2001), as well as the proliferation of lateral roots (Williamson et al., 2001). Since organic P can represent up to 80% of the total P content in some soils, roots release phosphatases (del Pozo et al., 1999) and RNases, as well as organic acids (Plaxton and Tran, 2011) in soil that increase the organic and

inorganic Pi scavenging capacity of the root system (Figure 2A). For example, the gene *ACP5* coding for an acid phosphatase was shown to be upregulated under Pi deficiency (del Pozo et al., 1999). The *pup1* (phosphatase-under producer) mutant, lacking one acid phosphatase isoform, showed reduced activation of extracellular root acid phosphatases during Pi starvation (Trull and Deikman, 1998).

Moreover, pathways that replace phospholipids with non-phosphorous-containing lipids, such as sulfolipids and galactolipids, are activated to increase the internal Pi uptake and PUE under Pi deficient conditions while maintaining the plasma membrane (PM) integrity (Figure 2B; Essigmann et al., 1998; Cruz-Ramírez et al., 2006). Thus, Pi deprivation is associated with an upregulation of the *SQD1* and *SQD2* genes encoding chloroplast proteins involved in sulfolipid biosynthesis (Essigmann et al., 1998; Yu et al., 2002) and the insertional inactivation of the *SQD2* gene resulted in a complete absence of sulfolipids (Yu et al., 2002). Additionally, to some extent Pi deficiency can enhance the symbiotic root mycorrhization improving plant's access to Pi by increasing the volume of soil explored for nutrients. The increase in mycorrhizal colonization is partly driven by strigolactone released from the Pi-deficient roots (Akiyama et al., 2005; Besserer et al., 2006). The kinetics of Pi transport into the root and across the plant tissues is carried through changes in transporter abundance, localization, and affinity for Pi. Plants optimize Pi uptake and utilization using various Pi transporters, encoded by the *PHT* gene family, for redistribution of Pi between tissues (sink versus source) and within cell organelles (e.g., vacuole, plastid).

Pi acquisition and internal cycling in plants

The Pi concentrations in soil range from 0.5 to 10 µM, whereas the cellular Pi concentrations are greater than 10 mM. Thus, the acquisition of extracellular Pi is energy consuming process since Pi must travel against a steep extracellular–intracellular concentration gradient (Raghothama, 2000). Moreover, as cells are also negatively charged, with an electrical potential of approximately –120 mV, Pi must also move against a charge gradient. Plants and fungi use an H^+ ATPase pump to generate

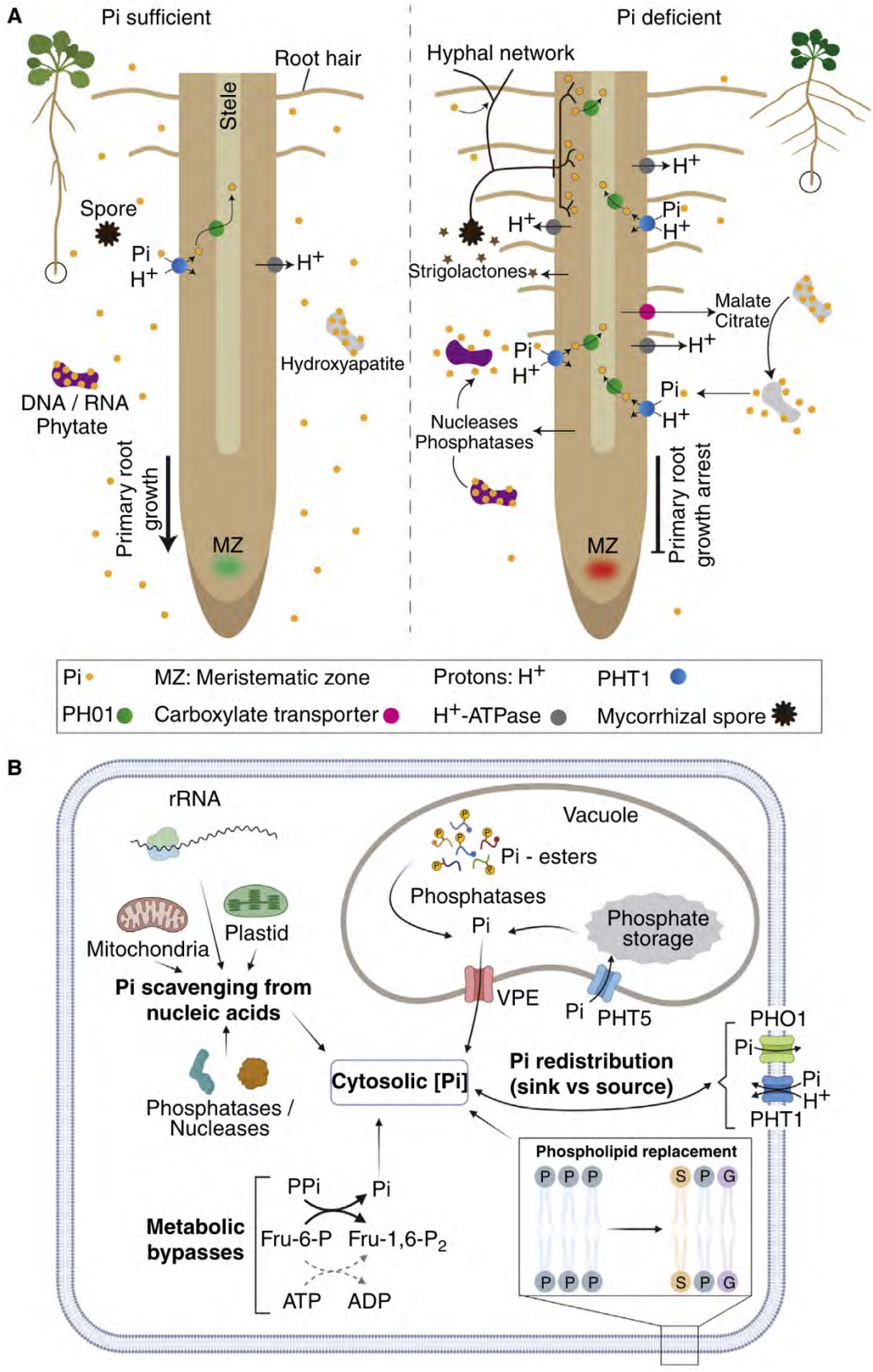

Figure 2. Developmental and metabolic adaptations of Pi-deficient plants. (A) An increase in PAE involves changes in several aspects of root biology such as shorter primary root, denser and longer secondary roots and root hairs in Pi-deficient plants

(right). The release of strigolactone enhances root mycorrhization (spore and hyphae are shown in black). Pi-deficient roots also release nucleases and phosphatases to mobilize Pi (yellow dots) from soil organic phosphate (Po), where the phosphate group is attached to a carbon atom via one of its oxygen atoms (e.g., DNA, RNA, and phytate) and from poorly soluble P forms (e.g., hydroxyapatite). The expression of the *PHT1* Pi-H^+ co-transporter (blue spheres) and vascular *PHO1* Pi exporter (green spheres) are enhanced under Pi deficiency. (B) An increase in PUE involves replacement of phospholipid by galacto- and sulfolipids, Pi scavenging from Po (including organellar DNA and ribosomal RNA) by nucleases and phosphatase, Pi redistribution between tissues and within cell organelles by various Pi transporters, as well as the activation of metabolic bypasses that do not use ATP. (From Poirier et al., 2022).

an electrochemical gradient across the PM by exporting H^+ to the apoplast at the expense of ATP (Figure 3). Thus, the proton gradient generated by H^+ ATPase is then used to drive Pi uptake via Pi/H^+ co-transporters in a secondary transport process with a stoichiometry of two to four protons per Pi (Ullrich-Eberius and van, 1984; Sakano, 1990; Schachtman et al., 1998).

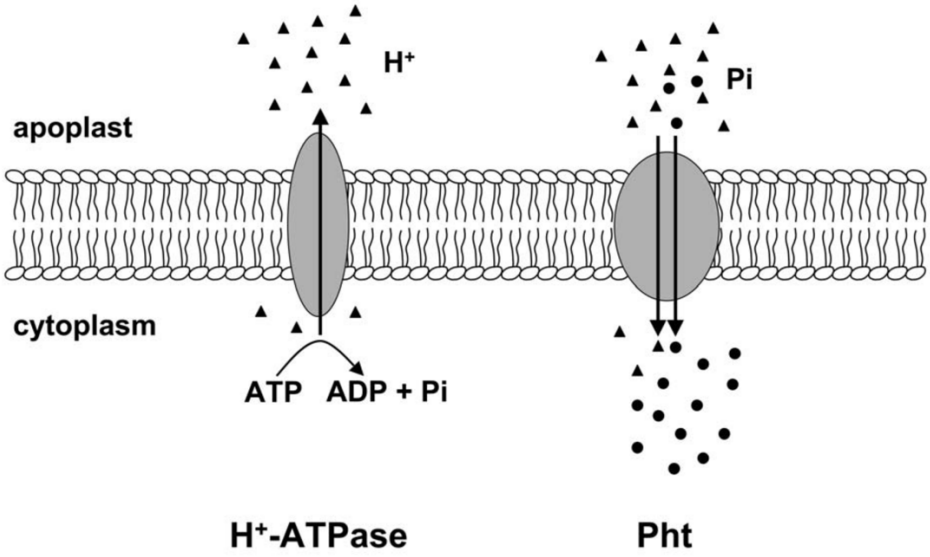

Figure 3. A model of phosphate transport of PHT coupled with H^+-ATPase across the membrane. The H^+ (triangles) gradient across the membrane is generated by the activity of the H^+-ATPase at the expense of ATP. H^+/Pi (circles) co-transport is mediated by the Pi transporter protein (PHT). (Adopted from Poirier and Bucher, 2002).

Plants rely on phosphate transporters (PHTs) to acquire Pi from soil and to transport it across the different tissues and organelles inside the plants. In Arabidopsis, *PHT*s are categorized into 5 subfamilies from *PHT1* to *PHT5*. Specifically, the most common PM-localized high-affinity H^+/Pi symporters that mediate Pi acquisition in the root

belong to the PHOSPHATE TRANSPORTER1 (PHT1) family (Muchhal et al., 1996; Raghothama, 2000; Chiou et al., 2001; Poirier and Bucher, 2002). Most PHT1 proteins are primarily located at the PM in root epidermal cells and root tip and moderately in the root cortical cells. Several *PHT1* genes are transcriptionally induced by Pi starvation (González et al., 2005; Morcuende et al., 2007; Bayle et al., 2011). Promoter-reporter fusions of *PHT1* members have demonstrated the Pi deficiency-induced expression of eight of the nine members in the roots of *A. thaliana* (Karthikeyan et al., 2002; Mudge et al., 2002). PHT1 transporters are characterized by 12 membrane-spanning domains that are very similar to the yeast high-affinity Pi transporter Pho84p (Muchhal et al., 1996). The Arabidopsis genome contains nine *PHT1* genes (*PHT1;1* to *PHT1;9*) encoding H^+/Pi cotransporters (Mudge et al., 2002), of which PM-localized PHT1;1 and PHT1;4 are extensively studied. Reverse genetics and the analysis of single and double Arabidopsis mutants for the *PHT1;1* and *PHT1;4* genes showed that these two transporters are the main contributors of Pi uptake in plants grown under Pi-sufficient and -deficient conditions (Misson et al., 2004; Shin et al., 2004; Ayadi et al., 2015). Similarly, the *PHT1;8* and *PHT1;9* genes have also been implicated in the uptake of Pi under Pi-deficient conditions (Remy et al., 2012).

Because of the crucial role of PHT1 transporters in Pi acquisition, it is not surprising that their expression, protein level, and localization is influenced by several transcriptional and post-translational mechanisms. For instance, the localization of at least a subset of PHT1 transporters to the PM is regulated by phosphorylation and interaction with the protein PHOSPHATE TRANSPORTER TRAFFIC FACILITATOR1 (PHF1, located in the ER; Bayle et al., 2011). The protein turnover of some PHT1 proteins is also controlled by ubiquitination *via* the E2 conjugase PHOSPHATE2 (PHO2) and the E3 ligase NITROGEN LIMITATION ADAPTATION1 (NLA1) protein (Liu et al., 2012a; Huang et al., 2013; Pan et al., 2019). These studies signify the important role of PHT1 members in the overall Pi uptake capacity of the root system from the rhizosphere. Considering the critical role of PHT1 members as the primary transporters responsible for the initial uptake of Pi, modulation of *PHT1* expression has been a focus of several studies aimed at improving PAE and PUE in transgenic plants (Gu et al., 2016).

Pi utilization and internal Pi cycling depend largely on the coordinated transport of Pi across different tissues and organelles. Within the plant cells, specific transporters located in different organelles uptake the Pi in exchange for other solutes or protons to maintain the Pi concentration. For example, PHT2;1 and all the members of the PHT4 family except PHT4;6 are localized to the chloroplast envelope or thylakoid (Versaw and Harrison, 2002; Guo et al., 2008). The *pht2;1* mutant showed an effect on Pi allocation between tissues under Pi-deficient condition including a higher Pi concentration in shoots but a lower Pi concentration in roots, and unchanged Pi translocation from old source leaves to young sink leaves compared to wildtype plants (Versaw and Harrison, 2002). The expression of all PHT4 members of Arabidopsis in yeast showed Pi transport activity which was enhanced by low pH and inhibited by a protonophore, suggesting the transport is dependent on the proton-motive force (Guo et al., 2008). PHT3 subfamily of proteins contain three members in Arabidopsis, PHT3;1 to PHT3;3, belonging to the mitochondrial carrier family and are involved in Pi transport across the inner mitochondrial membrane (Zhu et al., 2012). Vacuole is the main storage organ for Pi in the cell, representing up to 90% of the cell volume in leaves. Hence, the movement of Pi across its membrane (tonoplast) is crucial in buffering the effects of Pi deficiency on cellular metabolism. The transporters involved in the import and export of Pi across the tonoplast are only recently identified. The PHT5 subfamily, also named VACUOLAR PHOSPHATE TRANSPORTER (VPT) consisting of three members (PHT5;1 to PHT5;3) is involved in the uptake of Pi into the vacuole. These proteins harbour an SPX domain with binding affinity to inositol pyrophosphates (PPInsPs) for Pi signalling (Wild et al., 2016) as well as an MFS (MAJOR FACILITATOR23 SUPERFAMILY) domain (Marger and Saier, 1993), found in many transporters that carry small solutes. The *pht5;1* mutant showed hypersensitivity to both low-Pi and high-Pi conditions and the *pht5;1* isolated vacuole exhibited reduced Pi influx current compared to the wild-type based on the patch-clamp analysis (Liu et al., 2015). Another study showed that the *pht5;1* mutant accumulated less Pi and had a reduced vacuolar-to-cytoplasmic Pi ratio (Liu et al., 2016). Similarly, recently, VACUOLAR PHOSPHATE EFFLUX (VPE) transporters are shown to facilitate vacuolar Pi efflux in rice and Arabidopsis (Xu et al., 2019). The Arabidopsis *vpe2-1* mutant showed 1.2-fold higher vacuolar Pi content compared to WT (Xu et al., 2019).

Long-distance Pi transport

Generally, water and nutrients entering the root move radially through the epidermis, cortex, and endodermis and finally the central vascular cylinder. The endodermis is the innermost cortical cell layer that features Casparian strips (CS) that form a barrier to prevent the free diffusion of solutes from the soil to the stele. Root nutrient uptake and transport can occur through three different routes that can be interconnected in various ways: the apoplastic route, the symplastic route, and a coupled trans-cellular route (involving polarized influx and efflux carriers) (Figure 4; Barberon and Geldner, 2014). Through the apoplastic pathway, water and nutrients diffuse towards the stele through free spaces in the cell walls of the epidermis and cortex until they reach the CS which blocks the passive flow of solutes (Figure 4). The symplastic route to the vasculature implicates cell-to-cell movement via plasmodesmata (Figure 4). Plasmodesmata provides cytoplasmic continuity between each cell and its immediate neighbour enabling transport and communication between them (Burch-Smith and Zambryski, 2012). Finally, in the coupled trans-cellular pathway, transporters are polarly distributed, not only in the endodermis but also in cortical and epidermal cells. Thus, nutrients are transported from one cell to the other, passing from symplast to apoplast and again to symplast, in a mechanism similar to polar auxin transport (Löfke et al., 2013). Such a mechanism provides directional long-distance transport towards the stele and offers the advantage of a control mechanism over all cell layers, regardless of the mass flow of nutrients (Barberon and Geldner, 2014).

Plants acquire Pi by active uptake into the epidermal cells of the root through H^+/Pi symporters of the PHT1 family (Poirier and Bucher, 2002; Nussaume et al, 2011). Once in the root epidermal cells, Pi must move across different cell layers either apoplastically or symplastically until it reaches xylem parenchyma cells to eventually be loaded into the apoplastic space of the xylem. This exported Pi is then transported to the shoot by the transpiration stream and root pressure. Since the CS forms a barrier to the apoplastic flow of water and ions toward the root vascular cylinder, the movement of ions across the endodermal cells becomes a crucial step in the efflux of ions to the root xylem. In *A. thaliana*, very few proteins have been identified that export ions into the root xylem. For instance, STELAR K^+ OUTWARD RECTIFIER (SKOR), a member of the Shaker family expressed in the root stelar cells, encodes an outwardly rectifying K^+ channel and mediates the loading of potassium (K^+) in the xylem vessel

(Gaymard et al., 1998). Similarly, a boric acid exporter BOR1 also expressed in the root stelar cells mediates boron (B^-) efflux into the xylem vessel (Takano et al., 2002; Takano et al., 2005). NITRATE TRANSPORTER 1.5 (NRT1.5), NRT1/PTR FAMILY 2.4 (NPF2.4), and AMMONIUM TRANSPORTER 2;4 (AMT2;4) have also been implicated in the export and long-distance root-to-shoot transfer of nitrate, chloride, and ammonium ions respectively (Lin et al., 2008; Li et al., 2016; Giehl et al., 2017). Interestingly, all these genes are expressed primarily in root pericycle and xylem parenchyma cells. Like other nutrients, acquired Pi must be loaded into the xylem vessel for long-distance transfer to the shoot. This step is mediated by the Pi exporter *PHOSPHATE1 (PHO1),* also expressed in the xylem parenchyma cells (Poirier et al., 1991; Hamburger, 2002).

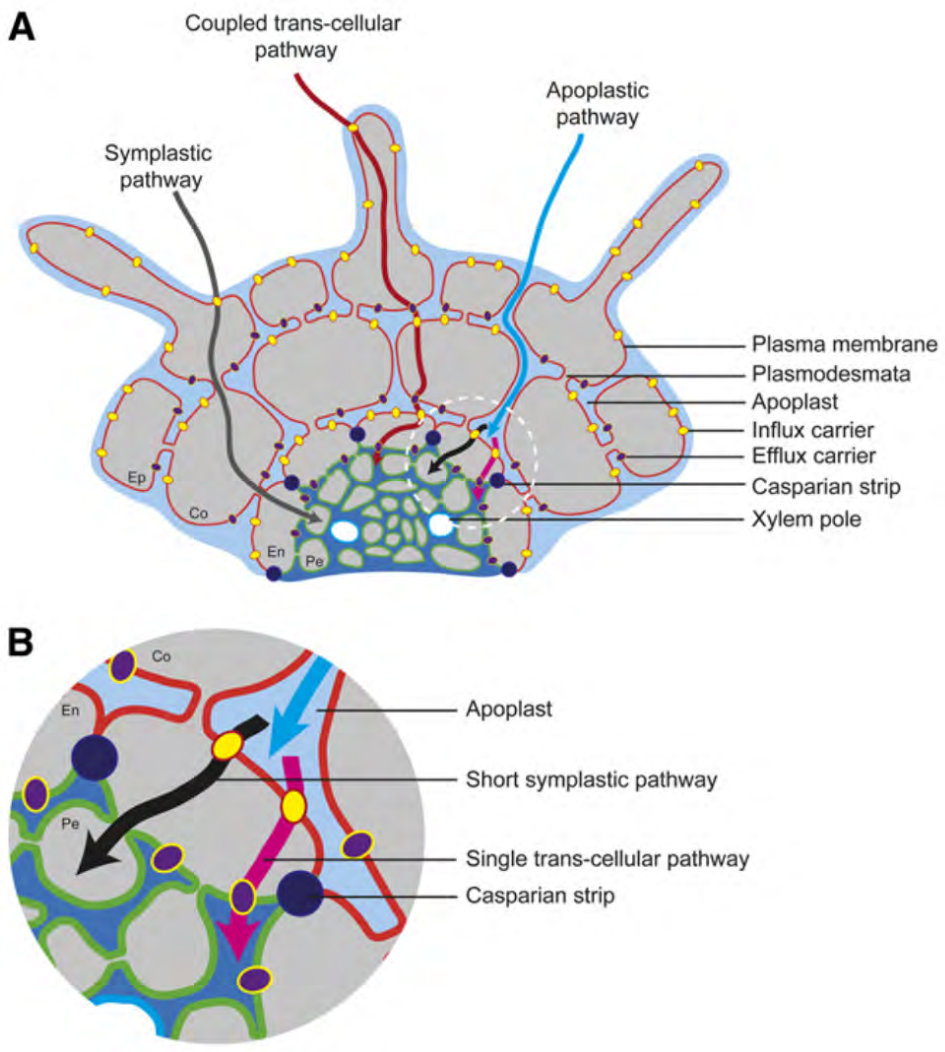

Figure 4. Three different pathways of nutrient transport in roots. (A) Schematic view of the three different pathways involved in the transport of nutrients from the soil

to the endodermis. The symplastic pathway (in gray), the coupled transcellular pathway (in red) and the apoplastic pathway (in blue). (B) Magnification of the circled area in A, focusing on the transport of nutrients from the apoplast to the endodermis. Transport routes through the endodermis involve a short symplastic pathway (in black) and a single trans-cellular pathway (in pink), restricted at the level of the endodermis. (Adapted from Barberon and Geldner, 2014).

PHO1 structure, activity, and expression

PHO1 and its closely related homolog PHO1; H1 are the only exporters known so far that mediate Pi export from root to shoot in plants. The *PHO1* gene was first identified from a mutant that could acquire Pi into the roots normally but could not load the acquired Pi into the xylem vessel for shoot transfer (Poirier et al., 1991). Later, the gene was identified by positional cloning and shown to encode a protein distinct from the known PHT Pi transporters (Hamburger, 2002). The Arabidopsis *pho1* mutant exhibits a defect in the transport of Pi from root to shoot (Figure 5A) and shows hallmarks associated with Pi deficiency that includes reduced shoot and primary root growth (Figure 5B), increased anthocyanin accumulation, and upregulation of genes associated with Pi deficiency (Poirier et al., 1991; Misson et al., 2005; Müller et al., 2007; Rouached et al., 2011). Experiments with *PHO1* promoter: GUS reporter assays have demonstrated strong activity of the promoter in the root stelar cells, including pericycle and some endodermal passage cells (Figure 6A-F; Hamburger, 2002). This pattern of *PHO1* expression is consistent with its role in Pi loading into the xylem cells. Although *PHO1* is primarily expressed in the roots, some expression is also detectable in the leaves, particularly in guard cells (Figure 6G; Zimmerli et al., 2012).

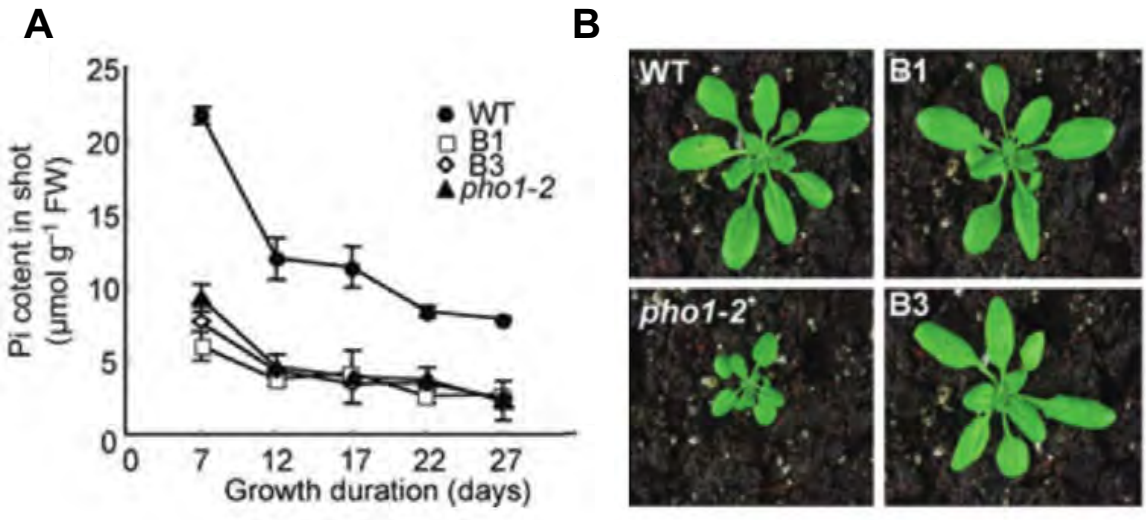

Figure 5. The function and phenotype of *pho1* mutant and transgenic plants underexpressing *PHO1*. (A) Inorganic phosphate (Pi) contents in aerial parts of wild-type (WT) plants, transgenic lines B1 and B3 underexpressing *PHO1*, as well as the null mutant *pho1-2* grown for 17-days in soil. (B) Phenotype of above-mentioned genotypes. (Adapted from Rouached et al., 2011).

The *A. thaliana* genome contains 10 *PHO1* homologs (*PHO1; H1 to PHO1; H10*), of which only *PHO1; H1* has been directly associated with the Pi export activity in root vasculature. *PHO1; H1* is strongly upregulated under Pi starvation (Stefanovic et al., 2007) and was shown to complement the *pho1* mutant phenotype when expressed under the *PHO1* promoter, indicating a role in Pi export. The implication of PHO1; H1 in Pi export into the root xylem was also shown by the analysis of *pho1 pho1; h1* double mutant. These mutants exhibit highly reduced shoot growth and reduced Pi transfer to the shoot (Figure 7A-B; Stefanovic et al., 2007). Finally, *PHO1; H1* is also expressed in the same tissues as *PHO1*, i.e: shoot and root vasculature (Figure 7C). The rest of the homologs are expressed in a range of different tissues and organs and might have distinct functions than long-distance Pi transport (Wang et al., 2004).

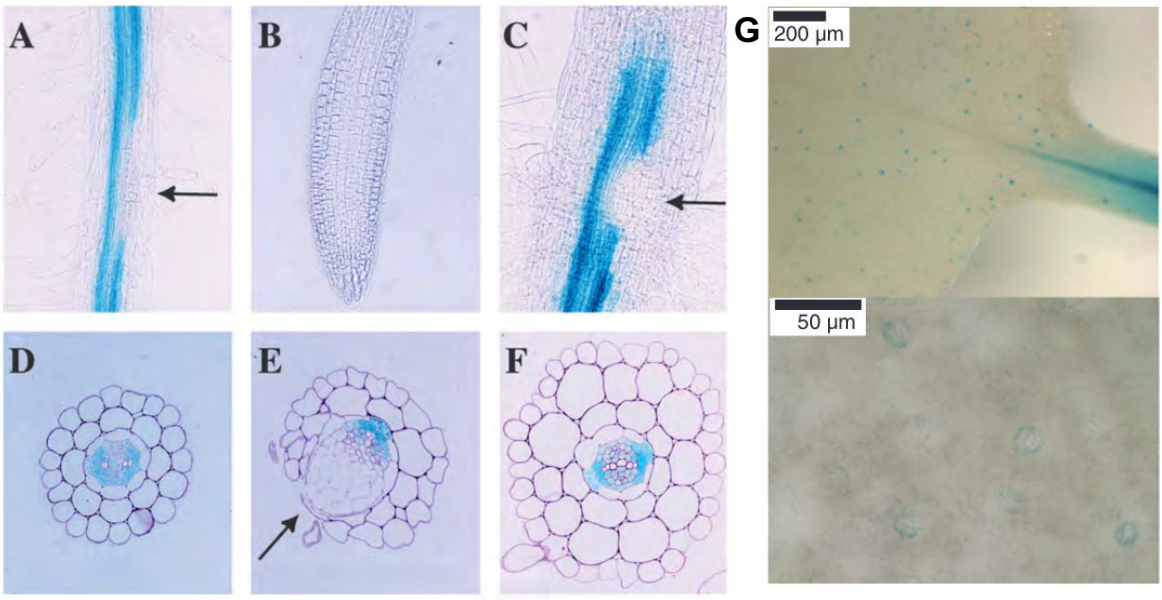

Figure 6. Expression pattern of the *PHO1* promoter. The GUS reporter gene was expressed under the control of a 2.1-kb (A, B, D, E, and G) or a 1.6-kb (C and F) fragment of the *PHO1* promoter region. Longitudinal and transverse views of the mature zone of roots (A, D, and E), root tip and elongation zone (B), hypocotyl-root junction (C), and hypocotyl (F) are shown. Arrows indicate regions where lateral roots are emerging. (A-F is adapted from Hamburger et al., 2002 and G from Zimmerli et al., 2012).

Pi export activity mediated by PHO1 was demonstrated in plants that overexpressed the protein in tissues other than the root vascular cylinder. Leaves from transgenic plants overexpressing PHO1 and immersed in an aqueous medium showed a rapid efflux of Pi into the apoplast, with a concomitant decrease in vacuolar Pi concentration (Stefanovic et al., 2011). Similarly, the expression of *PHO1* under an estradiol-inducible promoter showed that *PHO1* expression in leaf mesophyll cells led to a specific export of Pi to the apoplast (Arpat et al., 2012). This Pi export was only marginally affected by the addition of a proton-ionophore, indicating that Pi export was not coupled to the proton gradient.

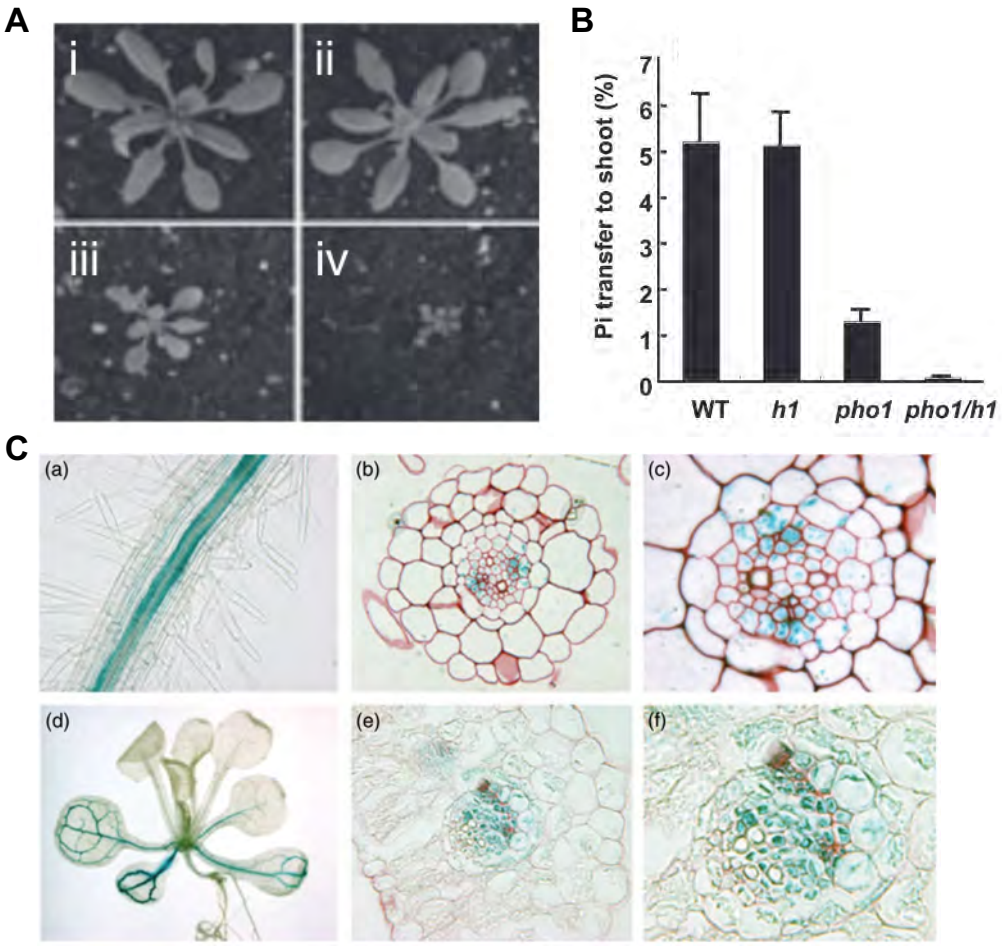

Figure 7. Expression pattern of the *PHO1; H1* promoter and characterization of the *pho1; h1-1* mutant and *pho1-4/pho1; h1-1* double mutant. (A) Phenotype of Col-0 (i), *pho1; h1-1* (ii), *pho1-4* (iii) and *pho1-4/pho1; h1-1* double mutant (iv). (B) The percent of ^{33}Pi transferred by root to the shoot in genotypes mentioned in (A). (C) The GUS reporter was expressed under the control of a 1-kb fragment of the *PHO1; H1* promoter. Longitudinal and transverse views of the root (a–c) and shoot (d–f) of inorganic phosphate (Pi)-replete plants are shown. Images (c) and (f) are magnifications of the sections shown in (b) and (e), respectively. (Adapted from Stefanovic et al., 2007).

The export of Pi to the xylem mediated by PHO1 (Poirier et al., 1991; Hamburger, 2002) or to the plant tissues other than root vasculature when *PHO1* is overexpressed (Stefanovic et al., 2011) has established PHO1 as a Pi exporter. Further evidence for the activity of PHO1 as a Pi exporter was obtained by the heterologous expression of rice (*Oryza sativa*) *PHO1* ortholog in both mammalian cell cultures and *Xenopus laevis* oocytes (Ma et al., 2021). PHO1-GFP chimeric protein under *PHO1* native promoter complemented *pho1-2* mutant and mediated Pi export (Arpat et al., 2012; Liu et al., 2012a). As predicted, GFP fluorescence was observed in pericycle cells surrounding xylem poles (Figure 8A), but surprisingly, the subcellular localization did not reveal GFP fluorescence at the PM. Rather, contrary to the expectation, PHO1-GFP was observed in punctate structures (Figure 8A), that localized to the Golgi, trans-Golgi network (TGN), and uncharacterized vesicles when expressed in onion epidermal cells or the mesophyll cells of *Nicotiana benthamiana* (Figure 8B; Arpat et al., 2012). The Pi export activity was observed in these PHO1-GFP transformed cells, which further confirmed the importance of not only PHO1 as an exporter but also of the Golgi and associated endosomes to mediate the Pi release outside of the cell.

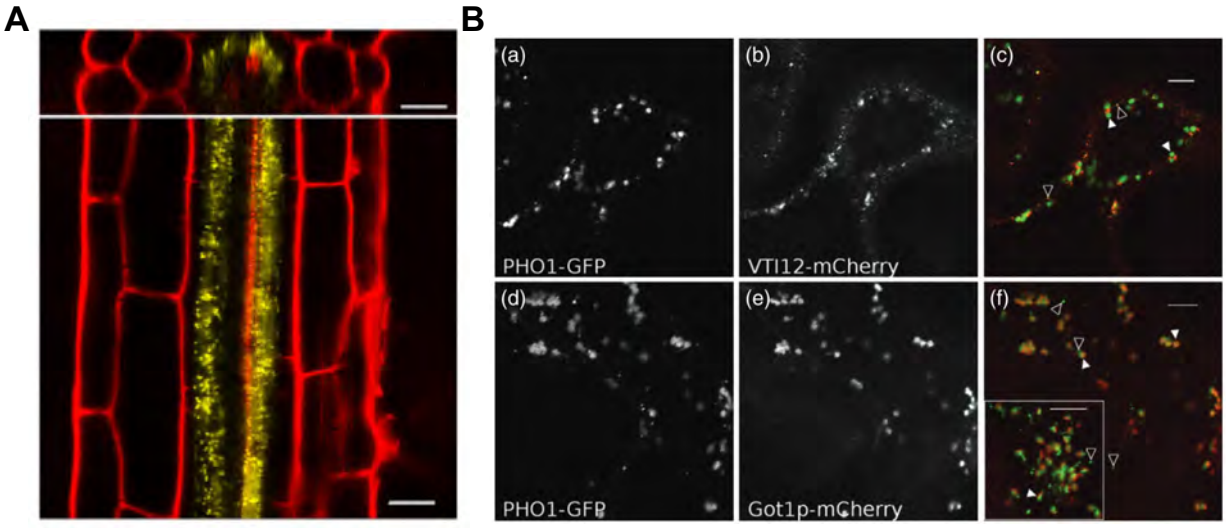

Figure 8. Subcellular localization of PHO1. (A) Cellular and subcellular localization of PHO1-YFP (*PHO1pro:gPHO1YFP*) in the Arabidopsis roots of a 5-d-old wild-type transgenic seedling. Scale bar, 20 µm. (Adapted from Liu et al., 2012). (B) Co-expression of PHO1-GFP construct with different subcellular markers in *N. benthamiana* epidermis. *N. benthamiana* leaves were co-infiltrated with an *Agrobacterium tumefaciens* strain harboring PHO1-GFP encoding plasmid together with other containing TGN marker VTI12-mCherry (a–c), and Golgi marker Got1p-mCherry (d–f). Green and red fluorescence are displayed at the left and in the middle of the row, respectively. Green-colored GFP and red-colored m-Cherry channels are

merged at the right. Open and closed arrowheads indicate examples of small and large vesicles, respectively. The inset within (f) depicts an overlay image from another cell. Scale bar, 10 μm. (Modified from Arpat et al., 2012).

PHO1 protein is composed of an N-terminal cytosolic tripartite SPX domain, and four transmembrane α-helices spanning domains (4TM), followed by another hydrophobic C-terminal EXS domain that spans the membrane twice (Figure 9; Wege et al., 2016). The SPX domain of PHO1 is involved in the sensing and binding of PPInsPs, the concentrations of which change in response to Pi availability (Wild et al., 2016; Jung et al., 2018). SPX binds PPInsP at high affinity via a series of conserved lysine residues (Wild et al., 2016). In plants, PPInsPs trigger the association of SPX proteins with PHR transcription factors to regulate Pi starvation responses (Wild et al., 2016).

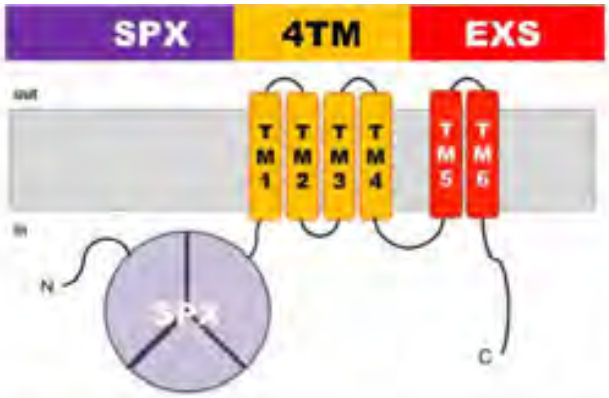

Figure 9. A schematic representation of PHO1 structure. PHO1 contains an SPX domain, four transmembrane domains (4TM), and an EXS domain. (Adapted from Wege et al., 2016).

The topology and domain-specific functions of PHO1 have been studied in detail (Wege et al., 2016). Functional analyses of different truncated forms of PHO1 showed that the EXS domain is essential for the proper localization of PHO1 to Golgi/TGN (Figure 10A), a feature that was essential for *pho1* mutant shoot phenotype complementation. Furthermore, a construct fusing only the EXS domain of PHO1 to GFP was also localized to the Golgi and TGN and co-localized with PHO1 (Figure 10A; Wege et al., 2016). The truncated form of PHO1 without the SPX domain (4TM-EXS) was able to export Pi when transiently expressed in *N. benthamiana* leaves, but it could not complement the *pho1* mutant phenotype in Arabidopsis (Figure 10 and Figure 11; Wege et al., 2016). This highlighted the role of the EXS domain in PHO1's localization to the Golgi/TGN, which was also important for its Pi export activity.

The low shoot Pi in the *pho1* mutant was initially thought to be the main cause of its reduced growth. However, transgenic plants that under-expressed *PHO1* showed

normal growth despite having low shoot Pi content similar to that of *pho1* mutants (Rouached et al., 2011). Interestingly, a similar phenomenon was found in the Arabidopsis *pho1-4* mutant transformed with only the EXS domain of PHO1 under the control of *PHO1* promoter, which lacked Pi transport activity, but was enough to rescue the shoot growth phenotype of *pho1* mutants, despite low shoot Pi levels (Figure 11; Wege et al., 2016). Both these studies showed that low Pi content can be dissociated from its main effect on growth and PHO1 could be involved in modulating the Pi-deficiency signaling cascade and its effect on growth.

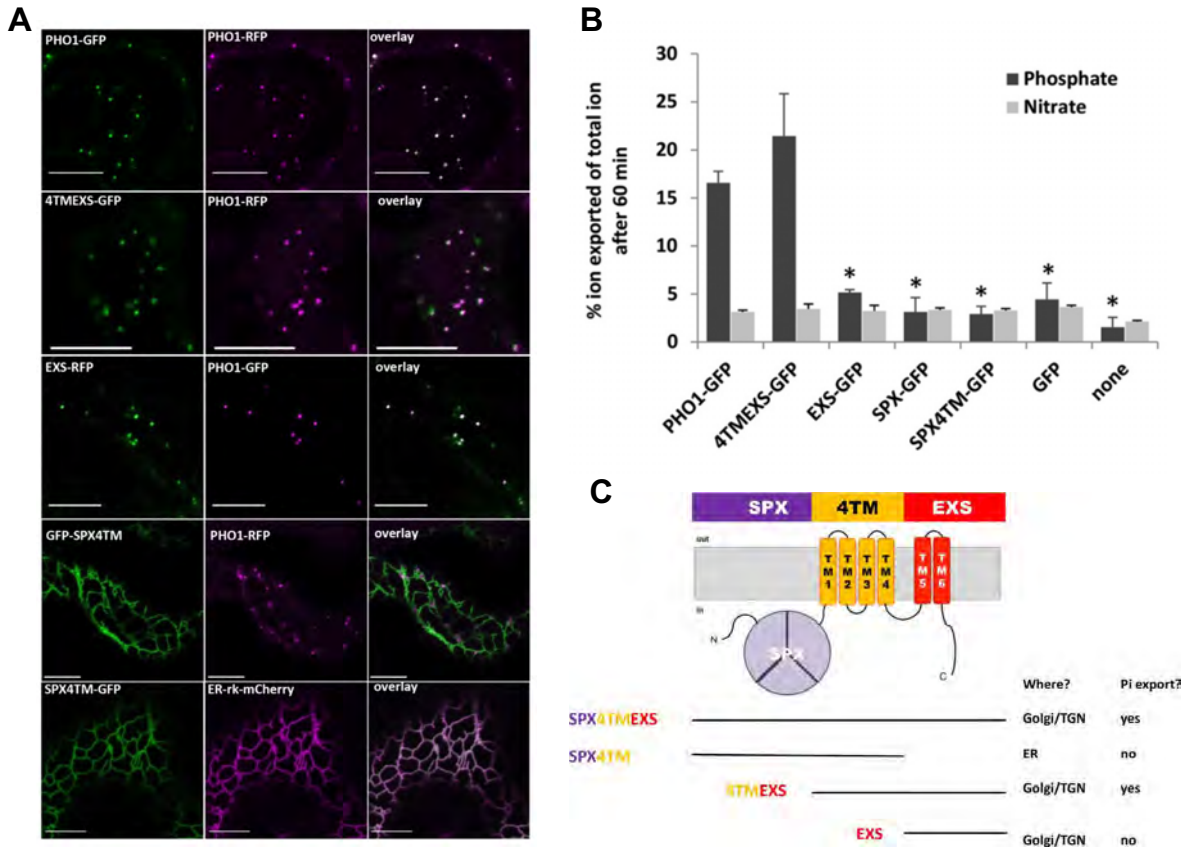

Figure 10. Subcellular localization and Pi efflux of various PHO1 truncations in *N. benthamiana*. (A) Subcellular localization of full-length and truncated PHO1-GFP constructs transiently expressed with full length PHO1-RFP in *N. benthamiana* epidermal cells. Scale bars, 10 mm. (B) Measurement of Pi and nitrate export mediated by PHO1 truncations, GFP and non-infiltrated control (none). (C) Schematic representation summarizing localization and Pi export function of different PHO1 truncations in transient assays. (Modified from Wege et al., 2016).

PHO1 expression is partially controlled by the transcription factors, WRKY6 and WRKY42, which act as repressors via binding to the W-box motifs in its promoter. Under Pi starvation conditions, the binding of WRKY6/42 to the *PHO1* promoter is

released, and thus the transcription of *PHO1* is activated (Chen et al., 2009; Su et al., 2015). *PHO1* expression is only weakly regulated at the transcriptional level by Pi deficiency, while its protein stability is controlled by ubiquitination via PHO2 (Liu et al., 2012). *PHO2* encodes a ubiquitin-conjugating E2 enzyme that ubiquitinates PHO1, leading to its degradation. The *pho2* mutant was originally identified in the genetic screen for mutants with abnormal distribution of Pi levels in leaves (Delhaize and Randall, 1995). *pho2* mutants show enhanced expression of both PHT1 and PHO1 proteins and exhibit a constitutively active phosphate-deficiency starvation response, leading to reduced growth associated with excessive shoot Pi content (Aung et al., 2006; Bari et al., 2006). When the supply of Pi is not limited, the ubiquitination of PHO1 and PHT1s in the post-ER compartments is mediated by PHO2 (Liu et al., 2012; Huang et al., 2013). PHO1 and PHO2 proteins are localized in the same subcellular compartment (Golgi/endosomes) and the proteins are shown to interact physically via the SPX domain of PHO1 (Liu et al., 2012). Thus, this seems to be, yet another mechanism of the regulation of Pi uptake and Pi translocation adopted by plants to maintain Pi homeostasis for their survival.

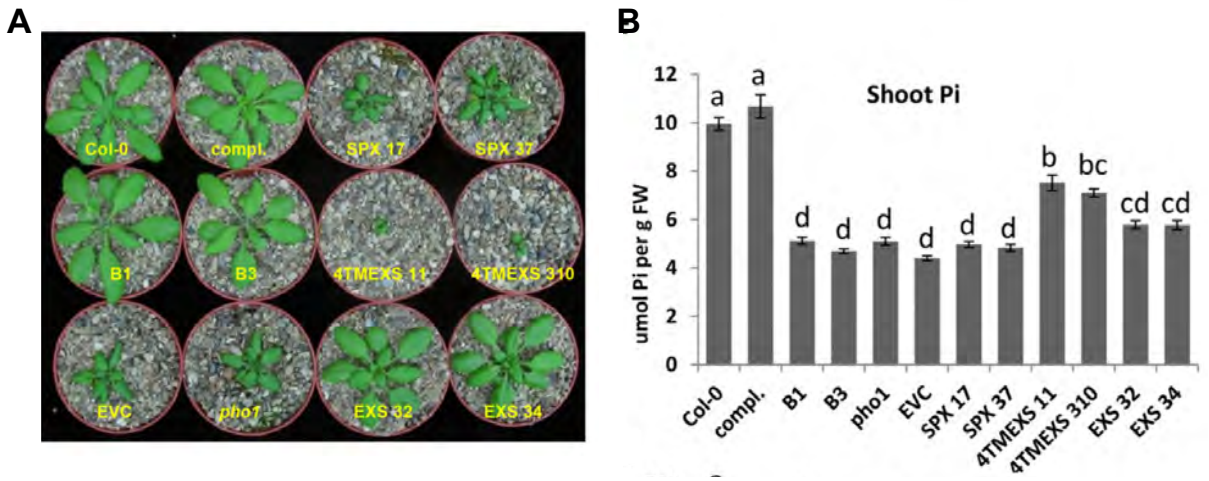

Figure 11. Phenotype and Pi export of various PHO1 truncations in *A thaliana*. (A) Phenotypes of two independent lines of each PHO1 truncation construct transformed in *pho1* mutant compared with Col-0, *pho1*, empty vector control (EVC) in the *pho1* background, *pho1* complemented with the full-length PHO1-GFP line (compl.), and the two *PHO1* knockdown lines B1 and B3 described previously (Rouached et al., 2011). (B) Shoot Pi content of the plants grown for 25 d in pots. (Adapted from Wege et al., 2016).

Nutrient homeostasis and vesicular trafficking in plants

Nutrient homeostasis is essential for plant growth and reproduction. It depends on the controlled flux of ions between cells and organs as well as across several subcellular compartments. Both uptake of ions into cells and their export out of cells are crucial for ion homeostasis, because the overaccumulation of essential nutrients, such as iron, manganese, and zinc, leads to toxicity, cell damage, and eventually death. In roots, the uptake and radial transport of nutrients toward the vascular tissues is achieved by an array of specialized membrane transporters. Therefore, regulating the abundance and the localization of these transporters at the PM appears to control their activity to maintain ion homeostasis in plants (Ivanov and Vert, 2021).

Vesicular trafficking is a fundamental cellular process, which in part controls the regulation of membrane transporters for inorganic nutrient transport (Figure 12; Ivanov and Vert, 2021; Gao and Chao, 2022). This control first involves the secretion of newly synthesized proteins to the plasma membrane from ER along the secretory pathway through the Golgi and TGN. Once secreted at the PM, membrane transport proteins are internalized through endocytosis and transported to membrane-bound organelles, early endosomes. Plants do not have early endosomes (EEs) similar to animals or yeast but this function is carried by TGN (Dettmer et al., 2006), where PM-proteins are either recycled to the PM or targeted to the vacuole for degradation (Robinson and Neuhaus, 2016). These mechanisms are often controlled by stresses, nutrient availability, and exo- or endogenous cues, allowing plants to adapt to the environment.

Great progress has been made in deciphering the molecular mechanisms underlying the regulation of vesicular trafficking in nutrient homeostasis, however, for the scope of this study, I will be only focusing on the endocytosis, a crucial and perhaps the most important step in the regulation of nutrient transporters.

Clathrin-mediated endocytosis

Endocytosis is a process by which cells internalize PM, membrane proteins, and extracellular material via endocytic vesicles (Figure 12). In plant cells, endocytosis occurs at the PM or the cell plate membrane (an immature complex of PM) during cell division (Otegui et al., 2001). The endocytic vesicles generated from the PM fuse with endosomes, membrane-bound organelles. Early endosomes are the first

compartment to receive the endocytic cargos from the PM, while late endosomes (LEs), including late multivesicular endosomes, are subject to fusion with vacuoles or lysosomes for degradation. Amongst the different types of endocytic mechanisms that exist in eukaryotes, endocytosis involving clathrin coat protein, commonly known as clathrin-mediated endocytosis (CME), is the most common endocytic pathway in plants (Dhonukshe et al., 2007) and controls the abundance of many transporters at

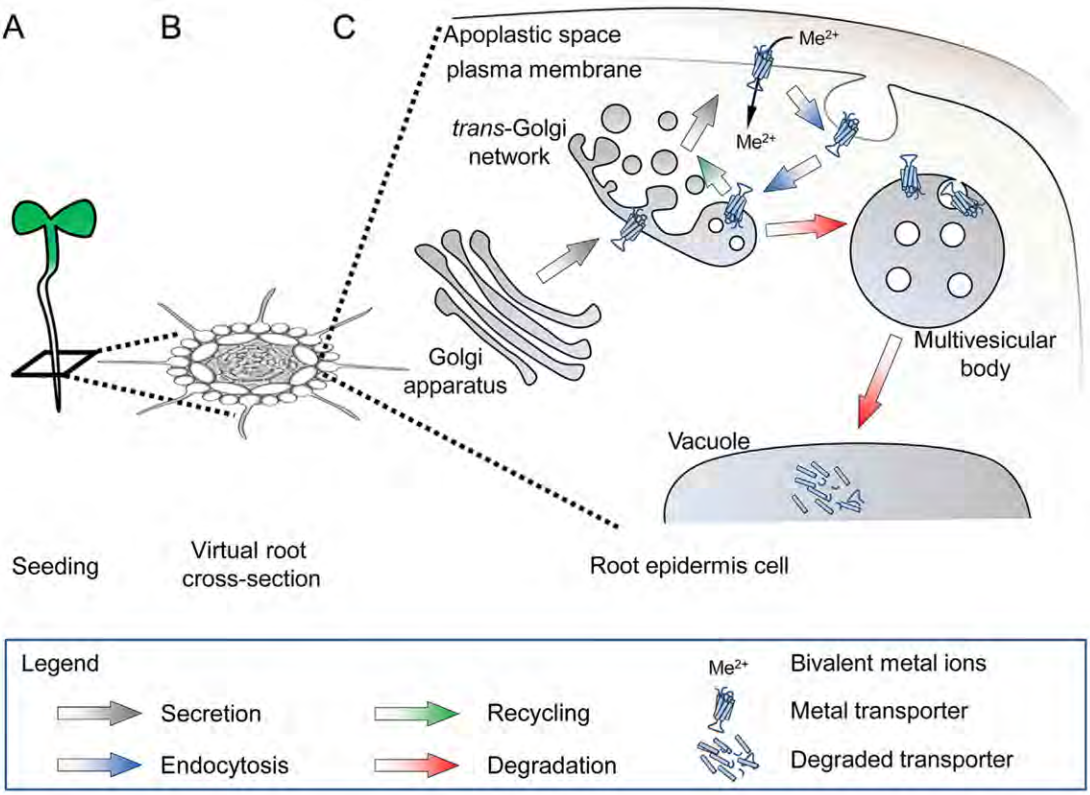

Figure 12. Schematic representation of the trafficking pathways for plasma membrane transporters in root epidermal cells (A) Root functions in the acquisition of nutrients, including metal ions from the soil. (B) The cross-section of the root of the model plant Arabidopsis consists of several layers of cells. The outermost layer, epidermis, is the main place where acquisition of nutrients occurs. (C) In epidermal cells, the availability of metal ion transporters at the plasma membrane is a result of complex trafficking events along the endomembrane system. (Taken from Ivanov and Vert, 2021).

the PM including iron transporter IRT1, the ammonium transporter AMT1;3, the aquaporin PIP2;1 and the manganese transporter NRAMP1, among the others (Barberon et al., 2011; Li et al., 2011; Wang et al., 2013; Barberon et al., 2014; Castaings et al., 2021).

Clathrin assembles into triskelia composed of three CLATHRIN HEAVY CHAINs (CHCs) and three CLATHRIN LIGHT CHAINs (CLCs). The assembly of triskelia forms the clathrin coat. CME involves five steps: nucleation, cargo selection, clathrin coat assembly, membrane fission, and uncoating (Figure 13; Paez Valencia et al., 2016; Dahhan and Bednarek, 2022). Clathrin-coated vesicle (CCV) formation is initiated through the recognition of PM-localized endocytic cargo and phosphatidylinositol phospholipids by adaptors, AP2 and TPLATE complex, that subsequently recruit clathrin triskelia to the PM. The polymerization of clathrin triskelia at the PM and the potential action of early adaptor proteins (EAPs) like TPLATE, drive membrane deformation to generate a clathrin-coated pit, which matures into a clathrin-coated vesicle. Clathrin EAPs confer specificity to the cargo sequestered into the clathrin-coated vesicle. This part of membrane is deforming toward the cytoplasm and undergoes scission from the PM to form a CCV through the action of dynamin-related proteins 1 and 2, which then deliver its cargo into the endocytic system along actin microfilaments. Clathrin mediates vesicle budding not only from the PM during endocytosis but also from the TGN and some other endosomes. Clathrin-coated pits were first visualized in mosquito oocytes internalizing yolk proteins in 1964 (Roth and Porter, 1964) through transmission electron microscopy. However, the role of CME in the internalization of the plant plasma membrane proteins has been shown only a decade ago (Dhonukshe et al., 2007).

CME requires an array of proteins including clathrin, adaptor, and accessory proteins for the selection and recruitment of the cargo (McMahon and Boucrot, 2011; Rodriguez-Furlan et al., 2019; Aniento et al., 2022). In *A. thaliana*, five ADAPTOR PROTEIN (AP) complexes have been identified (AP1 to AP5), but only the classical hetero-tetrameric ADAPTOR PROTEIN2 (AP2) complex has been implicated to function as an adaptor that recognizes select PM cargos destined for CME (Bashline et al., 2013; Di Rubbo et al., 2013; Kim et al., 2013; Yamaoka et al., 2013; Yoshinari et al., 2019). AP2 binds to clathrin, cargo proteins, and phosphatidylinositol 4,5-bisphosphate [PtdIns(4,5)P2] at the plasma membrane (Höning et al., 2005). AP2 complex consists of two large subunits (AP2A and AP2B), one medium subunit (AP2M), and one small subunit (AP2S) (Collins et al., 2002). The mutants of AP2 subunits, *AP2S* and *AP2M,* have been shown to reduce the endocytosis of auxin efflux transporters PIN1 and PIN2 respectively (Fan et al., 2013; Kim et al., 2013). Similarly,

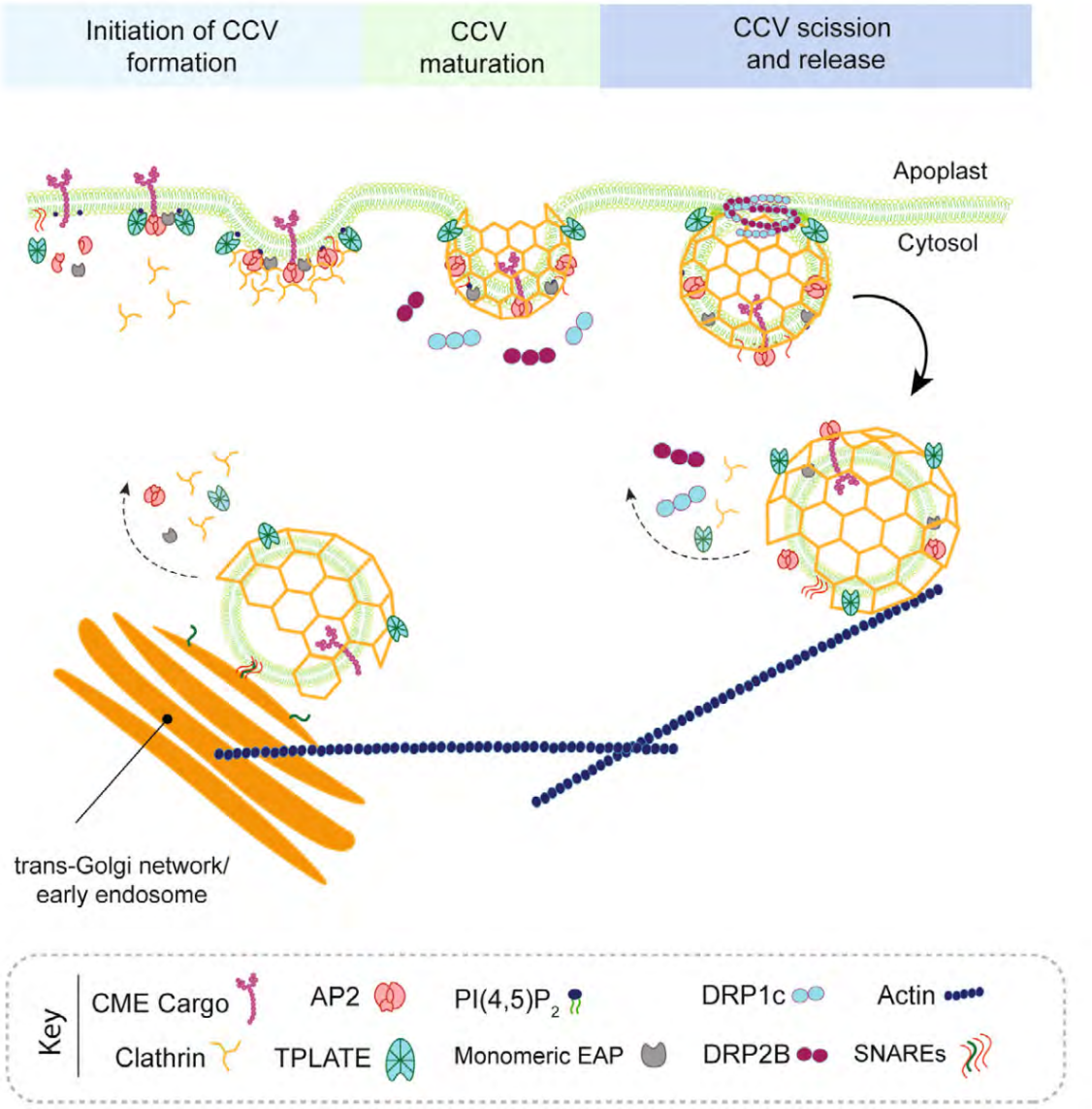

Figure 13. Stages of clathrin-coated vesicle formation. Three stages of clathrin-coated vesicle formation. Initiation of CCV formation through the recognition of plasma membrane-associated endocytic cargo and phosphatidylinositol phospholipids by adaptor proteins. Formed clathrin-coated pit then matures into a clathrin-coated vesicle. The final stage of CCV formation involves the action of dynamin-related proteins 1 and 2 that severs the budding endocytic vesicle from the membrane, releasing the CCV into the cytosol where it is trafficked to the TGN/EE along actin microfilaments. Sequential uncoating of the CCV indicated by dashed arrows occurs after cleavage and possibly up to the point when the endocytic CCV tethers to and fuses with the TGN/EE by the action of SNARE proteins. (Adapted from Dahhan and Bednarek, 2022).

the endocytosis of brassinosteroid receptor BRI1 was also compromised in a knockdown and dominant negative expression of AP2 subunits (Di Rubbo et al., 2013).

Surprisingly, unlike mammalian system, AP2 appears to be dispensable for plant endocytosis as Arabidopsis mutants defective in single AP2 subunits remain viable (Fan et al., 2013; Yamaoka et al., 2013). Recently, TPLATE complex (TPC) has emerged as an alternate adaptor complex and is absolutely essential for plant endocytosis and developement (Gadeyne et al., 2014). TPC is recruited to the PM prior to the recruitment of AP2 and clathrin and shows non-overlapping localization profiles to AP2 (Gadeyne et al., 2014). Therefore, it is important to check the involvement of AP2 in the endocytosis of different PM-localized proteins in plants, as already done for the brassinosteroid receptor BRI1 and auxin efflux carriers PIN. Nonetheless, based on the numerous reports in mammalian system and few in plants (cases of BRI1 and PINs), cargo selection of AP2-mediated CME is based on signals in the cytosolic regions of the PM proteins. These signals can be amino acid sequences, or post-transcriptional modifications, such as phosphorylation and ubiquitination (Traub, 2009; Dubeaux and Vert, 2017; Ivanov and Vert, 2020) and CME based on these sorting signals play a crucial role in plants in sensing and adaptation to different nutrient conditions (Discussed in later sections).

Endocytosis and endosomal trafficking are highly regulated processes and intersect with many other trafficking pathways. Endocytosis is tightly connected to exocytosis which involves the delivery of either newly synthesized or recycled proteins to the plasma membrane. Endocytosis and exocytosis share similar sorting mechanisms that are controlled by the same adaptor proteins, clathrin coat proteins, and other associated and accessory proteins at the plasma membrane and endosomes to control the sequestration, trafficking, and fate of the cargo molecules internalized by endocytosis.

Cargo selection

The control of PM protein abundance is dependent on the ability of CME machinery to recognize relevant cargo through intrinsic cytosolic peptide signals and post-translational modifications.

Peptide sequence

The subunits of the AP2 complex select cargo proteins via recognizing di-Leu motifs (DE)xxx (LLI) or DxxLL (x is any amino acid) and Tyr-based motifs Yxxϕ (ϕ is a bulky

hydrophobic amino acid; Diril et al., 2009; Traub, 2009). The endocytosis of the LeEix (pathogen-related LEUCINE-RICH-REPEAT RECEPTOR-LIKE PROTEIN) in tomato and the brassinosteroid receptor BRI1 in Arabidopsis depends on Tyr-based motifs in their cytoplasmic domains (Bar and Avni, 2009; Liu et al., 2020), suggests the conservation of these endocytic sorting signals in plants. Similarly, AP2M has been demonstrated to interact with the Tyr residue in three different YXXϕ motifs present in the cytoplasmic region of PIN1, though a single YXXϕ mutation did not alter PIN1 localization (Sancho-Andrés et al., 2016). Conversely, mutational analysis of three YXXϕ motifs in the cytoplasmic region of the Arabidopsis boron transporter BOR1 revealed that they are not required for CME but instead for the polar distribution of the protein in the inner PM domain of root cells (Takano et al., 2010).

Post-translational modification

Ubiquitination, a post-translational modification of cytoplasmic domains of transmembrane proteins has emerged as a critical signal recognized by the endocytic machinery to remove PM-localized plant proteins from the cell surface by endocytosis (Traub, 2009; Lauwers et al., 2010; Dubeaux and Vert, 2017). It is a process where ubiquitin molecule (mono-ubiquitination) can be conjugated to cargo proteins preferentially on lysine residue. In many cases, however, additional ubiquitin molecules can be conjugated, leading to the formation of ubiquitin chains (polyubiquitination). Both ubiquitination patterns can act as recognition signals for endocytosis as well as endosomal sorting of several plasma membrane proteins, including transporters and receptors. In addition to mono- and polyubiquitination, different types of chains can form depending on which amino acid residues of the ubiquitin molecule are conjugated to additional ubiquitins. The two most common chains are Lys48- and Lys63-linked chains. In mammals and yeast, Lys63 (K-63)-linked polyubiquitylation is frequently involved in endocytic trafficking (Haglund and Dikic, 2012; Tanno and Komada, 2013). This modification is also used as an endocytic signal in plants. Recently, K-63-linked polyubiquitylation of the pathogen-related receptor FLS2 (FLAGELLIN-SENSING 2), BRI1 and PIN2 generated by UBC35 and UBC36 has been shown to act as an early signal during initial internalization step of these cargos (Saeed et al., 2023). In plants, monoubiquitination of Pi transporter PHT1;1 by E3 ubiquitin ligase NITROGEN LIMITATION ADAPTION (NLA) is proposed

to control its internalization from the PM to regulate Pi uptake (Lin et al., 2013). Similarly, the trafficking of trans-Golgi localized iron transporter IRT1 between the cell surface and TGN/EE is dependent on mono-ubiquitination of cytosol-exposed lysine residues (Barberon et al., 2011). Ubiquitination-dead $IRT1_{K154RK179R}$ stabilizes at the PM as a consequence of a defect in internalization causing cytotoxicity in the cell due to the accumulation of metals, including Mn^{+2} (Barberon et al., 2011; Barberon et al., 2014). In animal cells, cytosolic serine, threonine, and cysteine residues have been reported to be ubiquitinated for the degradation of their substrate (Cadwell and Coscoy, 2005; Wang et al., 2007). Similarly, in Arabidopsis, IAA1, a member of Auxin/indole-3-acetic acid family (and a substrate of $SCF^{TIR1/AFB}$ ubiquitin ligase) was found to be ubiquitinated on Lys and Ser/Thr residues, which promoted its rapid degradation (Gilkerson et al., 2015). Ubiquitination can therefore occur on multiple different amino acid residues, which now introduces a great deal of complexity and flexibility. Nonetheless, whether the ubiquitination of non-lysine residues contribute to the internalization of the membrane proteins from the PM needs to be investigated.

Apart from ubiquitination, phosphorylation is also one of the signals to regulate the abundance of nutrient transporters at the PM. A recent study reported that the localization of the main manganese (Mn) transporter NATURAL RESISTANCE ASSOCIATED MACROPHAGE PROTEIN 1 (NRAMP1) is regulated by vesicle trafficking. The subcellular localization of NRAMP1 is Mn-dependent and high Mn availability in the media could induce the internalization of PM-localized NRAMP1 to endosomes through a CME pathway (Castaings et al., 2021). Moreover, the study also demonstrated that the serine residues Ser20, Ser22, and Ser24 of NRAMP1 could be phosphorylated, and phosphorylation of Ser20 is critical for NRAMP1 endocytosis (Castaings et al., 2021). Similarly, the phosphorylation of multiple serine residues in Arabidopsis PHT1 is shown to prevent it from reaching the PM (Bayle et al., 2011), while NITRATE TRANSPORTER NRT1.1; (Martín et al., 2008) and AQUAPORIN PIP2;1 (Prak et al., 2008) represent examples where their phosphorylation is required for their stabilization at the PM.

While a significant number of ubiquitylated and phosphorylated PM proteins and the enzymes that attach and recognize these modifications have been discovered in plants, if such mechanism existed for PHO1 was interesting to know. The regulation

of *PHO1* expression by transcription factors and its stability by PHO2 *via* ubiquitination is well established (Hamburger, 2002; Chen et al., 2009; Rouached et al., 2011; Liu et al., 2012; Ye et al., 2018; Xiao et al., 2022), however, the information on the control of PHO1 subcellular localization was largely unknown. The presence of PHO1 in Golgi/TGN as well as small fraction observed in EE and LE was surprising (Arpat et al., 2012; Liu et al., 2012), and did point towards the involvement of regulated trafficking mechanisms of PHO1. Due to the unequivocal importance of PHO1 in plant Pi homeostasis, we began exploring the localization and mechanism that could regulate its abundance and/or activity in Arabidopsis root vasculature cells.

Research outline

This thesis aims to investigate the subcellular localization of Arabidopsis PHO1 and the molecular mechanism that regulates its localization.

We sought to study this by adopting three different approaches:

1. Investigating if PHO1 can be transiently associated with PM by inhibiting the most common endocytic pathway, CME (Chapter 1).

2. A reverse genetic approach to find whether the post-translational modifications could control PHO1 localization (Chapter 2).

3. Comparative study of *PHO1* genes in *Arabidopsis thaliana* and *Medicago truncatula* to investigate the mechanism of their localization (Chapter 3).

Chapter 1

Chapter 1

The Arabidopsis PHOSPHATE 1 exporter undergoes constitutive internalization via clathrin-mediated endocytosis

Pallavi V. Vetal and Yves Poirier

Department of Plant Molecular Biology, University of Lausanne, 1015 Lausanne, Switzerland

Author for correspondence: Yves Poirier

Email: yves.poirier@unil.ch

Contributions

Yves Poirier and I wrote the manuscript. I performed all the experiments.

The findings from Chapter 1 are submitted to The Plant Journal.

Summary

In this work, we show that CME and vesicle trafficking in general contributes to plant Pi homeostasis by directly regulating the subcellular localization of PHO1, a known stele-localized exporter of Pi in *Arabidopsis thaliana*. We studied PHO1 localization using the overexpression of essential proteins and ubiquitination that is known to regulate endocytosis. By this strategy, we discovered that PHO1 localizes to the PM after CME inhibition, which otherwise is observed only at the Golgi/TGN. This suggested the existence of a constitutive internalization mechanism of PM-localized PHO1 via CME. Using a dominant negative *AP2MΔC* overexpressor line or *ap2m-1* mutant, we further demonstrated that PHO1 internalization does not require AP2. The reduced Pi export activity of PM-stabilized PHO1 provided evidence for the necessity of constitutive internalization and dynamic cycling of PHO1 between the PM and internal vesicular compartments. Here, we also demonstrated the importance of the EXS domain in the PM localization of PHO1. Though the signal driving this dynamic localization of PHO1 remains to be investigated, here, we were able to exclude the involvement of potential ubiquitination of cytosolic lysines in the EXS domain.

The Arabidopsis PHOSPHATE 1 exporter undergoes constitutive internalization via clathrin-mediated endocytosis

Pallavi V. Vetal and Yves Poirier

Department of Plant Molecular Biology, University of Lausanne, 1015 Lausanne, Switzerland

Author for correspondence: Yves Poirier
Tel: +41 21 692 4222
Email: yves.poirier@unil.ch

Running head: PHO1 undergoes clathrin-mediated endocytosis

One sentence summary: The phosphate exporter PHO1 localizes primarily at the Golgi and trans-Golgi network but transits to the plasma membrane and is constitutively retrieved from it via clathrin-mediated endocytosis.

Abstract

Inorganic phosphate (Pi) homeostasis is essential for plant growth and depends on the transport of Pi across cells. In *Arabidopsis thaliana*, PHOSPHATE 1 (PHO1) is present in the root pericycle and xylem parenchyma where it exports Pi into the xylem apoplast for its transfer to shoots. PHO1 consists of a cytosolic SPX domain followed by membrane-spanning α-helices and ends with the EXS domain, which participates in the steady-state localization of PHO1 to the Golgi and *trans*-Golgi network (TGN). However, PHO1 exports Pi across the plasma membrane (PM), making its localization difficult to reconcile with its function. To investigate whether PHO1 transiently associates with the PM, we inhibited clathrin-mediated endocytosis (CME) by overexpressing *AUXILIN-LIKE 2* or *HUB1*. Inhibiting CME resulted in PHO1 re-localization from the Golgi/TGN to the PM when *PHO1* was expressed in Arabidopsis root pericycle or epidermis or *Nicotiana benthamiana* leaf epidermal cells. However, localization of membrane-associated Golgi α-1,2-mannosidase I and PHT4;6 was not affected by *AUXILIN-LIKE 2* expression. A fusion protein between the PHO1 EXS region and GFP was stabilized at the PM by CME inhibition, indicating that the EXS domain plays an important role in sorting PHO1 to/from the PM. PHO1 internalization from the PM occurred independently of AP2 and was not influenced by Pi deficiency, the ubiquitin-conjugating E2 PHO2, or the potential ubiquitination of cytosolic lysines in the EXS domain. PM-stabilized PHO1 showed reduced root-to-shoot Pi export activity, indicating that CME of PHO1 may be important for its optimal Pi export activity and plant Pi homeostasis.

Introduction

Plants import mineral nutrients from the soil that are crucial for their growth and development. The acquisition of different ions by roots and their translocation to aerial tissues is a critical aspect of plant ion homeostasis. Of the 13 mineral nutrients required by plants, phosphorus (P) is one of the main elements limiting growth and productivity (Poirier et al., 2022). Plants acquire P in the form of inorganic orthophosphate (Pi) and functions as a structural element in nucleic acids and phospholipids, in energy metabolism as well as in the regulation of enzymes and signaling pathways. Pi limitation induces broad changes in gene expression and protein accumulation, leading to different developmental and metabolic acclimatory responses to improve Pi acquisition, storage and remobilization (Zhang et al., 2014; Gutiérrez-Alanís et al., 2018; Dissanayaka et al., 2021).

The uptake of Pi into roots and its export to vascular tissues are essential for Pi homeostasis. Following its acquisition by the root system via PHOSPHATE TRANSPORTER 1 (PHT1) H^+-Pi co-transporters (Nussaume et al., 2011), Pi is loaded into xylem vessels by PHOSPHATE 1 (PHO1) for its root-to-shoot transfer (Poirier et al., 1991; Hamburger, 2002). Arabidopsis (*Arabidopsis thaliana*) *PHO1* is expressed in the root pericycle and xylem parenchyma cells (Hamburger et al., 2002; Arpat et al., 2012). PHO1 expression in ectopic plant tissues, such as leaf mesophyll cells, leads to the rapid and specific export of Pi to the apoplast (Arpat et al., 2012; Wege et al., 2016). Further support for the activity of PHO1 as a Pi exporter was obtained by the heterologous expression of rice (*Oryza sativa*) *PHO1* orthologs in both mammalian cell cultures and *Xenopus laevis* oocytes (Ma et al., 2021). The Arabidopsis *pho1* mutant is defective in Pi translocation from roots to shoots and displays pleiotropic phenotypes expected for Pi deficiency, such as reduced shoot and root biomass and greater anthocyanin accumulation (Poirier et al., 1991). PHO1 has also been implicated in the transfer of Pi from maternal tissues to the embryo in both rice and Arabidopsis (Vogiatzaki et al., 2017; Ma et al., 2021). PHO1 orthologs in barrel clover (*Medicago truncatula*) mediate Pi transfer from infected nodule cells to nitrogen-fixing bacteroids (Nguyen et al., 2020).

PHO1 is composed of an N-terminal hydrophilic tripartite SPX (SYG1/Pho81/XPR1) domain that binds inositol pyrophosphate, an important mediator of Pi sensing and signaling (Wild et al., 2016; Jung et al., 2018), followed by four transmembrane-spanning α-helices (4TM) and a hydrophobic C-terminal EXS (ERD1, XPR1, SYG1) domain (Wege et al., 2016). PHO1 is primarily localized to the Golgi and partially to the trans-Golgi network (TGN) at steady-state levels in Arabidopsis root pericycle cells and when transiently expressed in *Nicotiana benthamiana* leaf epidermal cells (Arpat et al., 2012; Liu et al., 2012). This observation is in contrast to other transporters expressed in the root pericycle and involved in root-to-shoot ion transfer, such as REQUIRES HIGH BORON 1 (BOR1, for boron [B^-]; Takano et al., 2002; Takano et al., 2005), NITRATE TRANSPORTER 1.5 (NRT1.5, for nitrate [NO_3^-], Lin et al., 2008), NRT1/PTR FAMILY 2.4 (NPF2.4, for chloride ions [Cl^-]; Li et al., 2016) and AMMONIUM TRANSPORTER 2;1 (AMT2;1, for ammonium ions [NH_4^+]; Giehl et al., 2017), which localize to the plasma membrane (PM). The Golgi/TGN localization of PHO1 raises the question of how it mediates Pi export across the PM. As suggested by Arpat et al., 2012, one possibility is that only a minor fraction of PHO1 localizes to the PM to mediate Pi export. This situation would be analogous to that seen for the iron transporter IRON-REGULATED TRANSPORTER 1 (IRT1), which localizes to the TGN/EE in root hair cells at steady-state levels and functions in the uptake of reduced (ferrous) iron from the extracellular space (Barberon et al., 2011). IRT1 was observed at the PM only when its recycling from the PM via endocytosis was inhibited by treatment with the drug tyrphostin A23 or by blocking monoubiquitination. However, such stabilization of IRT1 at the PM resulted in severe growth defects and oxidative stress due to metal toxicity (Barberon et al., 2011). An alternative hypothesis is that PHO1 mediates Pi export by loading Pi into Golgi-derived vesicles, followed by the release of Pi into the extracellular space through exocytosis (Arpat et al., 2012).

Among the endocytic pathways described to date, clathrin-mediated endocytosis (CME) is the most common pathway in plants (Dhonukshe et al., 2007). CME modulates the abundance of many transporters at the PM, such as IRT1, the NH_4^+ transporter AMT1;3, the aquaporin PLASMA MEMBRANE INTRINSIC PROTEIN 2;1 (PIP2;1), the Pi transporter PHT1;1 and the manganese (Mn^{+2}) transporter NATURAL RESISTANCE-ASSOCIATED MACROPHAGE PROTEIN 1 (NRAMP1), among others

(Barberon et al., 2011; Li et al., 2011; Wang et al., 2013; Barberon et al., 2014; Castaings et al., 2021). CME requires an array of proteins, including heavy-chain and light-chain clathrins, together with adaptor and accessory proteins (McMahon and Boucrot, 2011; Paez Valencia et al., 2016; Rodriguez-Furlan et al., 2019; Aniento et al., 2022). In plants, the classical hetero-tetrameric ADAPTOR PROTEIN 2 (AP2) complex functions as a clathrin adaptor for CME and is implicated in the recognition of select PM cargoes destined for CME (Bashline et al., 2013; Di Rubbo et al., 2013; Kim et al., 2013; Yamaoka et al., 2013; Yoshinari et al., 2019). The AP2 complex consists of two large subunits (α2 and β2 or AP2A and AP2B), one medium subunit (μ2 or AP2M) and one small subunit (σ2 or AP2S) (Collins et al., 2002). Ubiquitination has emerged as a critical signal recognized by the CME machinery to remove PM-localized plant proteins from the cell surface (Dubeaux and Vert, 2017; Ivanov and Vert, 2021). For instance, the ubiquitination of IRT1 and the Pi transporter PHT1;1 induces their internalization via CME (Barberon et al., 2011; Lin et al., 2013; Shin et al., 2013).

In this study, we addressed the role of CME in PHO1 localization using genetic strategies that block CME at the PM. We observed that PHO1 reaches the PM and undergoes constitutive cycling to internal vesicular compartments. We also show that the internalization of PHO1 by CME occurs independently of AP2. Stabilization of PHO1 at the PM in Arabidopsis was associated with reduced Pi export from the root to the shoot. Taken together, our findings provide evidence for the dynamic trafficking of PHO1 to and from the PM and suggest that this cycling is important for maintaining Pi homeostasis.

Results

PHO1 is internalized from the PM via CME

To investigate whether PHO1 transits at the PM, we interfered with CME using a transient expression system in *Nicotiana benthamiana*. Overexpressing *AUXILIN-LIKE 2* inhibits CME by preventing the recruitment of clathrin to endocytic pits. This effect appears to be specific for the PM pool of clathrin without affecting the clathrin coating of other endosomal compartments (Adamowski et al., 2018). Accordingly, we

co-expressed a *PHO1-GFP* (green fluorescent protein) construct along with a construct encoding either the Golgi marker MAN1 (α-1,2-MANNOSIDASE I)-mCherry, the TGN marker VTI12 (VESICAL TRANSPORT V-SNARE 12)-mCherry or a PM-localized RFP (red fluorescent protein)-AUXILIN-LIKE 2 in *N. benthamiana* leaf epidermal cells using separate binary vectors. As previously reported (Arpat et al., 2012), we observed a high level of co-localization for PHO1-GFP and the Golgi marker in larger fluorescent bodies and a lower level of co-localization between PHO1-GFP and the TGN marker in the smaller and more mobile fluorescent bodies (Figure 1A, B). The transient expression of *AUXILIN-LIKE 2* led to the co-localization of PHO1-GFP with RFP-AUXILIN-LIKE 2 at the PM (Figure 1C; Supplemental Figure S1). To ensure that the observed effect of *AUXILIN-LIKE 2* expression on PHO1 re-localization to the PM was specific, we examined the effect of transient *AUXILIN-LIKE 2* expression on the localization of two other membrane-associated Golgi proteins, namely MAN1 (Nelson et al., 2007) and the phosphate transporter PHT4;6 (Guo et al., 2008; Cubero et al., 2009; Li et al., 2020). *AUXILIN-LIKE 2* expression did not shift the localization of these two Golgi membrane proteins towards the PM (Figure 1E, F; Supplemental Figure S2).

Overexpressing a construct encoding the C-terminal part of CLATHRIN HEAVY CHAIN1 (called HUB1) has a dominant-negative effect on CME due to the binding of HUB1 to and out-titrating the clathrin light chains (CLCs) (Liu et al., 1995; Dhonukshe et al., 2007; Kitakura et al., 2011). To further assess the contribution of CME to PHO1 localization, we transiently co-expressed *PHO1-GFP* with *RFP-HUB1* in *N. benthamiana* leaves. As shown in Figure 1D, PHO1-GFP localized at the PM when its encoding construct was co-expressed with *RFP-HUB1*. Together, these results reveal that PHO1 localizes to the PM in *N. benthamiana* leaves when CME is inhibited.

Overexpressing *AUXILIN-LIKE 2* in Arabidopsis stabilizes PHO1 at the PM of root pericycle cells

To study the effect of inhibiting CME on the subcellular localization of Arabidopsis PHO1 in the root pericycle, we introgressed the *XVE>>AUXILIN-LIKE 2* transgene from a previously characterized estradiol-inducible *XVE>>AUXILIN-LIKE 2* overexpressing line (Adamowski et al., 2018) into a *pho1-2* line complemented with a

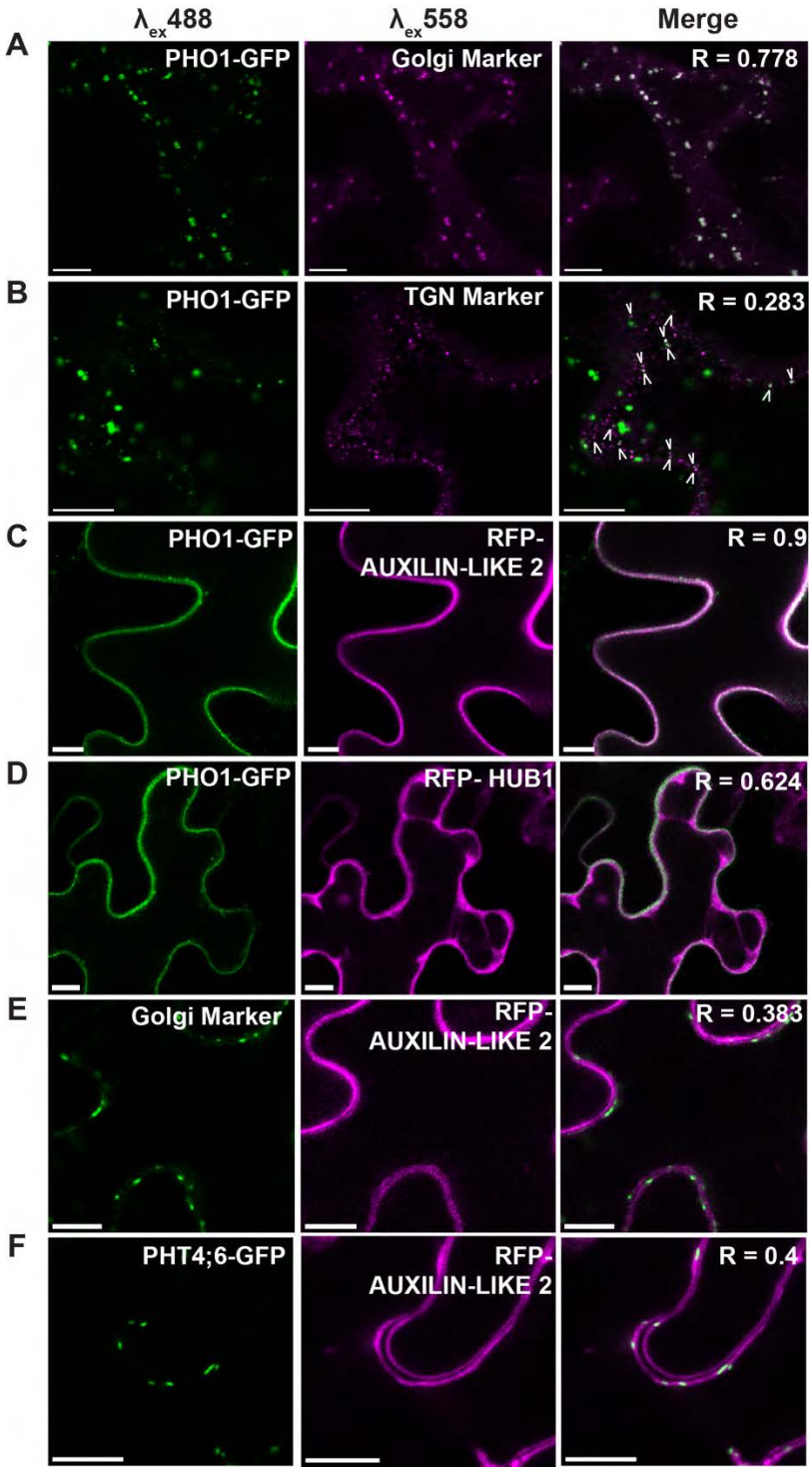

Figure 1. Overexpressing *AUXILIN-LIKE 2* or *HUB1* stabilizes PHO1-GFP at the plasma membrane in *N. benthamiana*. (A, B) Subcellular co-localization of full-length PHO1-GFP with markers for (A) the Golgi (MAN1-mCherry) or (B) TGN (VTI12-mCherry) in *N. benthamiana* epidermal cells. (C-D) Co-expression of *PHO1-GFP* with (C) *RFP-AUXILIN-LIKE 2* and (D) *RFP-HUB1*. (E-F) MAN1-GFP and PHT4;6-GFP (F) remain localized to the Golgi in cells co-expressing RFP-AUXILIN-LIKE 2. White arrowheads in B indicate partial co-localization of PHO1 with the TGN marker. R, Pearson's correlation coefficient of co-localization. Scale bars, 10 μm.

pPHO1:PHO1-YFP construct (hereafter referred to as line *P1-YFP*) to generate the *P1-YFP XVE>>AUXILIN-LIKE 2* line. In seedlings not expressing *AUXILIN-LIKE 2* (i.e., without estradiol treatment, DMSO mock control), PHO1-YFP showed a punctate pattern corresponding to the Golgi/TGN and some diffuse fluorescent signal likely representing protein degradation, with no signal visible at the PM (Figure 2A, upper panel). By contrast, upon estradiol induction, we observed a decrease in the PHO1-YFP punctate pattern and a significant increase in the PHO1-YFP signal at the PM that co-localized with the PM marker tdTomato-RCI2A (RARE-COLD-INDUCIBLE 2A) (Zhou et al., 2020) (Figure 2A, lower panel). Confocal cross-section images along with intensity line plots (Figure 2B, C) showed a shift of PHO1-YFP from the endomembranes to co-localization with the PM marker tdTomato-RCI2A in root pericycle cells upon *AUXILIN-LIKE 2* induction. We confirmed the overexpression of *AUXILIN-LIKE 2* in these lines after estradiol induction by RT-qPCR analysis (Supplemental Figure S3).

To evaluate if PHO1 could be stabilized at the PM when accumulating in a cell type other than root pericycle cells, we transformed Arabidopsis Col-0 and the *XVE>>AUXILIN-LIKE 2* overexpressing line with a construct encoding PHO1 fused to the fluorescent protein Dendra2 at its C-terminus under the control of an estradiol-inducible trichoblast-specific *WEREWOLF* promoter (*pWER>>XVE:PHO1-Dendra2*) (Lee and Schiefelbein, 1999; Siligato et al., 2016). In the presence of estradiol, we detected punctate-like structures in the epidermis of *pWER>>XVE:PHO1-Dendra2* cells that resembled native PHO1 localization in the root pericycle (Figure 2D, upper panel). The large PHO1-Dendra2 punctate structures co-localized well with the mCherry-GOT1 (GOLGI TRANSPORT 1) Golgi marker (Wave18R; Geldner et al., 2009), while smaller structures showed partial co-localization with the TGN marker mCherry-VTI12 (Wave13R; Geldner et al., 2009) (Supplemental Figure S4A; Arpat et al., 2012). However, upon co-induction of *AUXILIN-LIKE 2* overexpression in the *AUXILIN-LIKE 2* line background, we observed accumulation of PHO1-Dendra2 at the PM (Figure 2D, lower panel). We did not observe any fluorescent signal in these lines after mock (DMSO) treatment (Supplemental Figure S4B). These results suggest that PHO1 can cycle between the PM and Golgi/TGN in root cells other than the pericycle and that this dynamic localization is controlled by endocytosis via a CME pathway.

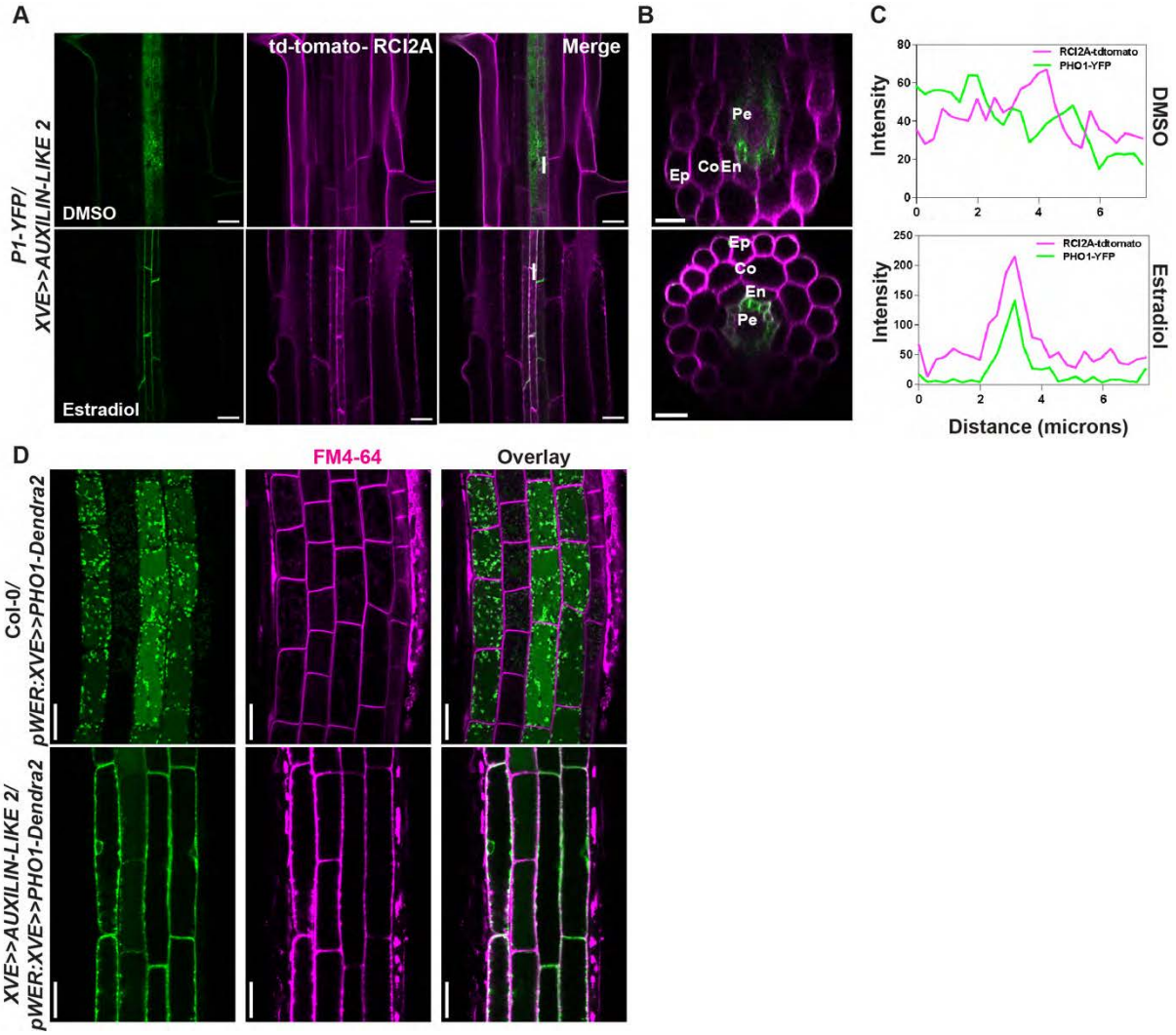

Figure 2. PHO1 internalization at the plasma membrane is regulated by CME. (A-C) A *P1-YFP* line was crossed to an estradiol-inducible *XVE>>AUXILIN-LIKE 2* line. (A) Confocal image showing the stabilization of PHO1-YFP at the plasma membrane (PM) following *AUXILIN-LIKE2* overexpression in the root of a 6-day-old Arabidopsis seedling treated with estradiol (lower panels). Mock (DMSO) treatment had no effect on PHO1 localization (upper panels). (B) Cross-section of a DMSO-treated Arabidopsis root showing punctate-like structures of PHO1-YFP (upper panel) and PM localization at the pericycle in estradiol-treated roots (lower panels). Ep, epidermis; Co, cortex; En, endodermis; Pe, pericycle. (C) Line plot showing the corresponding fluorescence intensity of PHO1-YFP and RCI2A td-tomato (PM marker) in Arabidopsis roots. The signal intensity of DMSO-treated roots is shown in the upper panel and estradiol-treated roots in the lower panel. Fluorescence intensity is drawn from the vertical white lines shown in A, right panels. (D) Subcellular localization of PHO1-Dendra2 encoded by a construct driving expression from an inducible epidermis-specific promoter (*pWER:XVE*) with (lower panels) or without (upper panels) *AUXILIN-LIKE 2* overexpression. In D, FM4-64 was used to define the PM of the epidermis. Scale bars, 20 µm.

Stabilization of PHO1 at the PM leads to reduced ^{33}Pi efflux from root to shoot

We investigated the effects of PM stabilization of PHO1 on its root-to-shoot Pi transfer function by analyzing the translocation of radiolabeled ^{33}Pi in the shoots of *P1-YFP XVE>>AUXILIN-LIKE 2*. Since the repression of CME in this line is not limited to the root pericycle, we first examined the effects of *AUXILIN-LIKE 2* overexpression on the uptake of ^{33}Pi from the medium to examine its possible influence on root Pi import. To this end, we transferred six-day-old *P1-YFP XVE>>AUXILIN-LIKE 2* and control (*pho1-2 XVE>>AUXILIN-LIKE 2,* Col-0 and *pho1-2*) seedlings to Murashige and Skoog (MS) plates containing estradiol for *AUXILIN-LIKE 2* induction or DMSO (mock control). Following 16 h of treatment, we exposed the roots to medium containing 10 μM Pi and 3 μCi ^{33}Pi with or without estradiol and calculated the total amount of ^{33}Pi acquired by the seedlings per root mg fresh weight. Pi uptake by the root system decreased in response to the induction of *AUXILIN-LIKE 2* expression compared to the DMSO control (Figure 3A). To circumvent this situation, we increased the amounts of Pi and ^{33}Pi 10-fold only for estradiol-treated seedlings. Under these conditions, whereas both Col-0 and *pho1-2* seedlings showed increased ^{33}Pi uptake from medium containing estradiol, the amount of ^{33}Pi acquired in the *XVE>>AUXILIN-LIKE 2* lines treated with estradiol matched that of the mock treatments (Figure 3B). We therefore used these conditions to evaluate the long-distance root-to-shoot transfer of Pi. We calculated the root-to-shoot transfer capacity of seedlings as the ratio of ^{33}Pi transferred to the shoot relative to the total amount of ^{33}Pi acquired by the seedlings via their roots. We observed a ~67% drop in the export of ^{33}Pi from roots to shoots in estradiol-induced *P1-YFP XVE>>AUXILIN-LIKE 2* seedlings compared to the non-induced DMSO-treated controls (Figure 3C). The export of ^{33}Pi from roots to shoots in seedlings where *AUXILIN-LIKE 2* was induced in the *pho1-2* mutant background also decreased to a similar extent (~54%). By contrast, we observed no reduction in ^{33}Pi transport in estradiol-treated Col-0 or *pho1-2* seedlings compared to their respective mock controls (Figure 3C).

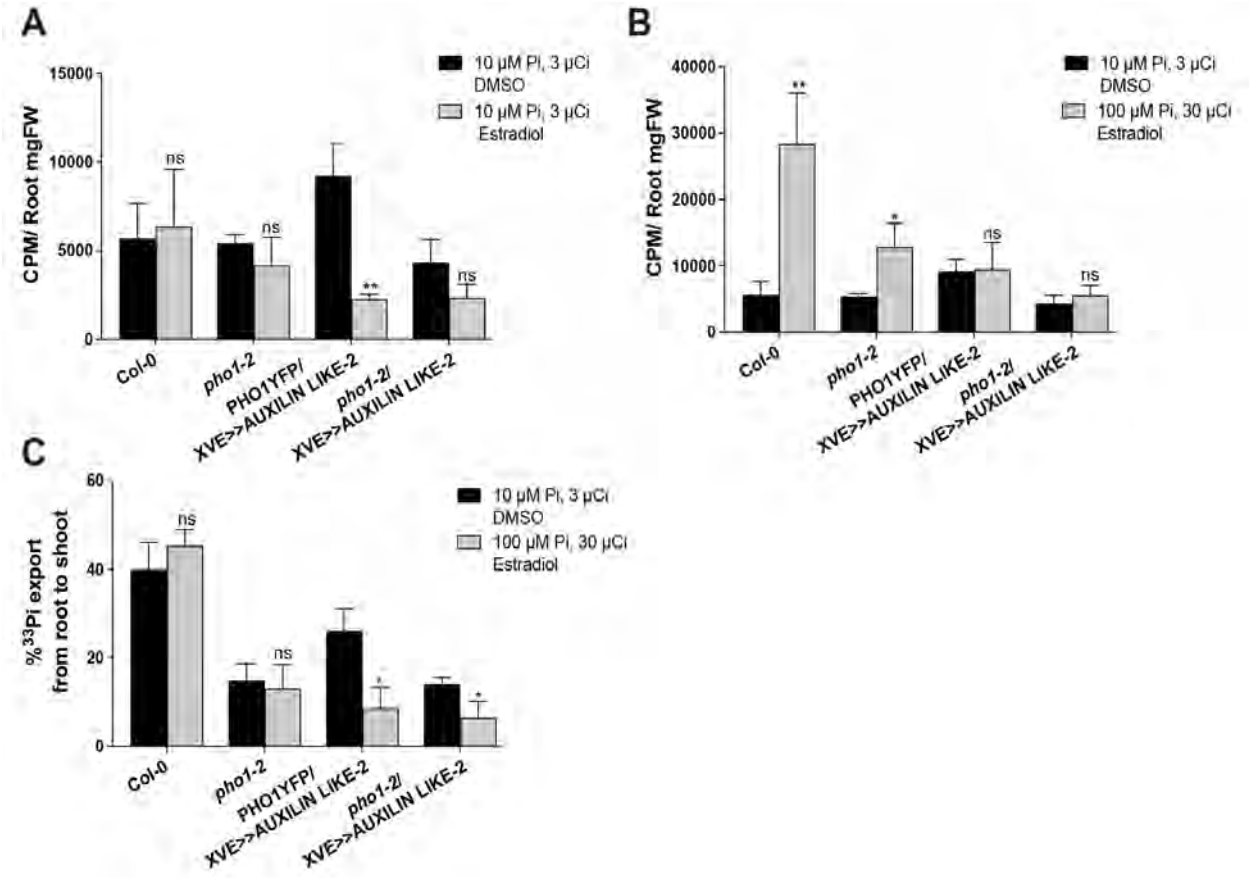

Figure 3. PHO1 stabilization at the PM affects Pi export from root to shoot. Six-day-old Col-0, *pho1-2*, *pho1-2 XVE>>AUXILIN-LIKE 2* and *P1-YFP XVE>>AUXILIN-LIKE 2* seedlings were treated with 5 µM estradiol or an equivalent volume of DMSO (mock) for 16 h and transferred to liquid MS medium containing ^{33}Pi and Pi for 1 h before quantification of ^{33}Pi uptake. (A, B) Measurement of ^{33}Pi import into the roots of seedlings on medium containing (A) 3 µCi ^{33}Pi and 10 µM Pi with DMSO (black bars) or estradiol (gray bars) and (B) 3 µCi ^{33}Pi and 10 µM with DMSO (black bars) or 30 µCi ^{33}Pi and 100 µM Pi with estradiol (gray bars). (C) Measurement of ^{33}Pi export from root to shoot in seedlings treated with 3 µCi ^{33}Pi and 10 µM Pi with DMSO (black bars) or 30 µCi ^{33}Pi and 100 µM Pi with estradiol (gray bars). Data are means ± standard deviation (n = 3, 10-12 plants were pooled for each biological replicate). Significant differences relative to the corresponding DMSO controls are indicated (**P <0.01, *P < 0.05; Student's t test).

Although the export of Pi into the root xylem is primarily mediated by PHO1, its closest homolog PHO1;H1 also contributes to Pi loading to the xylem (Stefanovic et al., 2007). Hence, to determine whether the reduced Pi transfer from roots to shoots in *pho1-2* is potentially associated with the localization of PHO1;H1 at the PM due to AUXILIN-LIKE 2-mediated CME inhibition, we generated lines expressing *PHO1;H1-GFP* under the control of the *PHO1* promoter in the *pho1-2 XVE>>AUXILIN-LIKE 2-mCherry*

background. Confocal microscopy showed that under mock treatment, PHO1;H1-GFP localizes to punctate-like structures, with a diffuse fluorescent signal likely representing protein degradation, with no signal at the PM visible in the root vasculature, similar to PHO1-YFP (Supplemental Figure S5, left panel). By contrast, we observed a change in the localization of PHO1;H1-GFP to the PM when we induced *AUXILIN-LIKE 2* overexpression by the addition of estradiol (Supplemental Figure S5, right panel).

CME of PHO1 occurs independently of AP2

The clathrin-dependent internalization of PHO1 from the PM prompted us to study the role of the AP2 complex in PHO1 endocytosis. Since the Arabidopsis *ap2m-1* mutant lacking the μ subunit of AP2 shows defects in endocytosis (Bashline et al., 2013), we examined the subcellular localization of PHO1-GFP in the *ap2m-1* background harboring a *pPHO1:PHO1-GFP* transgene. We did not observe any change in PHO1-GFP localization in the vasculature of *ap2m-1* (Figure 4A). The *ap2m-1* mutant has longer primary roots and defects in internalization of the endocytic tracer dye FM4-64 compared to the wild type (Bashline et al., 2013; Bashline et al., 2015); we observed the same features in *ap2m-1* carrying *pPHO1:PHO1-GFP* compared to the *P1-GFP* control (*pho1-2* complemented with the same *pPHO1:PHO1-GFP* construct) (Fig. 4B-D).

To independently examine the role of AP2 in PHO1 localization, we genetically interfered with AP2 function by overexpressing the dominant-negative *AP2MΔC* construct, where the AP2M C-terminal end responsible for cargo binding is deleted, in the *P1-YFP* genetic background (Bashline et al., 2013; Di Rubbo et al., 2013; Kim et al., 2013; Yamaoka et al., 2013). Upon induction of *AP2MΔC* expression, we did not detect any change in PHO1-YFP localization compared to the noninduced DMSO control (Figure 4E). RT-qPCR analysis showed that *AP2MΔC* is overexpressed 100-fold in seedlings treated with estradiol compared to mock treatment (Figure 4F). We also observed the decrease in root length and internalization of FM4-64 fluorescent puncta previously associated with the expression of *AP2MΔC* (Di Rubbo et al., 2013) in the *P1-YFP XVE>>AP2MΔC* line upon induction with estradiol relative to the DMSO control (Figure 4G-I). Altogether, these results indicate that the internalization of PHO1 via CME occurs independently of AP2.

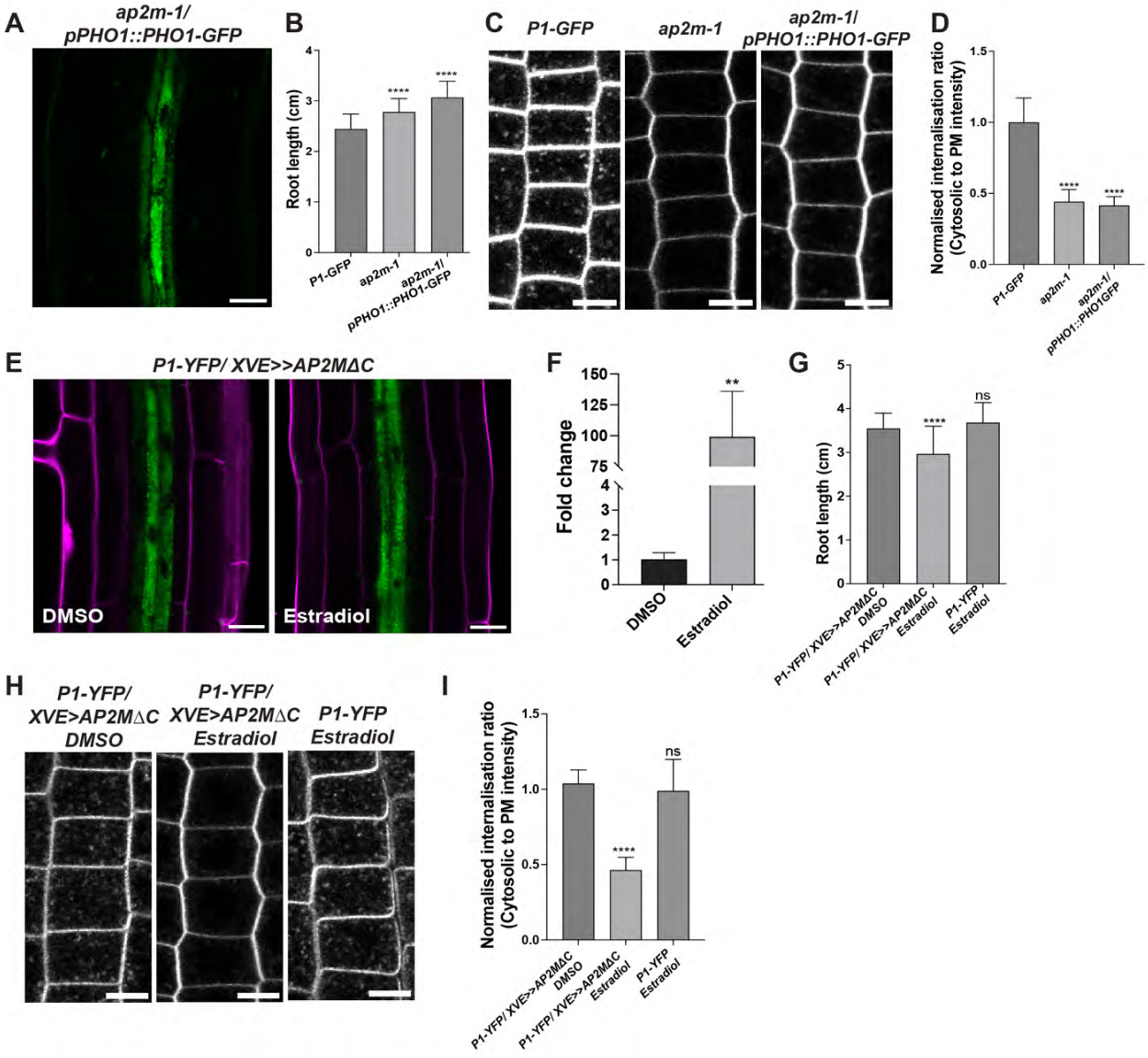

Figure 4. CME of PHO1 occurs independently of AP2. (A) Subcellular localization of PHO1-GFP in the roots of *ap2m-1*. (B) Measurement of root length in 7-day-old *P1-GFP*, *ap2m-1* and *ap2m-1 pPHO1:PHO1-GFP* seedlings. ANOVA ****P < 0.0001, *n* = *50-70* roots per genotype. (C) Imaging of FM4-64 puncta in the epidermal root cells of *P1-GFP*, *ap2m-1* and *ap2m-1 pPHO1:PHO1-GFP* seedlings. (D) Quantification of the ratio of intracellular-to-PM FM4-64 signal intensity normalized to that of the *P1-GFP* control. ANOVA ****P < 0.0001, n = 10-15 (~8 cells) roots per genotype. (E) Localization of PHO1-YFP after mock (DMSO) or estradiol induction of *AP2MΔC* expression (5 μM estradiol for 2 days). Propidium iodide staining (magenta) was used to define cell boundaries. (F) RT-qPCR analysis of *AP2M* expression in *P1-GFP XVE>>AP2MΔC* seedlings following induction with 5 μM estradiol for 2 days. Relative expression level after mock treatment (DMSO only) was set to 1. Student's t test, **P <0.01, n = 3 biological replicates. (G) Root length of *P1-YFP* and *P1-YFP XVE>>AP2MΔC* seedlings treated with estradiol or with an equivalent volume of DMSO (mock). Arabidopsis seeds were incubated for 7 days on inductive medium (5 μM estradiol). ANOVA ****P < 0.0001, n = 30-40 roots per genotype. Confocal images (H) and quantification (I) of cytosolic-to-PM ratios of FM4-64 internalization in the

genotypes mentioned in (G). ANOVA ****$P < 0.0001$, n = 10-13 (~8 cells) roots per genotype. Data are means ± SD. Scale bars, 20 µm.

PHO2 and the plant Pi status do not influence PHO1 localization

Pi availability affects PHO1 expression at both the transcriptional level and via ubiquitin-mediated degradation (Hamburger, 2002; Liu et al., 2012). We thus investigated if PHO1 localization is modulated by the plant Pi status by examining the localization of PHO1-YFP in the roots of seedlings grown for 6 days on Pi-sufficient or Pi-deficient medium. Confocal microscopy did not reveal a change in the localization of PHO1-YFP in roots under Pi-deficient conditions relative to Pi-sufficient conditions (Supplemental Figure S6), suggesting that the dynamic cycling of PHO1 between the Golgi/TGN and PM does not depend on the availability of Pi in the medium.

PHO2 encodes a ubiquitin-conjugating E2 enzyme that ubiquitinates PHO1, leading to its degradation (Liu et al., 2012). To determine if PHO2 influences the localization of PHO1, we transformed the *pho2* mutant with the *proPHO1:PHO1-YFP* construct and examined the localization of the encoded fusion protein by confocal microscopy. The punctate pattern associated with the Golgi/TGN localization of PHO1 in the *pho2* mutant background was similar to that seen in the *pho1-2* mutant, with no fluorescent signal associated with the PM (Figure 5A).

The effect of the EXS domain of PHO1 on PM localization is not dependent on ubiquitination

Previous studies on the structure of PHO1 showed that removing its C-terminal EXS domain resulted in the localization of the PHO1 truncated protein to the ER, while a fusion protein consisting of only the EXS domain of PHO1 fused to RFP resulted in co-localization with full-length PHO1-GFP to the Golgi/TGN (Wege et al., 2016). These findings highlight the important role of the EXS domain in the Golgi/TGN localization of PHO1. To investigate if the C-terminal EXS domain of PHO1 functions in its PM localization, we crossed the *pPHO1:EXS-GFP* line (producing only the EXS domain of PHO1 fused to GFP) with the *XVE>>AUXILIN-LIKE 2* line. Upon *AUXILIN-LIKE 2* overexpression by estradiol treatment, we observed stabilization of EXS-GFP at the

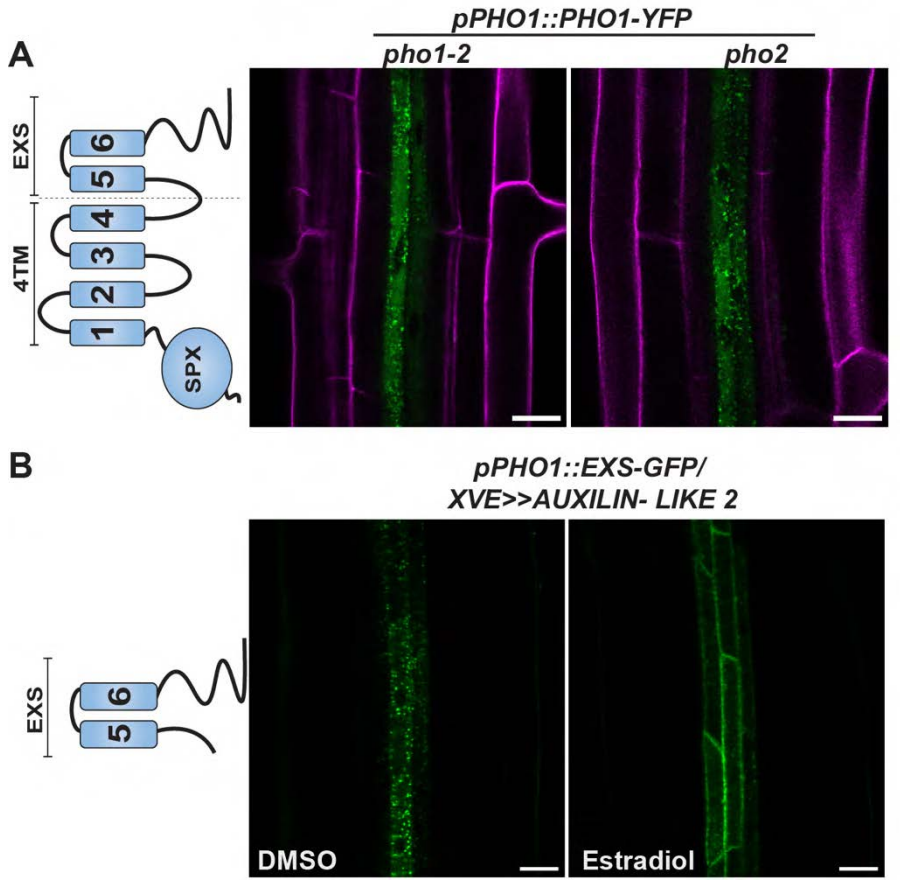

Figure 5. The EXS domain of PHO1 is involved in its trafficking from the Golgi/TGN to the plasma membrane. (A) Confocal microscopy of the localization of full-length PHO1-YFP in the *pho1-2* and *pho2* mutant backgrounds. A schematic diagram of PHO1-YFP (N-terminal SPX followed by four transmembrane α-helices [4TM] and ending with the EXS domain which includes the last two transmembrane α-helices) is shown on the left. Images show the overlay of GFP (green) and propidium iodide (magenta) fluorescence defining the cell wall boundaries. (B) Imaging of EXS-GFP in the roots of 6-day-old seedlings of the estradiol-inducible *AUXILIN-LIKE 2* overexpressor line treated with DMSO or estradiol for 16 h. Scale bars, 20 μm.

PM in the pericycle compared to the DMSO control (Figure 5B). These results suggest that the C-terminal EXS domain of PHO1 functions in PHO1 trafficking to the PM.

The PHO2-mediated degradation of PHO1 implicates the ubiquitination of the N-terminal half of PHO1 harboring the SPX domain (Liu et al., 2012). Considering that PHO1 localization is not affected in the *pho2* mutant, in addition to our observation that the EXS domain of PHO1 was stabilized to the PM in response to *AUXILIN-LIKE 2* overexpression, we examined whether lysine residues in the EXS domain and the preceding four transmembrane regions (4TM domain) could be ubiquitination sites involved in the localization of PHO1 to the PM. Based on the previously described

topology of PHO1 (Wege et al., 2016), we generated two PHO1 variants whose lysine residues facing the cytosol in the 4TM domain or EXS domain were changed to arginine residues. These variants contained mutations in three lysine residues in the 4TM region (K450R, K540R, and K548R) designated as TM K→R and seven lysine residues (K583R, K591R, K677R, K685R, K687R, K700R, and K769R) in the EXS denoted as EXS K→R (Figure 6A and Supplemental Figure S7). The K→R mutations in either the 4TM or EXS domain did not change the localization or function of PHO1 when we transiently expressed the encoding constructs in *N. benthamiana* leaves, as the variant proteins co-localized with Golgi and TGN markers (Figure 6B), and these lines showed greater Pi export to the apoplast compared to the empty vector control (Figure 6C). None of the PHO1 variants or controls showed any change in the level of nitrate exported to the medium, indicating that PHO1 specifically exports Pi.

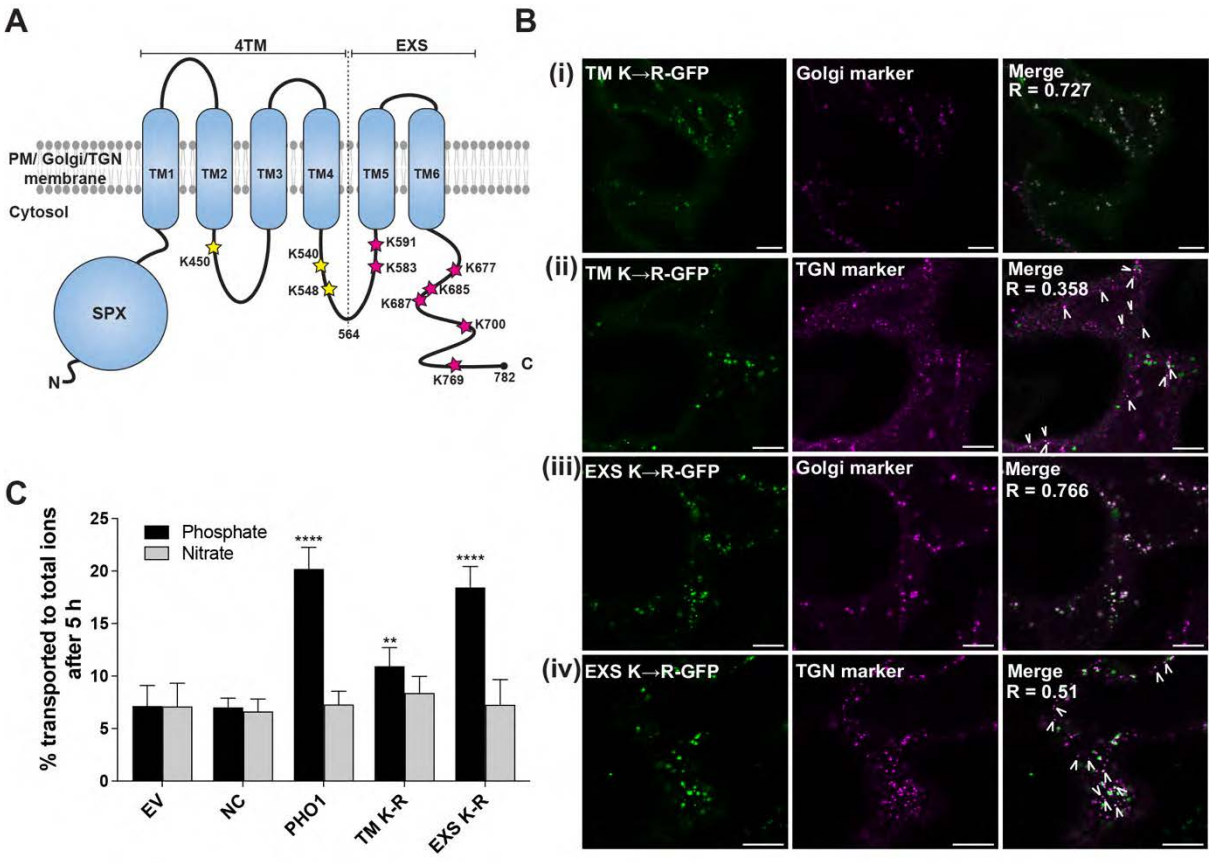

Figure 6. PHO1 TM K→R and EXS K→R mutants localize to the Golgi/TGN and export Pi into the extracellular space in *N. benthamiana* epidermal cells. (A) Topological model of Arabidopsis PHO1 showing the lysine residues (★) selected for mutagenesis. Two constructs encoding mutated PHO1-GFP were generated, one with three lysine-to-arginine mutations in the TM domain (TM K→R, ★ in yellow) and one with seven lysine-to-arginine mutations in the EXS domain (EXS K→R, ★ in magenta).

(B) Subcellular localization of PHO1 mutants transiently expressed in *N. benthamiana*. Co-localization of TM K→R PHO1-GFP (i and ii) and EXS K→R PHO1-GFP (iii and iv) to the Golgi/TGN with Golgi (MAN1-mCherry, i and iii) or TGN (VTI12-mCherry, ii and iv) markers. White arrowheads point to partial co-localization of PHO1 mutants with the TGN marker. R (Pearson's correlation coefficient) values for co-localization are reported in each merged image. (C) Measurement of Pi and NO_3^- exported by PHO1 TM and EXS mutants transiently expressed in *N. benthamiana* leaf discs. The amounts of Pi and NO_3^- exported to the apoplast were measured after 5 h of incubation. Pi and NO_3^- export were measured in leaf discs expressing *GFP* or non-infiltrated (NC) leaf discs as a control. Data are means ± SD, n = 5, 4-5 discs were pooled for each biological replicate. Asterisks represent statistically significant differences compared to the empty vector control, ANOVA; ****P < 0.0001; **P < 0.01. Scale bars, 10 µm.

Finally, we introduced GFP fusion constructs of these two TM K→R and EXS K→R PHO1 variants under the control of the *PHO1* promoter in the *pho1-2* mutant background to evaluate the effects of potential ubiquitination on the localization and Pi root-to-shoot transport activity of PHO1. Expressing the constructs encoding GFP fusions of both variants in the *pho1-2* background complemented the reduced shoot growth and low shoot Pi phenotypes of the *pho1-2* mutant to levels comparable to Col-0 and *P1-GFP* (Figure 7A, B). Both TM K→R and EXS K→R PHO1-GFP variants localized to punctate-like structures in the pericycle, similar to wild-type PHO1-GFP, which is indicative of Golgi/TGN localization (Figure 7C). These results indicate that the ubiquitination of these lysine residues is not likely to be involved in regulating the localization of PHO1 to the PM.

Discussion

Active internalization of PM-localized transporters via endocytosis has emerged as a powerful strategy to regulate ion homeostasis (Fuji et al., 2009; Zelazny and Vert, 2014; Ivanov and Vert, 2021). Here we demonstrated that endocytosis regulates the localization of the Pi exporter PHO1, since its PM localization only became apparent when we genetically impaired CME by overexpressing either *AUXILIN-LIKE 2* or *HUB1*. Importantly, localization of two other membrane-associated Golgi proteins, namely MAN1 and PHT4;6, was not modified by the overexpression of *AUXILIN-LIKE 2*. CME thus plays an important and specific role in the trafficking of PHO1 between the Golgi/TGN and the PM. This mechanism was not cell-type specific, as we not only observed the shift in the subcellular localization of Arabidopsis PHO1 mediated by CME impairment in root pericycle cells (the endogenous expression domain of *PHO1*

in roots) but also when we ectopically expressed *PHO1* in root epidermal cells and in *N. benthamiana* leaf epidermal cells. CME-mediated transporter internalization can be

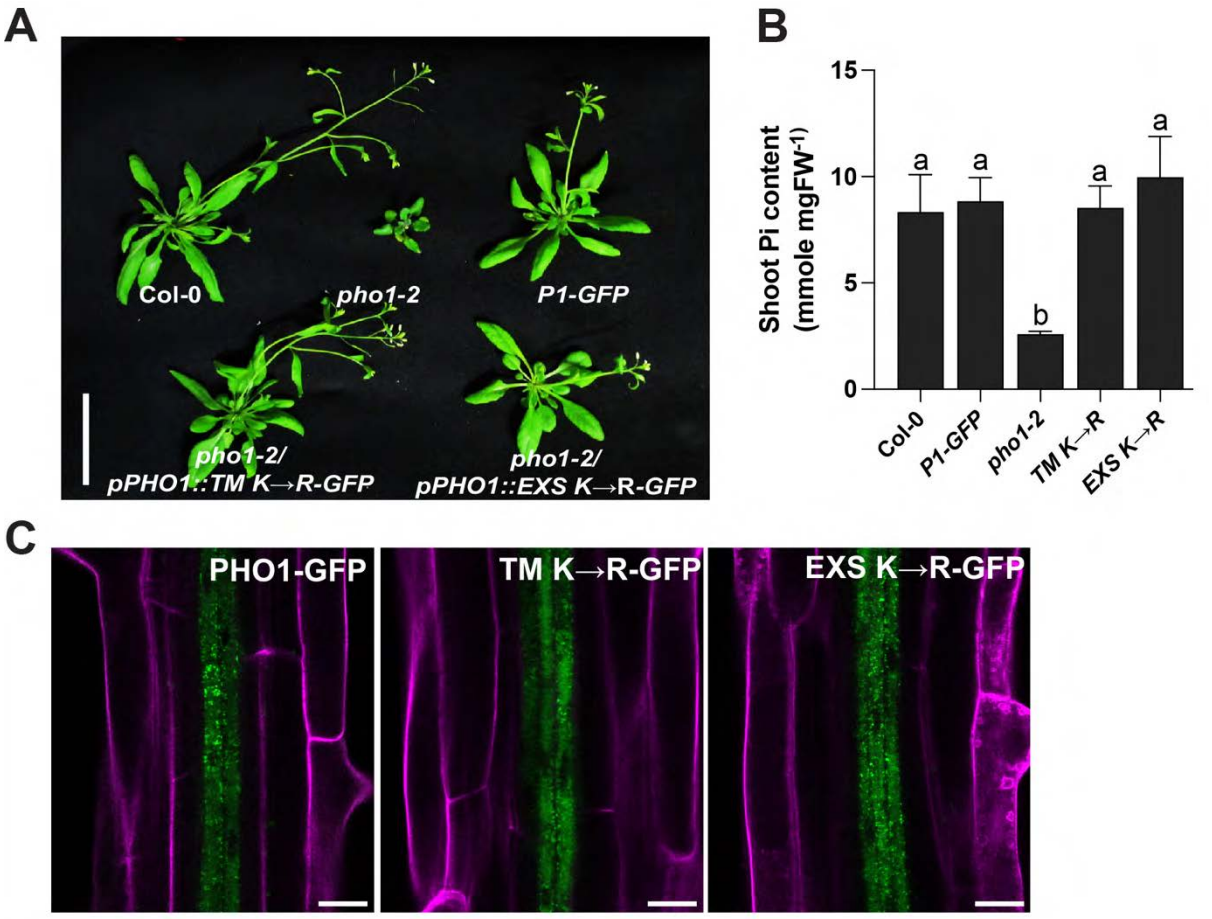

Figure 7. The potential ubiquitination sites in the cytosolic regions of PHO1 4TM and EXS do not control its internalization from the plasma membrane. (A) Phenotypes of plants transformed with constructs encoding each PHO1 K→R mutant in *pho1-2* compared to wild type (Col-0), *pho1-2* and *P1-GFP*. Plants were grown in pots for 32 days. Scale bar, 5 cm. (B) Pi contents of shoots from the lines mentioned in (A). Data are means ± SD, n = 5-7. For all histograms, different lowercase letters indicate significant differences, as determined by ANOVA with a Tukey Kramer test, $P < 0.05$. (C) GFP fluorescence in the root pericycles of *pho1-2* seedlings expressing full-length *PHO1-GFP*, TM K→R or EXS K→R mutant-GFP constructs. Images show the overlay of GFP (green) and propidium iodide (magenta) fluorescence defining the cell wall boundaries. Scale bars, 20 µm.

triggered by the abundance of the transporter substrate in the surrounding medium, representing a mechanism to regulate ion flux. Such CME-mediated internalization has been demonstrated for the plant transporters BOR1 by boron, NRAMP1 by manganese, and AMT1;3 by ammonium (Takano et al., 2002; Wang et al., 2013;

Castaings et al., 2021). Internalization of the PM-localized H^+-Pi co-transporter PHT1;1 into endosomes for subsequent recycling to the PM or the lytic vacuole under low and high Pi conditions, respectively, also contributes to the differential stability of PHT1;1 at the PM (Bayle et al., 2011). By contrast, we did not detect a shift in PHO1 localization to the PM in pericycle cells of roots grown in either low- or high-Pi medium. CME-mediated internalization of PHO1 from the PM thus appears to be constitutive, at least under the conditions tested here.

Most key components of the CME machinery are conserved among plants, fungi and animals (Chen et al., 2011; Baisa et al., 2013; Paez Valencia et al., 2016). The AP2M subunit of the AP2 complex has been implicated in the recognition of PM-localized protein cargoes destined for internalization (Bashline et al., 2013; Di Rubbo et al., 2013; Fan et al., 2013; Kim et al., 2013). The absence of PM localization for PHO1 in the dominant negative *AP2MΔC* overexpressing line and the *ap2m-1* mutant suggests the existence of an AP2-independent CME pathway for PHO1 internalization. AP2 is dispensable for plant endocytosis, as Arabidopsis mutants defective in single AP2 subunits remain viable (Bashline et al., 2013; Fan et al., 2013; Kim et al., 2013; Yamaoka et al., 2013). Mutations in the TPLATE complex (TPC) subunits are lethal, suggesting that this complex is an adaptor essential for CME (Van Damme et al., 2007; Gadeyne et al., 2014). Furthermore, one of the large subunits of the TPLATE complex has recently been shown to participate in the internalization of ubiquitinated plasma membrane cargo (Grones et al., 2022). Since the internalization of PHO1 appears to occur independently of the AP2 complex, it would be interesting to assess whether the TPC contributes to its internalization.

The C-terminal transmembrane region of PHO1, comprising the 4TM and EXS domains, was shown to be necessary and sufficient to mediate Pi export when transiently expressed in *N. benthamiana* (Wege et al., 2016). Furthermore, the EXS region was shown to be essential for the proper localization of PHO1 at the Golgi/TGN, and an EXS-RFP fusion protein co-localized with PHO1 (Wege et al., 2016). In the present study, we showed that inhibiting CME in seedling expressing an *EXS-GFP* fusion construct in the root pericycle also led to a shift of the fusion protein from the Golgi/TGN to the PM. Together, these results highlight the key role of the EXS domain of PHO1 in its localization and retrieval from the PM by CME.

Ubiquitination can trigger the internalization of transporters from the PM via CME. This observation was clearly demonstrated by the ubiquitination of two lysine residues of IRT1 facing the cytosol (K154 and K179) by the E3 ubiquitin ligase IRT1 DEGRADATION FACTOR 1 (IDF1) (Barberon et al 2011, Shin et al. 2013) and the action of the E3 ubiquitin ligase NITROGEN LIMITATION ADAPTATION (NLA) on PHT1 Pi importers (Lin et al, 2013). However, in the present study, mutating all the cytosol-facing lysine residues present in the 4TM or EXS region of PHO1 to arginine resulted in PHO1 variants still capable of complementing the *pho1* mutant. Moreover, these variant PHO1 proteins showed no shift in localization from the Golgi/TGN to the PM in transient expression assays in *N. benthamiana* leaves or in root pericycle cells.

Beyond endocytosis, ubiquitination is also involved in controlling the levels of transporters via sorting to multivesicular bodies (MVBs) and lytic vacuoles. For example, ubiquitination of BOR1 is essential for its degradation via sorting to MVBs (Kasai et al., 2011). Ubiquitination of the N-terminal half of PHO1 (containing the SPX domain) by the ubiquitin-conjugating E2 enzyme PHO2 led to increased degradation of PHO1 via its targeting to MVBs (Liu et al., 2012). As a result, the *pho2* mutant shows high PHO1 abundance and exhibits constitutively active Pi starvation phenotypes, leading to excessive shoot Pi content and reduced growth (Aung et al., 2006; Bari et al., 2006). The identities of the lysine residues ubiquitinated in the SPX domain of PHO1 by PHO2 are unknown. However, our results indicate that the localization of PHO1 between the PM and Golgi/TGN is not affected in the *pho2* mutant, indicating that PHO2-mediated ubiquitination does not contribute to the CME of PHO1. Although unlikely, it remains possible that the ubiquitination of the SPX region of PHO1 by other ubiquitin ligases plays a role in the PM localization of PHO1. However, mutating lysine residues in the SPX domain that are implicated in the binding of inositol pyrophosphates inactivated the Pi export activity of PHO1 without altering its steady-state localization at the Golgi/TGN (Wild et al., 2016).

Phosphorylation is an alternative mechanism that controls transporter localization in plants. For example, the phosphorylation of multiple serine residues at the C terminus of Arabidopsis PHT1;1 was shown to prevent its exit from the PM (Bayle et al., 2011). Conversely, phosphorylation of the NO_3^- transporter NRT1.1 (Martín et al., 2008), the aquaporin PIP2;1 (Prak et al., 2008) and the Mn^{+2} transporter NRAMP1 (Castaings et

al., 2021) are involved in the stabilization of these proteins at the PM. Whether phosphorylation of PHO1 contributes to its sorting to or from the PM deserves further investigation.

Stabilizing IRT1 at the PM by blocking ubiquitination resulted in an enhanced metal importing activity of IRT1, leading to oxidative damage and strongly limited plant growth associated with the excessive accumulation of Fe and Mn^{+2} (Barberon et al., 2011; Barberon et al., 2014). These results highlight the important role of IRT1 endocytosis in metal-importing activity, which is required for optimal metal homeostasis and plant survival. In an analogous manner, constitutive endocytosis can be seen as a way to prevent uncontrolled Pi export activity by PHO1. Overexpression of *PHO1* in leaves was previously shown to lead to the accumulation of very high levels of Pi in leaf xylem exudates, uncontrolled export of Pi into the leaf apoplastic space, and very poor growth, likely resulting from the metabolic costs of maintaining a futile cycle of Pi import and export (Stefanovic et al., 2011). In this context, it is surprising that the transient stabilization of PHO1 at the PM of the root pericycle via *AUXILIN-LIKE 2* induction led to a decrease in PHO1-mediated Pi export activity instead of an increase, which would be expected if the Pi export activity of PHO1 was mediated by a PM-localized protein. This impaired export activity might be associated with the lack of a partner protein or a post-translational modification that would be required for PHO1 to be functionally active. Alternatively, this lower Pi export activity may be due to the absence of lateral polarity of the PM-stabilized PHO1. Several ion transporters have been shown to exhibit lateral polarity in root cells, which may be associated with more efficient radial transfer of ions across the root for vascular ion loading (Barberon and Geldner, 2014). For example, the polar localization of BOR1 and LOW SILICON RICE 2 (LSI2), which are exporters of B^{-} in Arabidopsis and silicon in rice, respectively, on the inner (i.e. towards the xylem) side of the endodermis would favor the unidirectional movement of these ions to the xylem (Ma et al., 2007; Alassimone et al., 2010; Takano et al., 2010). Interestingly, overexpressing the late endosome phosphatidylinositol-3-phophstae-binding protein FYVE1 led to a lack of IRT1 polarity and lower metal contents in cells, likely due to the decreased radial transport of metals towards the xylem (Barberon et al., 2014). Although the reason behind the lower Pi export activity of PM-stabilized PHO1 is currently unclear, these findings support a role

for PHO1 internalization from the PM for its optimal activity in Pi transfer from root to shoot.

An attractive hypothesis for PHO1 Pi export activity is that this protein loads Pi into Golgi-derived vesicles, likely using the electrochemical proton gradient ($\Delta\mu H^+$) generated by the vacuolar ATPase (V-ATPase) as a driving force, followed by Pi unloading into the apoplastic space through exocytosis and the rapid recycling of PHO1 from the PM by endocytosis and endosomal trafficking (Arpat et al., 2012). This hypothesis would explain the presence of a large fraction of PHO1 in the Golgi/TGN and its near absence at the PM. The observed decrease in Pi export activity of PM-stabilized PHO1 may be explained by a reduction in the number of recycled endosomes available to participate in further rounds of vesicular Pi loading and export. Such a secretory pathway-mediated mechanism was previously proposed to explain how the trans-Golgi-localized Mn^{+2} transporter METAL TOLERANCE PROTEIN 11 (MTP11) could be associated with elevated intracellular levels of Mn^{+2} in the *mtp11* mutant and increased tolerance to excess Mn^{+2} in plants overexpressing *MTP11* (Delhaize et al., 2007; Peiter et al., 2007). A similar hypothesis was also put forward to explain the role of ENDOPLASMIC RETICULUM-TYPE CALCIUM-TRANSPORTING ATPASE 3 (ECA3) in calcium (Ca^{+2}) and Mn^{+2} homeostasis (Li et al., 2008). Support for such a synaptic-like transport pathway in plants was recently described for the export of nicotianamine in vascular tissues (Chao et al., 2021). Interestingly, recent work on the animal vesicular glutamate transporter VGLUT points to the possible evolution of a synaptic-like transport pathway for Pi. VGLUT belongs to the solute carrier (SLC) family and was originally discovered as a coupled sodium (Na^+)/Pi co-transporter (Ni et al., 1994; Aihara et al., 2002). Subsequently, VGLUT was shown to mediate the uptake of glutamate into neuronal synaptic vesicles using the $\Delta\mu H^+$ generated by V-ATPase (Bellocchio et al., 2000). A recent study using functional reconstitution and heterologous expression demonstrated that VGLUT can actually transport both Pi and glutamate into synaptic vesicles using a single substrate binding site (Preobraschenski et al., 2018). Whether PHO1 might export Pi via a similar synaptic-like pathway deserves further analysis.

Materials and Methods

Plant materials and growth conditions

All *Arabidopsis thaliana* plants used in this study, including mutants and transgenic plants, were in the Columbia (Col-0) background. For the *in vitro* experiments, seeds were surface sterilized by chlorine gas and transferred to the square plates containing half-strength Murashige and Skoog (MS) salts (Duchefa M0255), 1% (w/v) sucrose, and 1% (w/v) agar in continuous light for 6 days. Seedlings were either used for confocal microscopy or transferred to soil and grown in long-day conditions (16 h of light and 8 h of dark at 20 ^{0}C) for at least 25 days for phenotypic analysis and/or quantification of Pi content. For the Pi-deficient medium, MS salts without Pi (Caisson Labs, MSP11) were used. Pi buffer pH 5.7 (93.5% KH_2PO_4 and 6.5% K_2HPO_4) was added to obtain different Pi concentrations.

T-DNA insertion line *ap2m-1* (SALK_083693) (Fan et al., 2013; Kim et al., 2013; Yamaoka et al., 2013) was obtained from the Nottingham Arabidopsis Stock Centre. Previously published transgenic lines *Col-0 XVE>>AUXILIN-LIKE2* (Adamowski et al., 2018), *pho1-4 pPHO1::EXS-mGFP* (Wege et al., 2016), *pho1-2 pPHO1::PHO1-mGFP (P1-GFP)* (Wege et al., 2016), *pho1-2 pPHO1::PHO1-YFP (P1-YFP)* (Liu et al., 2012) and Wave marker line 13 and 18 (Geldner et al., 2009) were used for generating the crosses. Floral dip method was used for the generation of stable Arabidopsis transgenics (Clough and Bent, 1998). The constructs *XVE>>AP2MΔC* (Di Rubbo et al., 2013), WT *pPHO1::PHO1-mGFP* and mutated PHO1-GFP constructs were transformed into the line *P1-YFP*, *pho2* (Aung et al., 2006) and *pho1-2* (Hamburger et al., 2002) backgrounds, respectively.

Generation of constructs

PHO1 constructs with mutations at selected lysine residue in the 4TM and EXS domains were synthesized by GenScript (genscript.com). Genomic sequences of WT and mutated *PHO1* as well as the coding sequence of *C-HUB1* (Robert et al., 2010) were amplified and inserted into pENTR2B (Invitrogen) entry vector either by In-Fusion or Golden gateway strategy before being cloned into the binary plant expression vector pB7m34GW (Karimi et al., 2007) (modified with promoter *WEREWOLF* in the first and C-terminal Dendra2 fusion in the third position), pMDC32 (GFP C-fusion with the

original 2X35S promoter or modified *Arabidopsis PHO1* native promoter) (Curtis and Grossniklaus, 2003) and pK7WGR2 (RFP N-fusion with the CaMV 35S promoter) respectively by LR reaction (Invitrogen). The Man1-RFP (Golgi) and VTI12-mCherry (TGN) markers were previously described (Nelson et al., 2007; Geldner et al., 2009). The constructs were introduced into *Agrobacterium tumefaciens* pGV3101 and used for stable transformation in Arabidopsis by floral dipping (Clough and Bent, 1998) or transient expression in *Nicotiana benthamiana* (Arpat et al., 2012).

N. benthamiana infiltration and Pi export assay

Leaves of 4- to 5-week-old *N. benthamiana* plants were used for infiltration with *A. tumefaciens*. An overnight culture of *A. tumefaciens* carrying constructs grown at 28 ^{0}C was pelleted and resuspended in infiltration buffer containing 10 mM $MgCl_2$, 10 mM MES-KOH (pH 5.6), and 150 μM acetosyringone at a final OD = 0.4 to 0.6. The cultures were incubated further for 1-2 h at 28 ^{0}C on a shaker incubator. P19 expressed from a distinct binary vector was used to inhibit the silencing of the transgene. For co-infiltration, the *A. tumefaciens* strain carrying two constructs was mixed in an equal amount along with P19. Two days post-infiltration, leaves were cut randomly into 1-cm-diameter discs and taken either for confocal imaging or soaked in the buffer containing 5 mM glucose, 10 mM MES-KOH (pH 5.6), 1 mM KCl, 0.5 mM $CaCl_2$, 0.5 mM $MgSO_4$, and 0.01% Triton X-100 for Pi and NO_3^- export assay. Pi and NO_3^- released in the buffer were measured by the molybdate assay (Ames, 1996) and NO_3^- reductase assay (Barthes et al., 1995), respectively.

Pi content, ^{33}Pi import and ^{33}Pi root-to-shoot export assay in Arabidopsis

Pi levels in the shoot of soil-grown 4- to 5-week-old Arabidopsis were measured by releasing the cellular Pi content into the water by repeated freezing and thawing. Pi concentration was then quantified by molybdate assay using a standard curve.

To measure the uptake and transfer of ^{33}Pi from root to shoot, 7-day-old seedlings grown on half-strength (½) MS plates were incubated in liquid ½ MS with different concentrations of Pi and ^{33}Pi after the transgene induction by 5 μM estradiol or 0.05% DMSO treatment, ensuring that shoots do not touch the media. After an hour, roots and shoots were separated, washed with ice-cold water and liquid ½ MS (1 mM Pi),

blotted, and weighed before placing them in a scintillation vial with 10% SDS (w/v) for an hour at 55 ^{0}C. Radioactivity in the tissue was measured using Ultima Gold scintillation liquid and the Perkin Elmer tri-carb 2800TF scintillation counter.

Chemical treatment

Five to six-day-old seedlings were transferred to ½ MS plates containing 5 μM estradiol or solvent (0.05% DMSO) for 16-20 h for transgene induction. For FM4-64 uptake experiments, seedlings were incubated in liquid ½ MS medium supplemented with 2 μM FM4-64 dye (Thermo Fisher) for 8 min in the dark and on ice. Excess dye was washed off and the seedlings were mounted in ½ MS medium on microscopy slides at room temperature for imaging and internalization measurement. Propidium iodide (Sigma-Aldrich) was diluted 100 times in ½ MS medium with 1% (w/v) sucrose and roots were stained for 2 min before confocal laser scanning microscopy (CLSM) imaging.

Confocal microscopy and quantification

CLSM images of Arabidopsis roots and *N. benthamiana* leaves for subcellular localization were taken with a Leica Stellaris, a Zeiss LSM700, or a Zeiss LSM880 confocal microscope. FM4-64 internalization was quantified using the ImageJ software. The ratio between the difference of the average cytosolic fluorescence intensity and the mean cytosolic background intensity (background subtracted cytosolic) and the mean plasma membrane intensity was calculated. The average internalization ratio of each line was then normalized against the average internalization ratio of respective controls. Quantification of colocalization was conducted using the Fiji plugin JACoP (Bolte and Cordelières, 2006), in which Mander's coefficient and Pearson correlation coefficient were analyzed. Images were adjusted for color and contrast using ImageJ/Fiji software. Statistical analysis was done in Prism 9 (GraphPad Software, San Diego, CA, USA).

Quantitative RT-PCR

Total RNA from 7-d-old seedlings induced with 5 μM estradiol or DMSO control for 20 h was extracted using ReliaPrep™ RNA Miniprep Systems (Promega) according to

manufacturer's instructions. Two micrograms of RNA was reverse-transcribed using M-MLV Reverse Transcriptase (M3681, Promega) and oligo $d(T)_{15}$ according to the manufacturer's instructions. qRT-PCR was performed using SYBR Select Master Mix (4472908, Applied Biosystems) with primer pairs specific to genes of interest and *EF1A* (At1g07940) used for data normalization. Relative gene expression was calculated with the $2^{-\Delta\Delta CT}$ method (Livak and Schmittgen, 2001). Primer sequences are listed in Supplemental Table S1.

Acknowledgments

The authors are grateful to Dr. Jiri Friml (Institute of Science and Technology Austria) as well as Drs. Daniel van Damme and Eugenia Russinova (VIB Belgium) for sharing clones and materials involved in CME. We also thank the Geldner group (University of Lausanne) for providing clones and advice. This work was supported by a grant from the Swiss National Science Foundation (31003A-182462) to YP.

Author Contributions:

PVV and YP conceived the project and wrote the manuscript, and PVV performed all experiments. YP agrees to serve as the author responsible for contact and ensures communications.

The authors declare no conflict of interest.

References

Adamowski M, Narasimhan M, Kania U, Glanc M, De Jaeger G, Friml J (2018) A functional study of AUXILIN-LIKE1 and 2, two putative clathrin uncoating factors in *Arabidopsis*. Plant Cell **30**: 700–716

Aihara Y, Mashima H, Onda H, Hisano S, Kasuya H, Hori T, Yamada S, Tomura H, Yamada Y, Inoue I, et al (2002) Molecular cloning of a novel brain-type Na+-dependent inorganic phosphate cotransporter. J Neurochem **74**: 2622–2625

Alassimone J, Naseer S, Geldner N (2010) A developmental framework for endodermal differentiation and polarity. Proc Natl Acad Sci USA **107**: 5214–5219

Ames BN (1966) Assay of inorganic phosphate, total phosphate and phosphatases. Methods Enzymol **8**: 115-118.

Aniento F, Sánchez de Medina Hernández V, Dagdas Y, Rojas-Pierce M, Russinova E (2022) Molecular mechanisms of endomembrane trafficking in plants. Plant Cell **34**: 146–173

Arpat AB, Magliano P, Wege S, Rouached H, Stefanovic A, Poirier Y (2012) Functional expression of PHO1 to the Golgi and trans-Golgi network and its role in export of inorganic phosphate. Plant J **71**: 479-491

Aung K, Lin S-I, Wu C-C, Huang Y-T, Su C, Chiou T-J (2006) *pho2*, a phosphate overaccumulator, is caused by a nonsense mutation in a MicroRNA399 target gene. Plant Physiol **141**: 1000–1011

Baisa GA, Mayers JR, Bednarek SY (2013) Budding and braking news about clathrin-mediated endocytosis. Curr Opin Plant Biol **16**: 718–725

Barberon M, Dubeaux G, Kolb C, Isono E, Zelazny E, Vert G (2014) Polarization of IRON-REGULATED TRANSPORTER 1 (IRT1) to the plant-soil interface plays crucial role in metal homeostasis. Proc Natl Acad Sci USA **111**: 8293–8298

Barberon M, Geldner N (2014) Radial transport of nutrients: the plant root as a polarized epithelium. Plant Physiol **166**: 528–537

Barberon M, Zelazny E, Robert S, Conéjéro G, Curie C, Friml J, Vert G (2011) Monoubiquitin-dependent endocytosis of the IRON-REGULATED TRANSPORTER 1 (IRT1) transporter controls iron uptake in plants. Proc Natl Acad Sci USA **108**: E450–E458

Bari R, Datt Pant B, Stitt M, Scheible W-R (2006) PHO2, MicroRNA399, and PHR1 define a phosphate-signaling pathway in plants. Plant Physiol **141**: 988–999

Barthes L, Bousser A, Hoarau J and Deleens E (1995) Reassessment of the relationship between nitrogen supply and xylem exudation in detopped maize seedlings. Plant Physiol Biochem **33**: 173-183

Bashline L, Li S, Anderson CT, Lei L, Gu Y (2013) The endocytosis of cellulose synthase in *Arabidopsis* is dependent on μ2, a clathrin-mediated endocytosis adaptin. Plant Physiol **163**: 150–160

Bashline L, Li S, Zhu X, Gu Y (2015) The TWD40-2 protein and the AP2 complex cooperate in the clathrin-mediated endocytosis of cellulose synthase to regulate cellulose biosynthesis. Proc Natl Acad Sci USA **112**: 12870–12875

Bayle V, Arrighi J-F, Creff A, Nespoulous C, Vialaret J, Rossignol M, Gonzalez E, Paz-Ares J, Nussaume L (2011) *Arabidopsis thaliana* High-Affinity phosphate transporters exhibit multiple levels of posttranslational regulation. Plant Cell **23**: 1523–1535

Bellocchio EE, Reimer RJ, Fremeau RT, Edwards RH (2000) Uptake of glutamate into synaptic vesicles by an inorganic phosphate transporter. Science **289**: 957–960

Bolte S, Cordelières FP (2006) A guided tour into subcellular colocalization analysis in light microscopy. J Microsc **224**: 213–232

Castaings L, Alcon C, Kosuth T, Correia D, Curie C (2021) Manganese triggers phosphorylation-mediated endocytosis of the *Arabidopsis* metal transporter NRAMP1. Plant J **106**: 1328–1337

Chao Z-F, Wang Y-L, Chen Y-Y, Zhang C-Y, Wang P-Y, Song T, Liu C-B, Lv Q-Y, Han M-L, Wang S-S, et al (2021) NPF transporters in synaptic-like vesicles control delivery of iron and copper to seeds. Sci Adv **7**: eabh2450

Chen X, Irani NG, Friml J (2011) Clathrin-mediated endocytosis: the gateway into plant cells. Curr Opin Plant Biol **14**: 674–682

Clough SJ, Bent AF (1998) Floral dip: a simplified method for Agrobacterium-mediated transformation of *Arabidopsis thaliana*. Plant J **16**: 735–743

Collins BM, McCoy AJ, Kent HM, Evans PR, Owen DJ (2002) Molecular architecture and functional model of the endocytic AP2 complex. Cell **109**: 523–535

Cubero B, Nakagawa Y, Jiang XY, Miura KJ, Li F, Raghothama KG, Bressan RA, Hasegawa PM, Pardo JM (2009) The phosphate transporter PHT4;6 Is a determinant of salt tolerance that Is localized to the golgi apparatus of Arabidopsis. Mol Plant **2:** 535-552

Curtis MD, Grossniklaus U (2003) A gateway cloning vector set for high-throughput functional analysis of genes in *planta*. Plant Physiol **133**: 462–469

Delhaize E, Gruber BD, Pittman JK, White RG, Leung H, Miao Y, Jiang L, Ryan PR, Richardson AE (2007) A role for the *AtMTP11* gene of *Arabidopsis* in manganese transport and tolerance. Plant J **51**: 198–210

Dhonukshe P, Aniento F, Hwang I, Robinson DG, Mravec J, Stierhof Y-D, Friml J (2007) Clathrin-mediated constitutive endocytosis of PIN auxin efflux carriers in *Arabidopsis*. Curr Biol **17**: 520–527

Di Rubbo S, Irani NG, Kim SY, Xu Z-Y, Gadeyne A, Dejonghe W, Vanhoutte I, Persiau G, Eeckhout D, Simon S, et al (2013) The clathrin adaptor complex AP-2 mediates endocytosis of BRASSINOSTEROID INSENSITIVE1 in *Arabidopsis*. Plant Cell **25**: 2986–2997

Dissanayaka DMSB, Ghahremani M, Siebers M, Wasaki J, Plaxton WC (2021) Recent insights into the metabolic adaptations of phosphorus-deprived plants. J Exp Bot **72**: 199–223

Dubeaux G, Vert G (2017) Zooming into plant ubiquitin-mediated endocytosis. Curr Opin Plant Biol **40**: 56–62

Fan L, Hao H, Xue Y, Zhang L, Song K, Ding Z, Botella MA, Wang H, Lin J (2013) Dynamic analysis of *Arabidopsis* AP2 σ subunit reveals a key role in clathrin-mediated endocytosis and plant development. Development **140**: 3826–3837

Fuji K, Miwa K, Fujiwara T (2009) The intracellular transport of transporters: membrane trafficking of mineral transporters. Curr Opin Plant Biol **12**: 699–704

Gadeyne A, Sánchez-Rodríguez C, Vanneste S, Di Rubbo S, Zauber H, Vanneste K, Van Leene J, De Winne N, Eeckhout D, Persiau G, et al (2014) The TPLATE adaptor complex drives clathrin-mediated endocytosis in plants. Cell **156**: 691–704

Gaymard F, Pilot G, Lacombe B, Bouchez D, Bruneau D, Boucherez J, Michaux-Ferrière N, Thibaud J-B, Sentenac H (1998) Identification and disruption of a plant shaker-like outward channel involved in K+ release into the xylem sap. Cell **94**: 647–655

Geldner N, Dénervaud-Tendon V, Hyman DL, Mayer U, Stierhof Y-D, Chory J (2009) Rapid, combinatorial analysis of membrane compartments in intact plants with a multicolor marker set. Plant J **59**: 169–178

Giehl RFH, Laginha AM, Duan F, Rentsch D, Yuan L, von Wirén N (2017) A critical role of AMT2;1 in root-to-shoot translocation of ammonium in *Arabidopsis*. Mol Plant **10**: 1449–1460

Grones P, De Meyer A, Pleskot R, Mylle E, Kraus M, Vandorpe M, Yperman K, Eeckhout D, Dragwidge JM, Jiang QH, et al (2022) The endocytic TPLATE complex internalizes ubiquitinated plasma membrane cargo. Nature Plants **8:** 1467-1483

Guo B, Jin Y, Wussler C, Blancaflor EB, Motes CM, Versaw WK (2008) Functional analysis of the Arabidopsis PHT4 family of intracellular phosphate transporters. New Phytol **177:** 889-898

Gutiérrez-Alanís D, Ojeda-Rivera JO, Yong-Villalobos L, Cárdenas-Torres L, Herrera-Estrella L (2018) Adaptation to phosphate scarcity: tips from *Arabidopsis* roots. Trends Plant Sci **23**: 721–730

Hamburger D, Rezzonico E, MacDonald-Comber Petétot J, Somerville C, Poirier Y (2002) Identification and characterization of the arabidopsis PHO1 gene involved in phosphate loading to the xylem. Plant Cell **14**: 889–902

Ivanov R, Vert G (2021) Endocytosis in plants: Peculiarities and roles in the regulated trafficking of plant metal transporters. Biol Cell **113**: 1–13

Jung J-Y, Ried MK, Hothorn M, Poirier Y (2018) Control of plant phosphate homeostasis by inositol pyrophosphates and the SPX domain. Curr Opin Biotechnol **49**: 156–162

Karimi M, Depicker A, Hilson P (2007) Recombinational cloning with plant gateway vectors. Plant Physiol **145**: 1144–1154

Kasai K, Takano J, Miwa K, Toyoda A, Fujiwara T (2011) High boron-induced ubiquitination regulates vacuolar sorting of the BOR1 borate transporter in *Arabidopsis thaliana*. J Biol Chem **286**: 6175–6183

Kim SY, Xu Z-Y, Song K, Kim DH, Kang H, Reichardt I, Sohn EJ, Friml J, Juergens G, Hwang I (2013) Adaptor protein complex 2–mediated endocytosis is crucial for male reproductive organ development in *Arabidopsis*. Plant Cell **25**: 2970–2985

Kitakura S, Vanneste S, Robert S, Löfke C, Teichmann T, Tanaka H, Friml J (2011) Clathrin mediates endocytosis and polar distribution of PIN auxin transporters in *Arabidopsis*. Plant Cell **23**: 1920–1931

Lee MM, Schiefelbein J (1999) WEREWOLF, a MYB-related protein in *Arabidopsis*, is a position-dependent regulator of epidermal cell patterning. Cell **99**: 473–483

Li B, Byrt C, Qiu J, Baumann U, Hrmova M, Evrard A, Johnson AAT, Birnbaum KD, Mayo GM, Jha D, et al (2016) Identification of a stelar-localized transport protein that facilitates root-to-shoot transfer of chloride in *Arabidopsis*. Plant Physiol **170**: 1014–1029

Li RL, Wang JL, Xu L, Sun MH, Yi KK, Zhao HY (2020) Functional analysis of phosphate transporter OsPHT4 family members in rice. Rice Science **27:** 493-503

Li X, Chanroj S, Wu Z, Romanowsky SM, Harper JF, Sze H (2008) A distinct endosomal Ca2+/Mn2+ pump affects root growth through the secretory process. Plant Physiol **147**: 1675–1689

Li X, Wang X, Yang Y, Li R, He Q, Fang X, Luu D-T, Maurel C, Lin J (2011) Single-molecule analysis of PIP2;1 dynamics and partitioning reveals multiple modes of *Arabidopsis* plasma membrane aquaporin regulation. Plant Cell **23**: 3780–3797

Lin S-H, Kuo H-F, Canivenc G, Lin C-S, Lepetit M, Hsu P-K, Tillard P, Lin H-L, Wang Y-Y, Tsai C-B, et al (2008) Mutation of the *Arabidopsis NRT1.5* nitrate transporter causes defective root-to-shoot nitrate transport. Plant Cell **20**: 2514–2528

Lin W-Y, Huang T-K, Chiou T-J (2013) NITROGEN LIMITATION ADAPTATION, a target of MicroRNA827, mediates degradation of plasma membrane–localized phosphate transporters to maintain phosphate homeostasis in *Arabidopsis*. Plant Cell **25**: 4061–4074

Liu S-H, Wong ML, Craik CS, Brodsky FM (1995) Regulation of clathrin assembly and trimerization defined using recombinant triskelion hubs. Cell **83**: 257–267

Liu T-Y, Huang T-K, Tseng C-Y, Lai Y-S, Lin S-I, Lin W-Y, Chen J-W, Chiou T-J (2012) PHO2-dependent degradation of PHO1 modulates phosphate homeostasis in *Arabidopsis*. Plant Cell **24**: 2168–2183

Livak KJ, Schmittgen TD (2001) Analysis of relative gene expression data using real-time quantitative PCR and the $2^{-\Delta\Delta CT}$ method. Methods **25**: 402–408

Ma B, Zhang L, Gao Q, Wang J, Li X, Wang H, Liu Y, Lin H, Liu J, Wang X, et al (2021) A plasma membrane transporter coordinates phosphate reallocation and grain filling in cereals. Nat Genet **53**: 906–915

Ma JF, Yamaji N, Mitani N, Tamai K, Konishi S, Fujiwara T, Katsuhara M, Yano M (2007) An efflux transporter of silicon in rice. Nature **448**: 209–212

Martín Y, Navarro FJ, Siverio JM (2008) Functional characterization of the *Arabidopsis thaliana* nitrate transporter CHL1 in the yeast Hansenula polymorpha. Plant Mol Biol **68**: 215–224

McMahon HT, Boucrot E (2011) Molecular mechanism and physiological functions of clathrin-mediated endocytosis. Nat Rev Mol Cell Biol **12**: 517–533

Nelson BK, Cai X, Nebenführ A (2007) A multicolored set of *in vivo* organelle markers for co-localization studies in *Arabidopsis* and other plants. Plant J **51**: 1126–1136

Nguyen NNT, Clua J, Vetal PV, Vuarambon DJ, De Bellis D, Pervent M, Lepetit M, Udvardi M, Valentine AJ, Poirier Y (2020) PHO1 family members transport phosphate from infected nodule cells to bacteroids in *Medicago truncatula*. Plant Physiol **185:** 196-209

Ni B, Rosteck PR, Nadi NS, Paul SM (1994) Cloning and expression of a cDNA encoding a brain-specific Na(+)-dependent inorganic phosphate cotransporter. Proc Natl Acad Sci USA **91**: 5607–5611

Nussaume L, Kanno S, Javot H, Marin E, Pochon N, Ayadi A, Nakanishi TM, Thibaud MC (2011) Phosphate import in plants: focus on the PHT1 transporters. Front Plant Sci **2**: 83

Paez Valencia J, Goodman K, Otegui MS (2016) Endocytosis and endosomal trafficking in plants. Annu Rev Plant Biol **67**: 309–335

Peiter E, Montanini B, Gobert A, Pedas P, Husted S, Maathuis FJM, Blaudez D, Chalot M, Sanders D (2007) A secretory pathway-localized cation diffusion facilitator confers plant manganese tolerance. Proc Natl Acad Sci USA **104**: 8532–8537

Poirier Y, Jaskolowski A, Clúa J (2022) Phosphate acquisition and metabolism in plants. Curr Biol **32**: R623–R629

Poirier Y, Thoma S, Somerville C, Schiefelbein J (1991) A mutant of arabidopsis deficient in xylem loading of phosphate. Plant Physiol **97**: 1087-1093

Prak S, Hem S, Boudet J, Viennois G, Sommerer N, Rossignol M, Maurel C, Santoni V (2008) Multiple phosphorylations in the C-terminal tail of plant plasma membrane aquaporins: role in subcellular trafficking of *At*PIP2;1 in response to salt stress. Mol Cellular Proteomics **7**: 1019–1030

Preobraschenski J, Cheret C, Ganzella M, Zander JF, Richter K, Schenck S, Jahn R, Ahnert-Hilger G (2018) Dual and direction-selective mechanisms of

phosphate transport by the vesicular glutamate transporter. Cell Reports **23**: 535–545

Robert S, Kleine-Vehn J, Barbez E, Sauer M, Paciorek T, Baster P, Vanneste S, Zhang J, Simon S, Čovanová M, et al (2010) ABP1 mediates auxin inhibition of clathrin-dependent endocytosis in *Arabidopsis*. Cell **143**: 111–121

Rodriguez-Furlan C, Minina EA, Hicks GR (2019) Remove, recycle, degrade: regulating plasma membrane protein accumulation. Plant Cell **31**: 2833–2854

Shin L-J, Lo J-C, Chen G-H, Callis J, Fu H, Yeh K-C (2013) IRT1 DEGRADATION FACTOR1, a RING E3 ubiquitin ligase, regulates the degradation of IRON-REGULATED TRANSPORTER1 in *Arabidopsis*. Plant Cell **25**: 3039–3051

Siligato R, Wang X, Yadav SR, Lehesranta S, Ma G, Ursache R, Sevilem I, Zhang J, Gorte M, Prasad K, et al (2016) MultiSite gateway-compatible cell type-specific gene-inducible system for plants. Plant Physiol **170**: 627–641

Stefanovic A, Arpat AB, Bligny R, Gout E, Vidoudez C, Bensimon M, Poirier Y (2011) Over-expression of PHO1 in Arabidopsis leaves reveals its role in mediating phosphate efflux. Plant J **66**: 689–699

Stefanovic A, Ribot C, Rouached H, Wang Y, Chong J, Belbahri L, Delessert S, Poirier Y (2007) Members of the PHO1 gene family show limited functional redundancy in phosphate transfer to the shoot, and are regulated by phosphate deficiency via distinct pathways. Plant J **50**: 982–994

Takano J, Miwa K, Yuan L, von Wiren N, Fujiwara T (2005) Endocytosis and degradation of BOR1, a boron transporter of *Arabidopsis thaliana*, regulated by boron availability. Proc Natl Acad Sci USA **102**: 12276–12281

Takano J, Noguchi K, Yasumori M, Kobayashi M, Gajdos Z, Miwa K, Hayashi H, Yoneyama T, Fujiwara T (2002) *Arabidopsis* boron transporter for xylem loading. Nature **420**: 337–340

Takano J, Tanaka M, Toyoda A, Miwa K, Kasai K, Fuji K, Onouchi H, Naito S, Fujiwara T (2010) Polar localization and degradation of *Arabidopsis* boron transporters through distinct trafficking pathways. Proc Natl Acad Sci USA **107**: 5220–5225

Van Damme D, Coutuer S, De Rycke R, Bouget F-Y, Inzé D, Geelen D (2007) Somatic cytokinesis and pollen maturation in *Arabidopsis* depend on TPLATE, which has domains similar to coat proteins. Plant Cell **18**: 3502–3518

Vogiatzaki E, Baroux C, Jung J-Y, Poirier Y (2017) PHO1 exports phosphate from the chalazal seed coat to the embryo in developing *Arabidopsis* seeds. Curr Biol **27**: 2893-2900

Wang Q, Zhao Y, Luo W, Li R, He Q, Fang X, Michele RD, Ast C, von Wirén N, Lin J (2013) Single-particle analysis reveals shutoff control of the *Arabidopsis* ammonium transporter AMT1;3 by clustering and internalization. Proc Natl Acad Sci USA **110**: 13204–13209

Wang Y, Secco D, Poirier Y (2008) Characterization of the *PHO1* gene family and the responses to phosphate deficiency of *Physcomitrella patens*. Plant Physiol **146**: 646–656

Wege S, Khan GA, Jung J-Y, Vogiatzaki E, Pradervand S, Aller I, Meyer AJ, Poirier Y (2016) The EXS domain of PHO1 participates in the response of shoots to phosphate deficiency via a root-to-shoot signal. Plant Physiol **170**: 385–400

Wild R, Gerasimaite R, Jung J-Y, Truffault V, Pavlovic I, Schmidt A, Saiardi A, Jessen HJ, Poirier Y, Hothorn M, et al (2016) Control of eukaryotic phosphate homeostasis by inositol polyphosphate sensor domains. Science **352**: 986–990

Yamaoka S, Shimono Y, Shirakawa M, Fukao Y, Kawase T, Hatsugai N, Tamura K, Shimada T, Hara-Nishimura I (2013) Identification and dynamics of *Arabidopsis* adaptor protein-2 complex and its involvement in floral organ development. Plant Cell **25**: 2958–2969

Yoshinari A, Hosokawa T, Amano T, Beier MP, Kunieda T, Shimada T, Hara-Nishimura I, Naito S, Takano J (2019) Polar localization of the borate exporter BOR1 requires AP2-dependent endocytosis. Plant Physiol **179**: 1569–1580

Zelazny E, Vert G (2014) Plant nutrition: Root transporters on the move. Plant Physiol **166**: 500–508

Zhang Z, Liao H, Lucas WJ (2014) Molecular mechanisms underlying phosphate sensing, signaling, and adaptation in plants. J Integr Plant Biol **56**: 192–220

Zhou F, Emonet A, Dénervaud Tendon V, Marhavy P, Wu D, Lahaye T, Geldner N (2020) Co-incidence of damage and microbial patterns controls localized immune responses in roots. Cell **180**: 440-453

Supplemental Figures

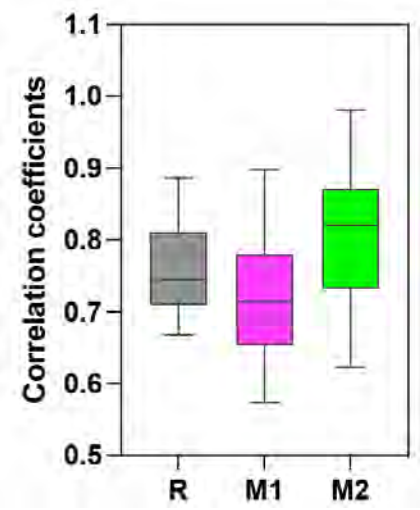

Figure S1. Correlation coefficients between PHO1-GFP and RFP-AUXILIN LIKE 2 expressed in *N. benthamiana* epidermal cells. R, Pearson's correlation coefficient. Mander's coefficient test was used for the fraction of RFP-AUXILIN- LIKE 2 in PHO1-GFP (M1) and the fraction of PHO1-GFP in RFP-AUXILIN-LIKE 2 (M2). *n* = 14 cells.

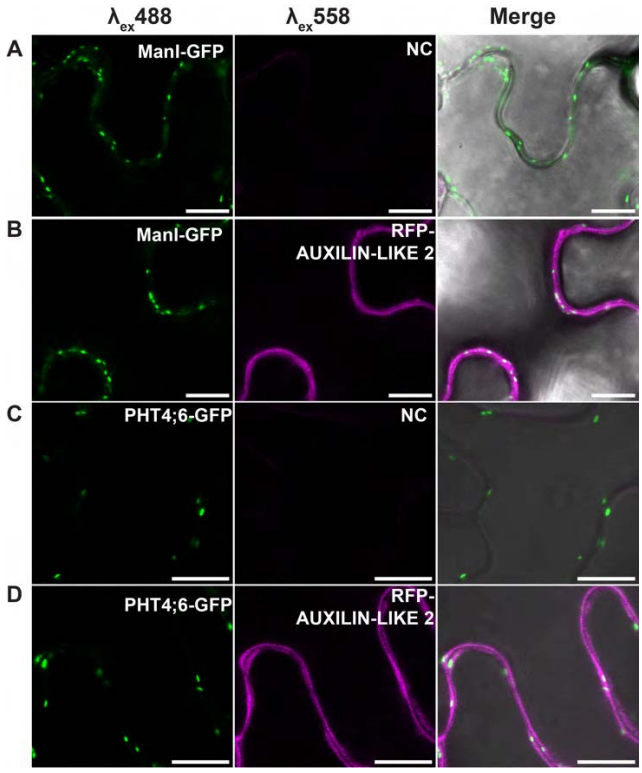

Figure S2. Localization of the Golgi proteins MAN1 and PHT4;6 is not modified by AUXILIN-LIKE2 overexpression. Subcellular localization of MAN1-GFP (A,B) or PHT4;6-GFP (C,D) in *N. benthamiana* epidermal cells in the absence (NC) and

presence of RFP-AUXILIN-LIKE 2. Third panel shows the merge of images from bright field image, panel 1 and 2. Scale bars, 10 µm.

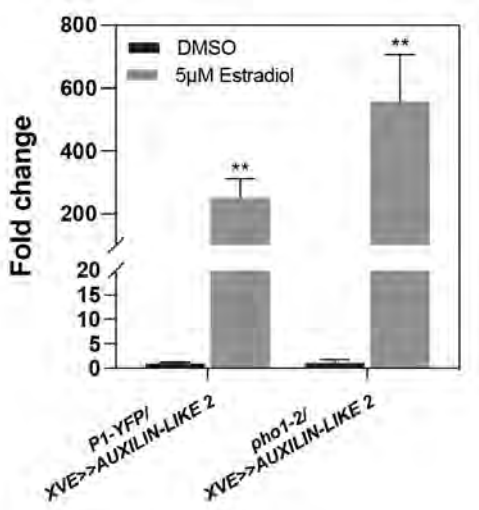

Figure S3. Quantitative RT-PCR of *AUXILIN-LIKE 2*. RT-qPCR to check the expression of *AUXILIN-LIKE 2* in the *XVE>>AUXILIN-LIKE 2* line following induction with estradiol (5 µM) or mock control (DMSO). Data significantly different from the corresponding DMSO controls are indicated (*n = 3*, DMSO versus estradiol treatment, **P <0.01; Student's t test).

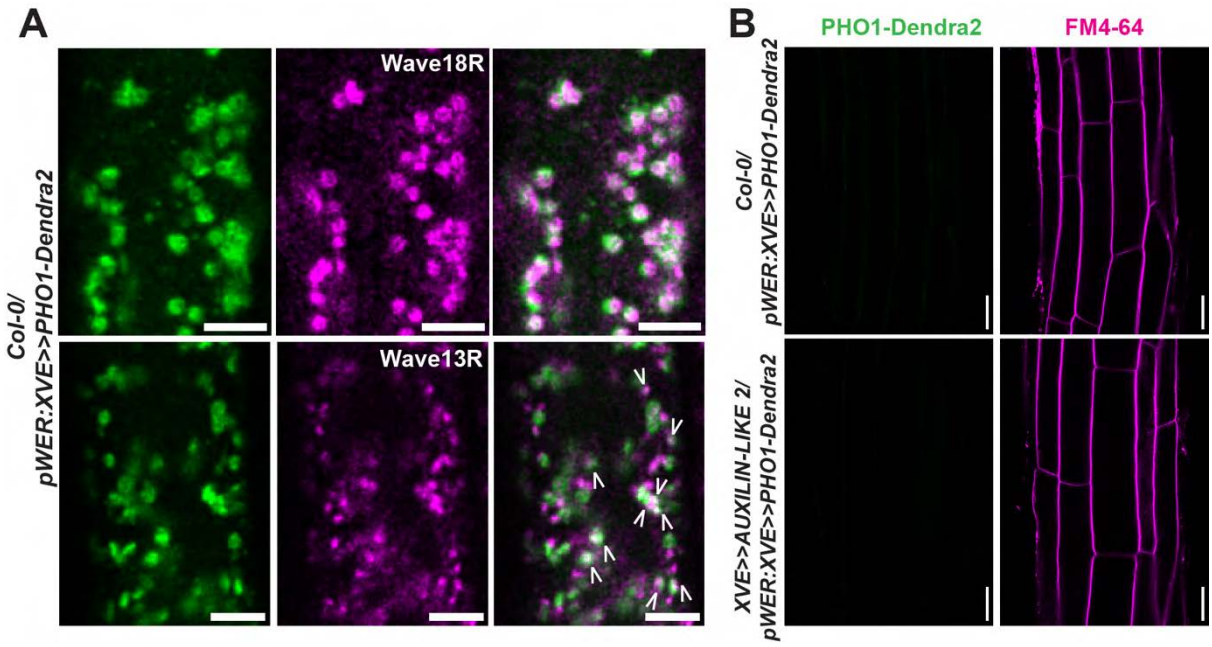

Figure S4. PHO1 localizes to Golgi and TGN in the epidermal cells of Arabidopsis roots. (A) Subcellular co-localization of PHO1-Dendra2 with Golgi (Got1p-mCherry; Wave18R) and TGN (VTI12-mCherry; Wave13R) markers. White arrows indicate the partial co-localization of PHO1 with the TGN marker. Scale bar, 5 µm. (B) Confocal

image showing the absence of PHO1-Dendra2 expression in the epidermis of Col-0 and *XVE>>AUXILIN-LIKE 2* lines transformed with *pWER>>XVE::PHO1-Dendra2* transgene upon mock (DMSO) treatment in roots of *A. thaliana*. Bright field images with FM4-64 staining help to visualize cell boundaries. Scale bars, 20 µm.

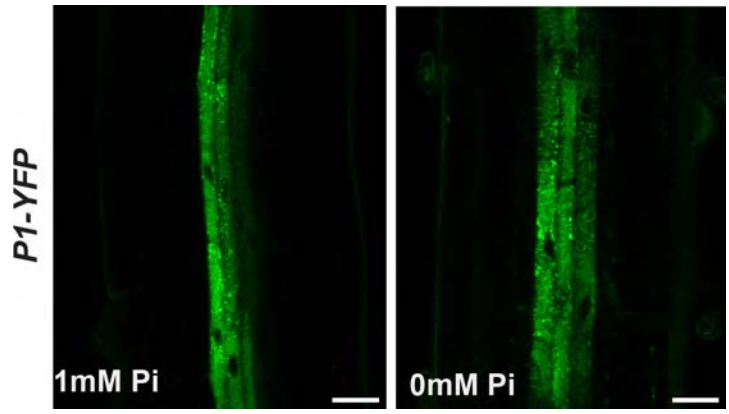

Figure S5. Over-expression of *AUXILIN-LIKE 2* stabilizes the PHO1 homolog PHO1;H1 at the PM. The subcellular localization of PHO1;H1-GFP under the control of *PHO1* promoter with mock and estradiol treatment. Scale bar, 10 µm.

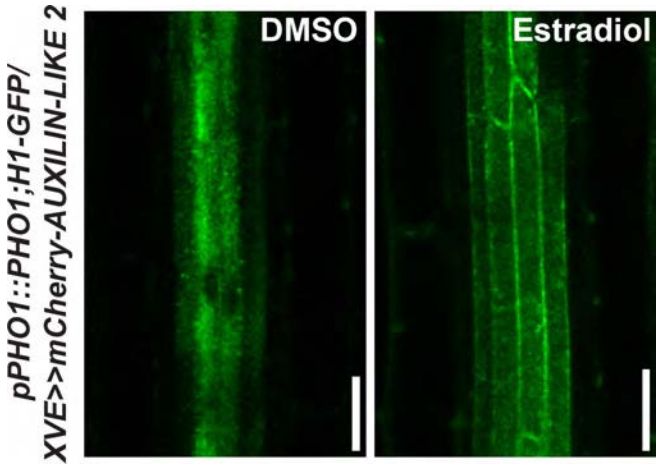

Figure S6. Subcellular localization of PHO1-YFP in roots grown under Pi-sufficient and Pi- deficient conditions. PHO1-YFP in the Arabidopsis roots of 5-day old *P1-YFP* transgenic seedlings under +Pi (1 mM) and - Pi (0 mM) conditions. Scale bar, 20 µm.

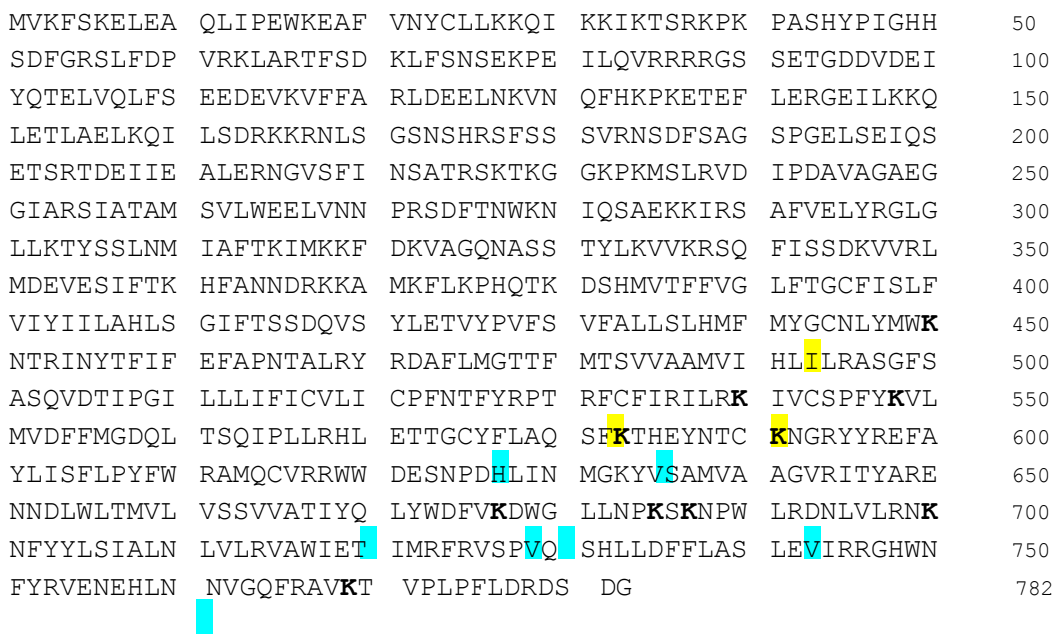

Figure S7. Arabidopsis PHO1 protein sequence highlighting mutated lysine residues. Bold letters indicate the lysine residues that were mutated (at potential ubiquitination sites). Putative residues in TM and EXS regions are highlighted in yellow and cyan respectively.

Supplemental Table S1. List of primers used in this study.

No	Primer name	Sequence (5'→3')	Purpose
1	PHO1_SPX FP PHO1_SPX RP	TTACGTCTCACATTATGGTGAAGTTCTCGAAGGA TAACGTCTCTCTTATCAGAGCTGATAAATTGCGATC	The cloning of synthesized *PHO1 4TM K→R* and *EXS K→R* mutations
2	PHO1_TM FP PHO1_TM RP	TTACGTCTCATAAGGTAAAATAAAAGGAGGTCTTATG TAACGTCTCTTGAAGTTGCATAACTTAGTTTTAC	
3	PHO1_EXS FP PHO1_EXS RP	TTACGTCTCATTCAATAGATGGTGACGACATCTAATT TAACGTCTCTTCATTGAACCAGATCCACCTC	
4	PHO1;H1_FP/ pENTR2B PHO1;H1_RP/ pENTR2B	CCGGTACCGAATTCGATGGTCAAGTTCACAAAGCAATTC ATATCTCGAGTGCGGGTCTTCTTCATCCACTTCTCTGAAAG	Cloning of *PHO1;H1*
5	AUXILIN-LIKE2_FP/ p2rp3 AUXILIN-LIKE2_RP/ p2rp3	GGGGACAGCTTTCTTGTACAAAGTGGTTATGGATGATTTCACAGGATTG GGGGACAACTTTGTATAATAAAGTTGTTCAAAAGAGTTCCTCTGAGTTG	Cloning of *AUXILIN-LIKE2*
6	C-Hub1_FP/ pENTR2B C-Hub1_RP/ pENTR2B	CCGGTACCGAATTCGAAGAAGTTTAACTTAAATGTTCAGGC ATATCTCGAGTGCGGTTAGTAGCCGCCCATCGGTGG	Cloning of *C-HUB1*
7	pPHO1_attB4 F pPHO1_attB1r R	GGGGACAACTTTGTATAGAAAAGTTGTTTCAGTTTTAGCCTCTATTATTCCTAT GGGGACTGCTTTTTTGTACAAACTTGTCCGTTTTGATTAATTGCTAATAGTG	Promoter *PHO1* cloning
8	pho1-2_snp_F pho1-2_snp_R	GGCAGCTCGTTGAATATGATAGC GACCTCCTTTTATTTTACCTTATCAGAGCTGATCAATT	*pho1-2* mutant genotyping
9	pho2_F pho2_R	GACCACCACGATGGTCAACATACC GCAGAAAGAGTCAGAACTAACTCGG	*pho2* mutant genotyping
10	SALK_083693 LP SALK_083693 RP	GCACAAAGAAAAGTCAGTGGC GCAATGCTAATGTTGCTTGTG	*ap2m* mutant genotyping
11	AUXILIN-LIKE2_FP AUXILIN-LIKE2_RP	AACAATTTGGGGAAGAAAGAGAGTG TGGATCAGTGAACCCTCCTGT	RT-qPCR analysis
12	AP2M_FP AP2M_RP	CGATTGCTTGGTTTGGAAGATAAG AGACCAGATGCTGTGAACATTG	RT-qPCR analysis
13	EF1A_FP EF1A_RP	TGCTGTTGTAACAAGATGGATGCC GGGTTGTATCCGACCTTCTTCAGG	RT-qPCR analysis

Chapter 2

Chapter 2

Deciphering potential post-translational modifications required for PM localization of PHO1 by site-directed mutagenesis

Aim

Several studies have shown how membrane proteins, like ion transporters, undergo regulation at various trafficking steps and get post-translationally modified to maintain ion homeostasis at the cellular level during stress conditions. These post-translational modifications include phosphorylation (serine, threonine, and tyrosine residue) and ubiquitination (lysine), mostly on exposed cytosolic C-terminal protein region (Prak et al., 2008; Barberon et al., 2011; Martins et al., 2015). Moreover, adaptor protein-mediated (AP2) recognition of dileucine-based (DE)xxx (LLI) or DxxLL or tyrosine-based Yxxϕ or NPxY signal motifs for internalization is also known to be responsible for sorting and/or trafficking of membrane-localized proteins to and from the PM (Diril et al., 2009; Takano et al., 2010). Our results from the previous chapter demonstrate that PHO1 is localized at the PM. However, the mechanism that controls this localization is still unknown. Due to the increasing reports suggesting the role of post-translational mechanisms to control the localization of membrane proteins, in this chapter, we investigated the potential role of these modifications on PHO1 localization.

We employed site-directed mutagenesis (SDM) to mutate putative cytosolic residues or signal motifs in 4TM and EXS domains of PHO1 to their mimic and non-mimic residues. We chose 4TM and EXS domains, because according to Wege et al., 2016, only 4TMEXS truncation of PHO1 could export Pi and localize properly to Golgi/TGN when transiently expressed in *N. benthamiana* highlighting their importance in the Pi export function and the localization of PHO1. From the previous results, we already know that the ubiquitination of the putative lysine residues in the 4TMEXS region of PHO1 does not control its localization. Thus, here, we mainly discuss the role of phosphorylation as a signal that might control PHO1 trafficking in Arabidopsis. We used a transient expression system in *N. benthamiana* to have a primary indication of the functionality of different mutations generated in PHO1. It is a valuable system for this study, since the expression of Arabidopsis *PHO1* in *N. benthamiana* mediates

specific Pi export, making *N. benthamiana* an appropriate system for PHO1 localization study (Arpat et al., 2012).

Material and methods

Plant materials and growth conditions

The *pho1-3* allele as a *pho1* knockout mutant (Hamburger, 2002) and *Arabidopsis thaliana* transgenic lines used in this study are all in Col-0 background. Seeds were surface sterilized by chlorine gas method and transferred to the square plates containing ½ Murashige and Skoog's (MS) media, 1% (w/v) sucrose, and 0.8% (w/v) agar in continuous light for 6 days and used for confocal microscopy or transferred to soil in long-day conditions (16 h of light and 8 h of dark at 20^{o}C) for 25 days for phenotypic analysis and/or quantification of shoot Pi content. The floral dip method was used for stable Arabidopsis transformation of mutated PHO1 constructs in *pho1-3* background (Clough and Bent, 1998).

Generation of constructs

Mutations in 4TM and EXS regions of the *cPHO1* constructs were synthesized from *GeneScript*. Wild-type (WT), chimeric, or mutated PHOs from Arabidopsis were first cloned in pENTR2B (Invitrogen) entry vector either by infusion or Golden gateway strategy and then transferred into the suitable binary plant expression vectors, like pMDC32 (with original 2X35S promoter or modified Arabidopsis *PHO1* native promoter) by LR reactions (Curtis and Grossniklaus, 2003; Engler et al., 2008).

N. benthamiana infiltration and Pi export assay

The leaves of 4 to 5-week-old *N. benthamiana* plants were used for infiltration. An overnight culture of *A. tumefaciens* carrying constructs grown at 28 ^{o}C was pelleted and resuspended in infiltration buffer containing 10 mM $MgCl_2$, 10 mM MES-KOH (pH 5.6), and 150 μM acetosyringone to OD = 0.4 to 0.6. The cultures were incubated further for 1-2 h at 28 ^{o}C on a shaker incubator. P19 was used to inhibit the silencing of the transgene. For co-infiltration, the *Agrobacterium* strain carrying two constructs was mixed in an equal amount along with P19. Two days post infiltration, leaves were cut randomly into 1-cm-diameter discs and taken either for confocal imaging or soaked

in the buffer containing 5 mM glucose, 10 mM MES-KOH (pH 5.6), 1 mM KCl, 0.5 mM $CaCl_2$, 0.5 mM $MgSO_4$, and 0.01% Triton X-100 for Pi and nitrate export assay. Pi released in the buffer was measured by the molybdate assay (Ames, 1996).

Phosphate content assay

Pi levels in the shoot of soil grown 4 to 5-week-old soil grown Arabidopsis plants were measured by releasing the cellular Pi content into the water by repeated freeze and thaw method. Pi concentration was then quantified by molybdate assay using a standard curve.

Confocal microscopy

CLSM images of Arabidopsis roots and *N. benthamiana* leaves for subcellular localization of GFP and OFP fusion proteins were taken with a Leica Stellaris, a Zeiss LSM700, or a Zeiss LSM880 confocal microscope.

Results

Chimeric PHO1-GFP complements the *pho1* mutant.

It has been observed for PHO1 as well as for several of its homologs that attempts to clone full-length cDNA directly into *E. coli* using plasmids consistently resulted in the recovery of aberrant clones having *E. coli* transposon inserted into the gene, resulting in the truncation of the open-reading frame (unpublished results). Since the cDNA of PHO1 is unclonable in *E. coli*, we generated a chimeric *PHO1-GFP* fusion (*cPHO1-GFP*) construct, which comprised only exons in the SPX domain and both exons and introns in the 4TM-EXS domains (Figure 8A). cPHO1-GFP co-localized with the Golgi marker and exported Pi in the external medium when transiently co-expressed in *N. benthamiana* (Figure 8B-C). To check if *cPHO1-GFP* is functional, several transgenic lines were generated under *PHO1* native promoter in the *pho1-3* mutant background. Analysis of transgenic plants (referred to as $cPHO1_{compl}$) showed that *cPHO1-GFP* was able to complement the *pho1-3* mutant phenotype with levels of Pi export comparable to WT PHO1 complemented *pho1-3* mutant line (*P1-GFP*) (Figure 8D-E). Confocal analysis of $cPHO1_{compl}$ showed punctate-like structures indicative of

Golgi/TGN localization in the Arabidopsis root vasculature (Figure 8F). This construct was used further to generate mutations.

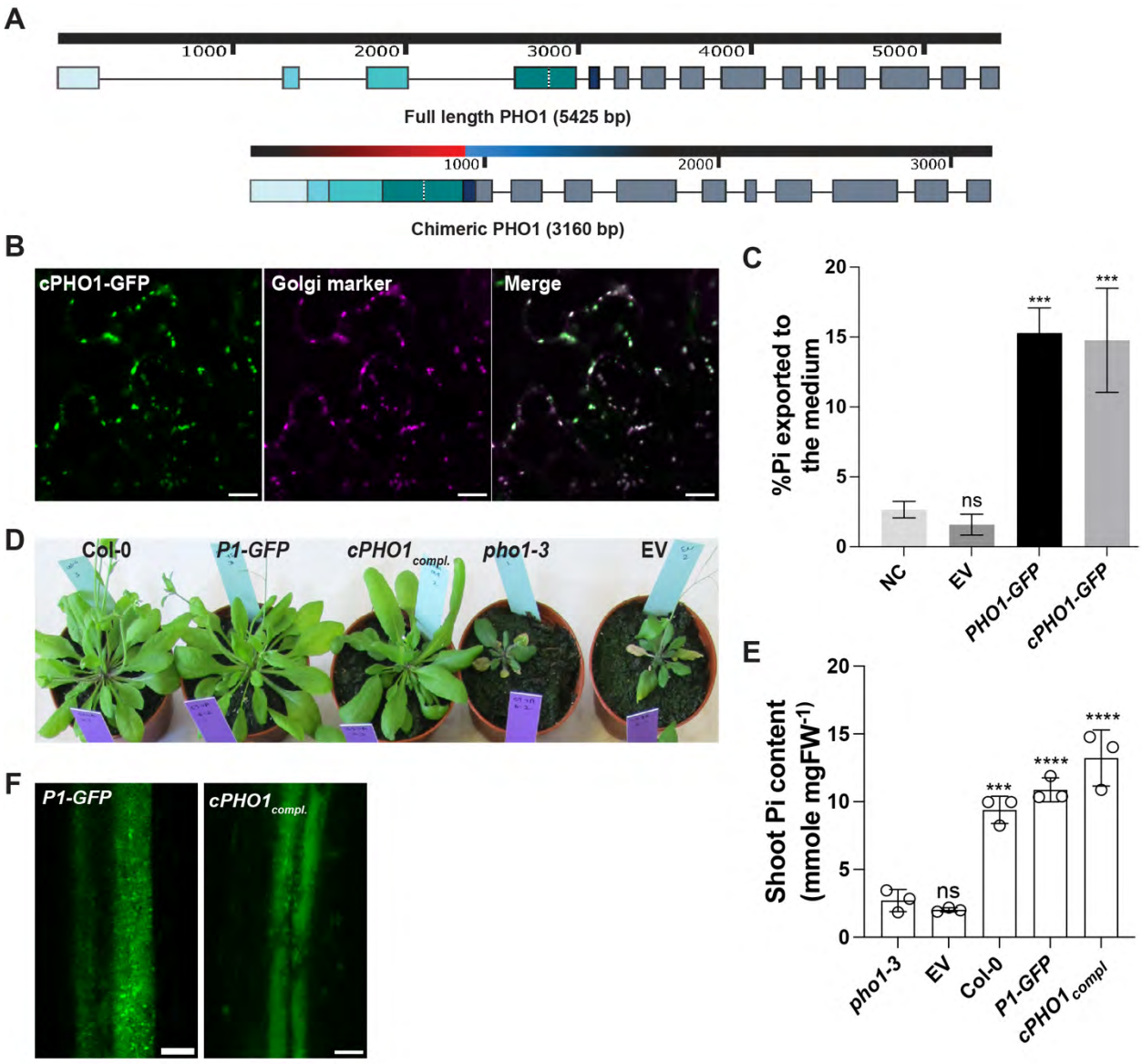

Figure 8. Chimeric *PHO1* construct is functional in *N. benthamiana* and Arabidopsis. (A) Schematic representation of WT genomic *PHO1* and synthesized *cPHO1* without introns in the SPX domain. (B) Co-localization of GFP fluorescence from the expression of cPHO1-GFP with Golgi marker ManI-mCherry to punctate structures when transiently expressed in *N. benthamiana.* (C) Export of Pi from *N. benthamiana* leaves infiltrated with *cPHO1-GFP*, *PHO1-GFP* and EV constructs compared to NC (non-infiltrated control leaf) after 5h. (D) Phenotypic comparison of 3-week-old plants from *pho1-3* mutant stably transformed with cPHO1-GFP *($cPHO1_{compl}$)* with full-length PHO1-GFP complemented *pho1-3 (P1-GFP)*, Col-0, *pho1-3* mutant and empty vector line (EV; *pho1-2* transformed with *pPHO1: ccdb: pMDC32*). (E) Total shoot Pi content of genotypes mentioned in (D) compared with *pho1-3* mutant. (F) Subcellular localization of WT PHO1 and cPHO1-GFP in the root vasculature of *A. thaliana.* Error bars represent SD (*n* = *3*). Asterisks represent

statistically significant differences compared with *pho1-3* (B) and non-infiltrated control (C) (ANOVA; ****P < 0.0001; ***P < 0.001). Scale, 10 μm.

Extensive mutagenesis in 4TM and EXS domains disrupts PHO1 protein function

We generated 11 constructs of PHO1-GFP fusion, where 5 contain mutations in the 4TM domain and 6 in the EXS domain in the *cPHO1* backbone (Figure 9A). The number of residues mutated in each domain is shown in Figure 9B. We selected all the putative amino acids predicted to be on the cytosolic region of the 4TM and EXS domains of PHO1 for mutagenesis. The mutations include cytosolic serine (S) and threonine (T) to alanine (A; non-phosphomimic) and aspartate (D; phosphomimic), tyrosine (Y) to glutamate (E; phosphomimic) and phenylalanine (F; non-phosphomimic), lysine (K) to arginine (R) and dileucines (LL) to alanine (AA). Mutated genes were cloned under a CaMV 35S and native *PHO1* promoter for transient expression in *N. benthamiana* and stable transgenic line generation in the *pho1-3* mutant background, respectively. In Arabidopsis, out of all the mutations, only *cTM ST→A* and *cTM Y→F* mutants could partially complement *pho1-3* mutant phenotype (Figure 10A) and localize in the vasculature with slight increase in the shoot Pi content compared to *pho1-3* mutant (Figure 10B-D). None of the *cEXS* mutants could functionally complement the *pho1* mutant. Mutants *cTM Y→E* and *cTM Y→F* showed punctate like-structures but could not export Pi in the medium when transiently expressed in the epidermal cells of *N. benthamiana* (Figures 11A-B). *cTM ST→A* mutant was found to be localized in ER and Golgi-like structures with less Pi export in the medium (Figure 11A-B). *cEXS* mutants neither localized to punctate structures nor exported Pi in transient assays (Figure 11C-D).

A

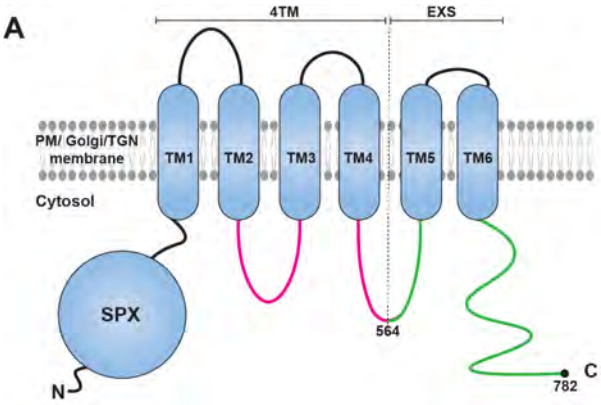

B

TM Mutants	No. of residues mutated	EXS Mutants	No. of residues mutated
TM ST→A	7	EXS ST→A	18
TM ST→D	7	EXS ST→D	18
TM Y→E	5	EXS Y→E	8
TM Y→F	5	EXS Y→F	8
TM K→R	3	EXS LL→AA	3
		EXS K→R	7

Figure 9. Schematic of PHO1 domains and mutations. (A) Schematic of PHO1 showing cytosolic region of 4TM (in Magenta) and EXS (in Green) domains selected for generating mutations. (B) Number of mutations generated in the cytosolic region of 4TM and EXS domain of *cPHO1*.

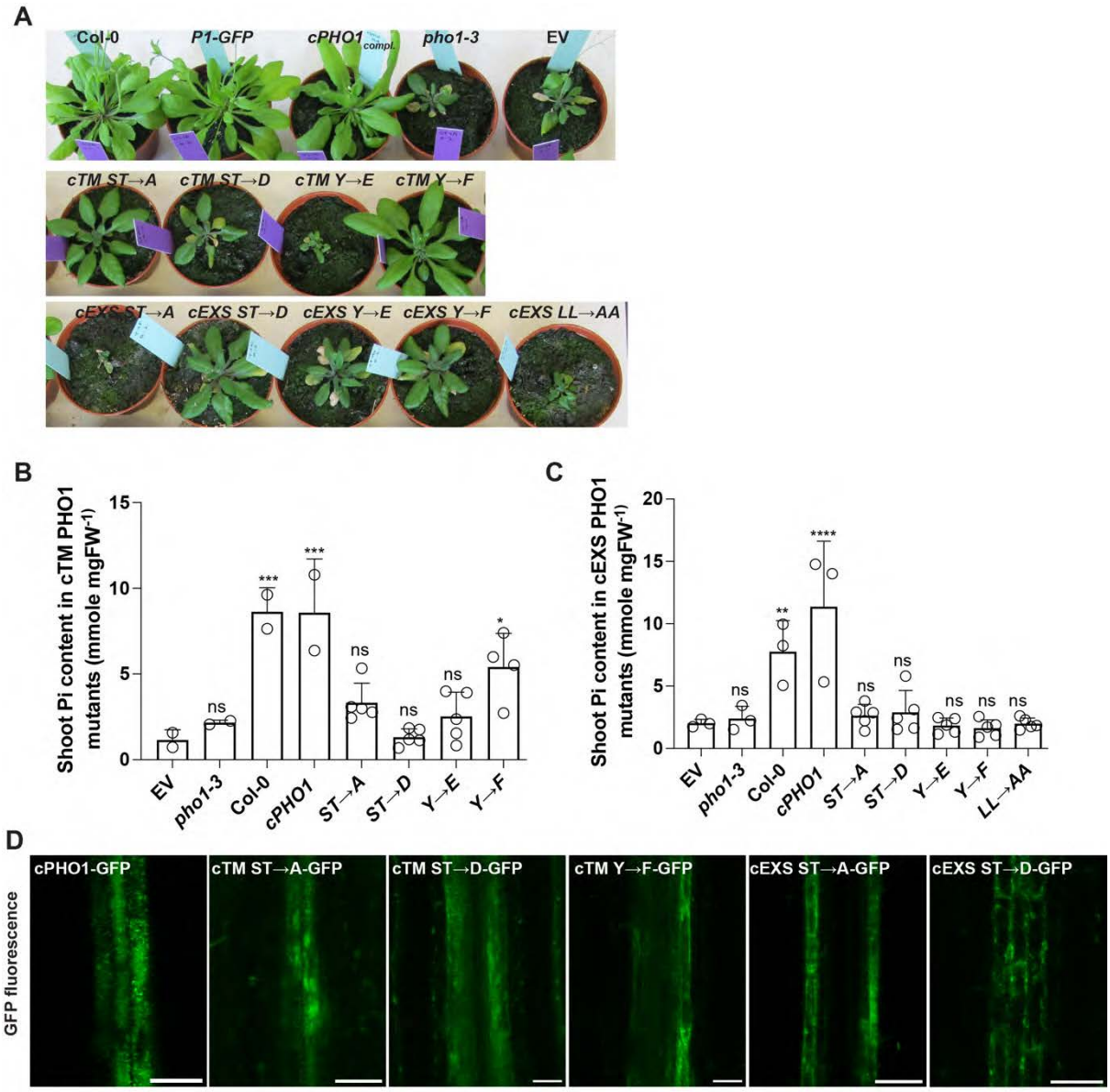

Figure 10. Mutations in 4TM and EXS domains of PHO1 do not complement *pho1-3* mutant. (A) Phenotypic analysis of *pho1-3* stably transformed with mutated *cTM* and *cEXS* constructs compared to Col-0, *P1-GFP, cPHO1*$_{compl}$, *pho1-3* and empty vector (EV) line. Shoot Pi content of 3-week-old *cTM* mutants (B) and *cEXS* (C) mutants and other lines compared with EV. (C) Localization of cTM and cEXS PHO1-GFP mutants in the root vasculature. Error bars represent SD (*n = 2-5*). For all histograms, columns with asterisks are significantly different from EV (ANOVA; ****P < 0.0001; ***P < 0.001; **P <0.01; *P <0.05). Scale, 20 μm.

The effect of serine, threonine, and tyrosine mutations in three EXS sub-fragments of PHO1

From this point, we focused on the role of phosphorylation on the EXS domain because the EXS domain alone could stabilize at the PM after CME inhibition (see Chapter 1; page 54). To reduce the mutational load, we divided the EXS domain into three fragments (EXS1, EXS2, and EXS3), since extensive mutations in the EXS domain could not functionally complement the *pho1-3* mutant. Moreover, all the mutations mentioned hereafter are done in genomic *PHO1* background to eliminate the introduction of possible mutations in the coding region of PHO1. In the EXS1 domain, all the cytosolic S, T were mutated to A (non-phosphomimic), whereas Y were mutated to E (phosphomimic) and F (non-phosphomimic) starting from residue 564 to 614 (Figure 12A and Figure 13A). Similar mutations were generated in the EXS2 domain from residue 615 to 707, and the EXS3 domain spanning from 708 to 782 (Figure 12A and Figure 13A). Their subcellular localization and Pi export were studied by transient expression in *N. benthamiana* and stable transformation in Arabidopsis *pho1-3* mutant. GFP fusions of all three fragments with *EXS ST→ A* mutations (non-phosphomimic) showed localization to Golgi-like structures and exported Pi compared to non-infiltrated control in *N. benthamiana* except for EXS2 fragment which exported less Pi compared to WT (Figure 12B-C). Similarly, in Arabidopsis, these mutants could complement the *pho1-3* mutant phenotype and exported Pi to the shoot (Figure 12D-E). EXS2 fragment mutant showed slightly reduced Pi export activity similar to when transiently expressed in *N. benthamiana*. Since the mutations in S and T did not affect the PHO1 localization, we did not pursue them further.

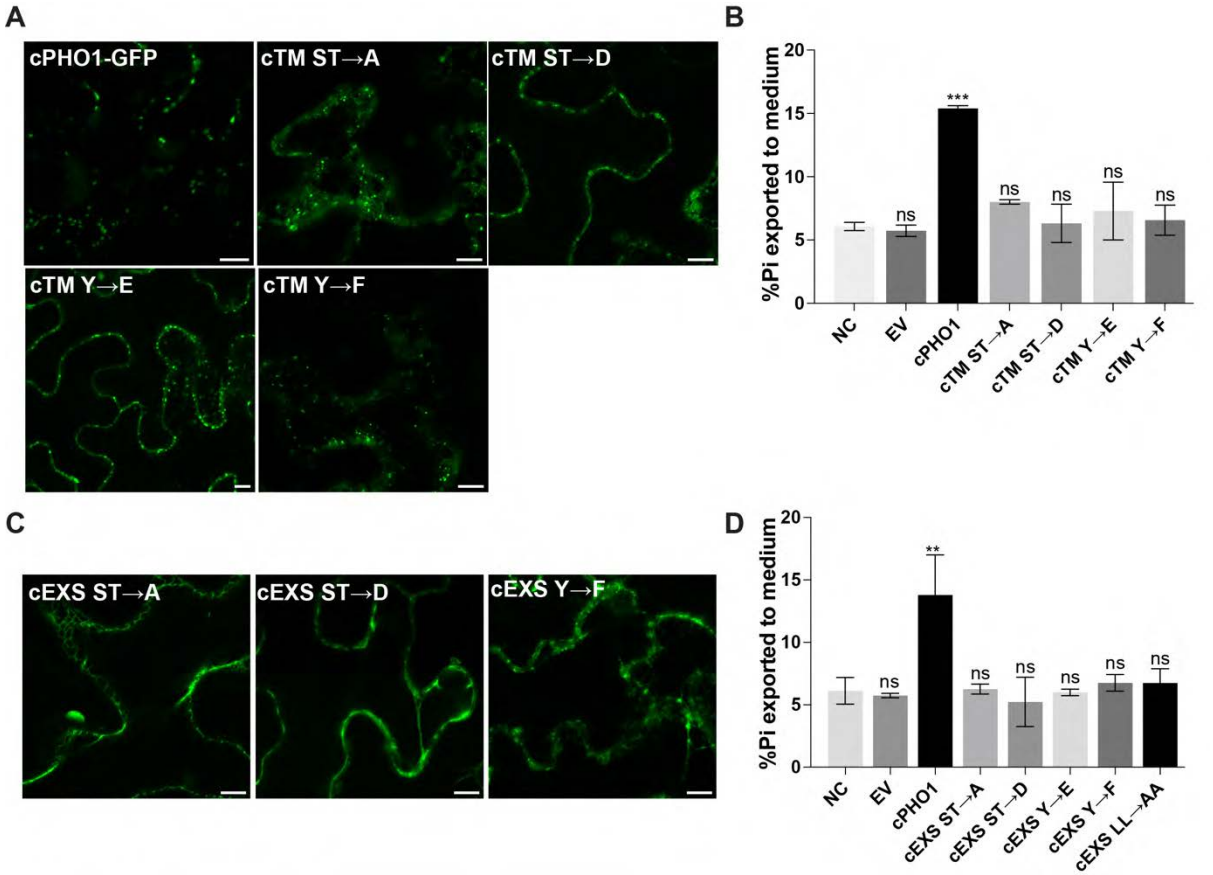

Figure 11. Subcellular localization and Pi export activity of *cTM* and *cEXS PHO1* mutants in *N. benthamiana.* Subcellular localization (A,C) and Pi export (B,D) mediated by GFP fused cTM and cEXS mutated constructs in transiently expressed in *N. benthamiana* leaf discs. EV and non-infiltrated (NC) leaves were used as controls for determination of Pi export activity. Error bars represent SD (*n* = *3*, 5-6 discs were pooled for each biological replicate). Asterisks represent statistically significant differences compared with NC (ANOVA; ***P < 0.001; **P <0.01). Scale, 10 μm.

Similar to S and T mutations, the phosphomimic and non-phosphomimic tyrosine residue mutations in EXS1 and EXS3 fragments did not show any change in their localization and Pi export activity compared to PHO1-GFP fusion construct when expressed transiently in *N. benthamiana* (Figure 13B-C). However, surprisingly Y→E mutations in the EXS2 fragment exhibited PM localization with no apparent export of Pi into the medium (Figure 13B-C). Unlike EXS2 Y→E, the non-phosphomimic EXS2 Y→F was localized to ER-like structures in the epidermal cells of *N. benthamiana* (Figure 13B). When these constructs were transformed in Arabidopsis, *EXS2 Y→E* phosphomimic did not complement *pho1-3* mutant, however, its GFP fusion showed PM-like localization with no Pi export activity (Figure 13D-F). We think that this is an artifact since this was observed in very few seedlings and the observed GFP fluorescence was in the cell layer (possibly endodermis) other than where PHO1 is

usually expressed (pericycle). Its non-phosphomimic *EXS2 Y→F* as well could not complement *pho1-3* mutant with almost non-detectable GFP fluorescence in the vasculature (Figure 13D-F).

The effect of tyrosine residue mutations in the EXS2 fragment of PHO1

Multiple sequence alignment of PHO1 homologs from different plant species shows high protein sequence similarity in the EXS region of PHO1 (Figure 14). Particularly, in the EXS2 region of the EXS domain, the putative tyrosine residues seem to be conserved across the homologs. Moreover, the EXS2 region contains two potential AP2 binding sequence motifs, YWDF and YYLSI. Thus, to investigate if these residues contribute to PHO1 localization, we generated GFP fusion constructs where we substituted tyrosine residues to phospho- and non-phosphomimic. When transiently expressed in *N. benthamiana*, most of the single Y mutants exhibited punctate-like structures (Figure 15A). The phosphomimic mutants Y669E, Y703E, and Y704E showed additional localization to ER along with punctate structures and exported relatively less Pi to the medium compared to their non-phosphomimics (Figure 15A-B). Surprisingly, a Y703,704E double mutant was localized at the PM when co-expressed with the PM marker in *N. benthamiana* and failed to export Pi in the medium (Figure 15A-C). Its non-phosphomimic neither changed the localization nor demonstrated a defect in Pi export activity. Mutants, where three Y (at 669, 703 and 704 positions) were mutated to E and F, were functionally inactive and presented different localization than WT PHO1 with much less protein expression observed in the confocal microscopy experiments (Figure 15A-B). In Arabidopsis, all the mutants complemented the *pho1-3* mutant phenotype by exporting Pi to the shoot; except for the phosphomimic of Y703,704 and Y669,703,704 where two and three residues were mutated respectively (Figure 16A-B). The confocal microscopy of Y647E, Y647F, Y669F, Y672E, Y672F, and Y704F PHO1 variants exhibited punctate-like structures, whereas other mutants either showed ER-like strands or very low diffused GFP fluorescence (Figure 16C).

Y703E and Y704E phosphomimic mutants contained consecutive tyrosine at 704 and 703 positions, respectively, that was not mutated. Hence, to avoid the likelihood of non-mutated tyrosine controlling the function and localization while the other is

mutated, we substituted Y with another non-polar amino acid leucine (L) at 703 and/or 704 amino acid positions.

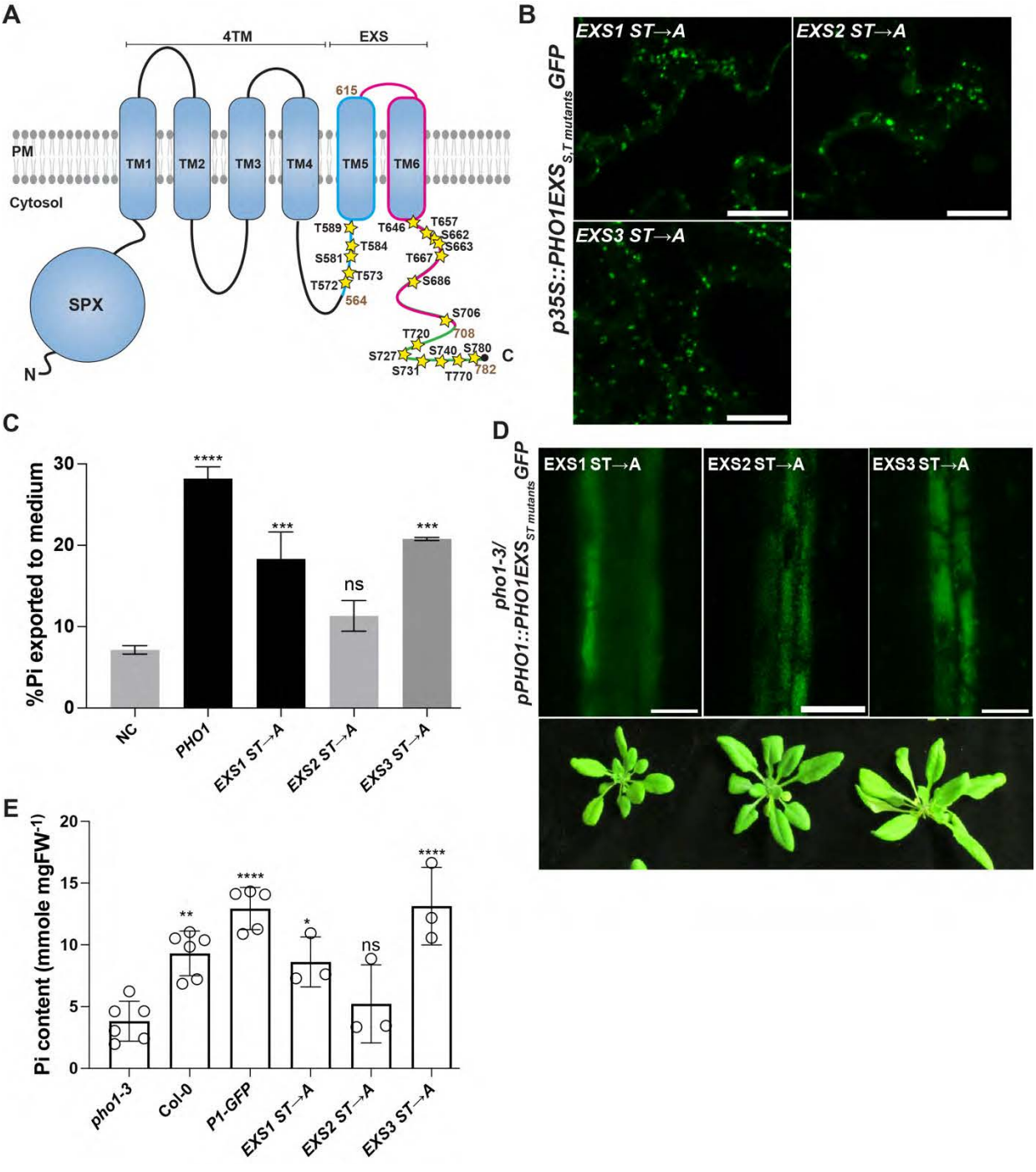

Figure 12. Non-phosphomimic mutations of serine and threonine residue in EXS domain complements *pho1-3* mutant. The schematic representation of PHO1 highlighting the serine, threonine residue (A) and tyrosine residue (B) of the EXS domain selected for mutagenesis (★ in yellow). Three different regions of EXS domain selected for mutagenesis referred as EXS1 (in Cyan), EXS2 (in Magenta) and EXS3 (in Green). (C) Localization of *PHO1 EXS ST→A* mutants to punctate structures when transiently expressed in *N. benthamiana.* (D) Export of Pi from *N. benthamiana* leaves

infiltrated with *PHO1 EXS ST→A* mutated constructs compared to NC (non-infiltrated control leaf) after 5h. *n* = *3*, 5-6 discs were pooled for each biological replicate (E) Phenotypic analysis and subcellular localization of *EXS ST→A* mutants in *pho1-3* mutant background. (F) Total shoot Pi content of *EXS ST→A* mutants compared with *pho1-3* mutant. *n= 3-6*. Error bars represent SD. Asterisks represent statistically significant differences compared with NC (ANOVA; ****P < 0.0001; ***P < 0.001; **P <0.01; *P <0.05). Scale, 20 μm.

In *N. benthamiana* YY→ LE and YY→ EL phosphomimic with L at 703 and 704 positions (respectively) localized to the PM, while non-phosphomimic YY→ LL was observed at both punctate-like and PM subcellular localizations (Figure 17A). However, GFP fusions of these mutants did not show PM localization in Arabidopsis (Figure 23A). These mutants were able to complement the *pho1-3* mutant (Figure 17C). YY→ LE and YY→ EL mutants where E mimics phosphorylated Y and L mimics non-phosphorylated version showed Pi export activity in *N. benthamiana* and Arabidopsis (Figure 17B-D).

Discussion

Due to the absence of detailed data regarding the structure of PHO1, the only available information is from *in silico* predictions and few structure-function studies (Wege et al., 2016; Wild et al., 2016). Thus, the predicted topology is not yet unambiguously determined (Wege et al., 2016). Nonetheless, based on the existing data, the PHO1 protein consists of an N-terminal hydrophilic SPX domain, which is followed by six hydrophobic membrane-spanning domains named 4TM and EXS domains with the N- and C-termini facing the cytosol. The analysis of the expression of different combinations of PHO1 domains has allowed to study their involvement in the localization and activity of PHO1 when expressed transiently in *N. benthamiana* as well as stably in transgenic *pho1* mutants (Wege et al., 2016). Recently, we have shown that the EXS domain not only controls PHO1 localization to Golgi/TGN but also to the PM. However, the information about signal sequence or motif that drives PHO1 localization is still lacking. Hence, in this study, we performed SDM screen of 4TM and EXS domains of PHO1.

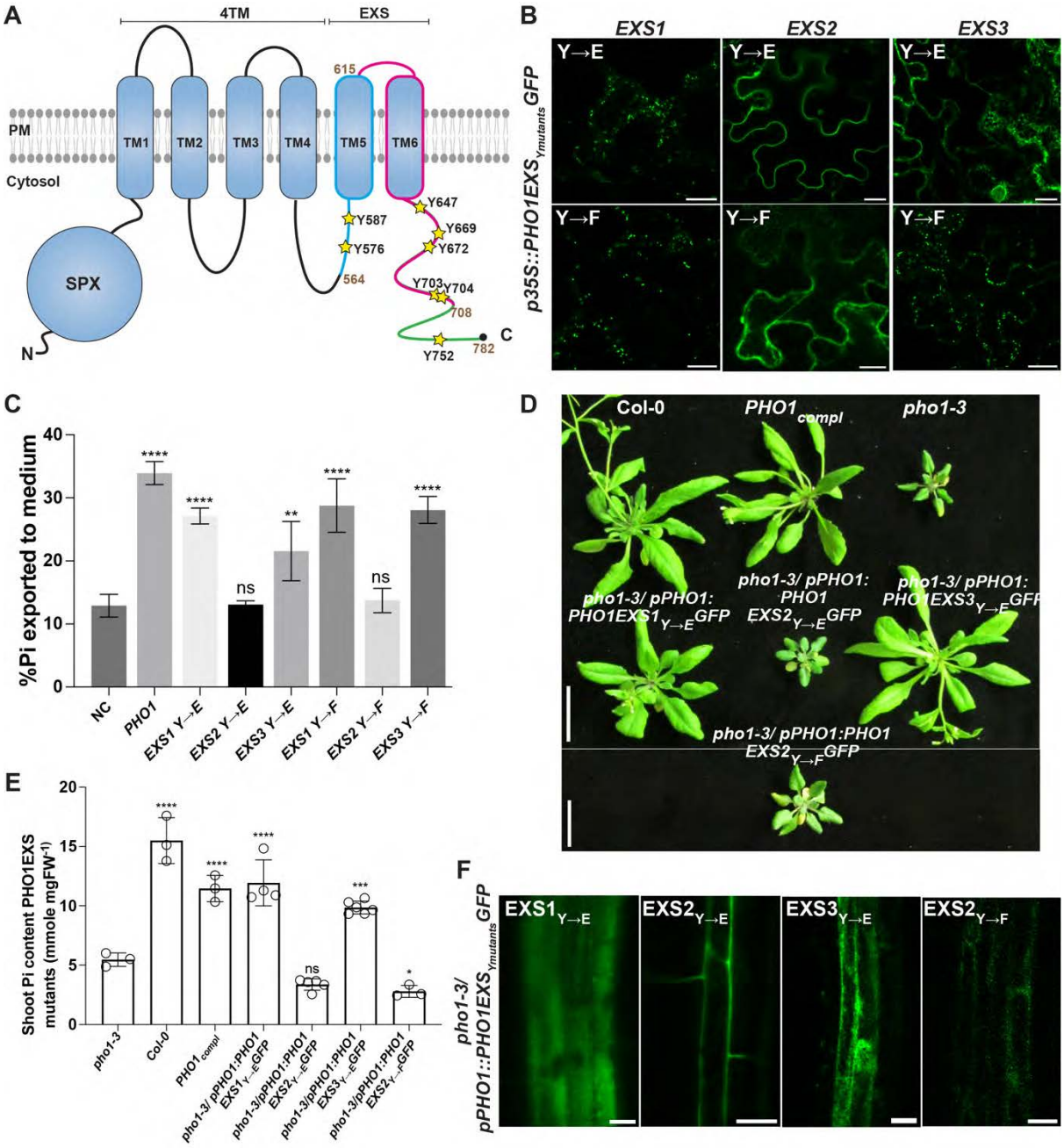

Figure 13. Phosphomimic of tyrosine residue in EXS2 fragment localizes to the PM in *N. benthamiana*. (A) Subcellular localization of *PHO1 EXS Y→E* (phosphomimic) and *EXS Y→F* (non-phosphomimic) mutants and Pi export (B) to the medium when transiently expressed in *N. benthamiana.* Scale, 20 μm. *n = 3*, 5-6 discs were pooled for each biological replicate. (C) Phenotypic analysis and shoot Pi content (D) of tyrosine phospho- and non-phosphomimic EXS fragment mutants in *pho1-3* mutant background. *n= 3-6*. Scale, 5 cm. (E) The expression pattern of PHO1 EXS Y→E and EXS2 Y→F in the vasculature of *A. thaliana*. Scale, 10 μm. Error bars represent SD. Asterisks represent statistically significant differences compared with NC (ANOVA; ****P < 0.0001; ***P < 0.001; **P <0.01; *P <0.05).

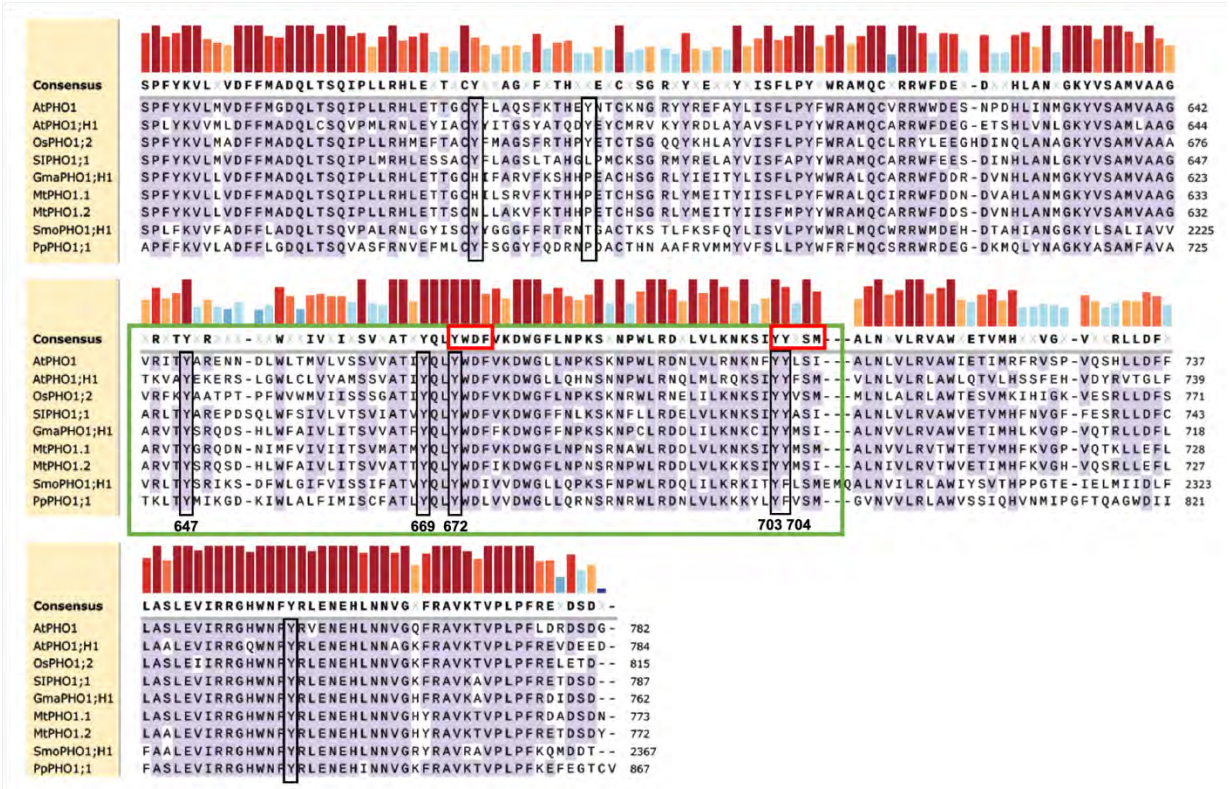

Figure 14. Multiple sequence alignment of EXS domain of PHO1 protein sequences. Alignment of EXS domain of AtPHO1 and its putative orthologs in rice (Os), tomato (Sl), soyabean (Gma), *Medicago* (Mt), *Selaginella* (Smo) and *Physcomitrella* (Pp). Alignment was done in Snapgene using MUSCLE method. The sequence conservation is depicted as coloured bars on the top. The tyrosine amino acids studied are shown in the black box. Green box indicates the protein sequence spanning the EXS2 region. Red boxes at the top of EXS2 region highlight the putative Yxxϕ signal sequence.

Most of the PHO1 variants with many mutations could neither complement *the pho1-3* mutant nor export Pi in Arabidopsis and *N. benthamiana*. Their GFP-fusions were not detected in transformants generated in *pho1-3* background. We speculate that these extensive mutations in 4TM and EXS regions of PHO1 result in a misfolded protein that eventually gets degraded. However, of these mutants, *cTM ST→ A* and *cTM Y→ F* 4TM mutants were at least partially functional in Arabidopsis (Figure 10). Whether partial functional complementation is the result of differences in the protein levels remains to be investigated. Since the purpose of this screen was to decipher the signals that affect PHO1 localization, we did not check protein stability or protein levels of analyzed mutants in the present screen.

Although the data on cTM and cEXS mutants was not conclusive, it provided important information on the unlikely involvement of serine and threonine residues of the 4TM domain in PHO1 localization. High sequence similarity of the EXS domain between PHO1 homologs and its involvement in the stabilization of PHO1 at the PM narrowed our search for potential amino acids that could act as a signal for its trafficking. We mutated putative tyrosine residues in the EXS domain to their phospho- and non-phosphomimic. In this study, we observed that all the phosphorylation dead (non-phosphomimic) PHO1 mutants could complement the *pho1* mutant phenotype in a manner that is similar to the WT PHO1 protein (Figures 16-17). Since these phosphorylation dead variants of tyrosine as well as serine/threonine residues in the EXS domain show PHO1-like localization and adequate Pi export to the shoot, it suggests that the phosphorylation of these residues is not necessary for the localization and activity of PHO1.

Most of the single phosphomimic tyrosine mutants, on the other hand, complemented the *pho1* mutant growth phenotype while maintaining relatively low shoot Pi content compared to their non-phosphomimic counterpart (Figures 16-17). Uncoupling of low shoot Pi from its effects on shoot growth has been previously shown for plants that under-expressed *PHO1 via* silencing, indicating a role of PHO1 in modulating the response of the shoot to Pi deficiency (Rouached et al., 2011).

We generated a double mutant construct where two consecutive tyrosine residues Y703 and Y704 were mutated to avoid the possible phosphorylation of adjacent tyrosine in the single mutants. The phosphomimic mutant Y703,704E localized to the PM in *N. benthamiana*, however, its localization in Arabidopsis was neither PHO1-like nor at the PM (Figures 15B, 16B). Replacing tyrosine residue with either E (phosphomimic) and/or L (non-phosphomimic) at 703 and/or 704 positions did not result in any significant change concerning localization and Pi export activity in Arabidopsis. But these mutants did localize to the PM similar to the Y703,704E mutant when transiently expressed in *N. benthamiana*. We speculate that the discrepancy of Y703,704E localization between *N. benthamiana* and Arabidopsis may be attributed to the involvement of different proteins/interactors or molecular mechanisms that might regulate the trafficking of membrane proteins differently in two distinct systems.

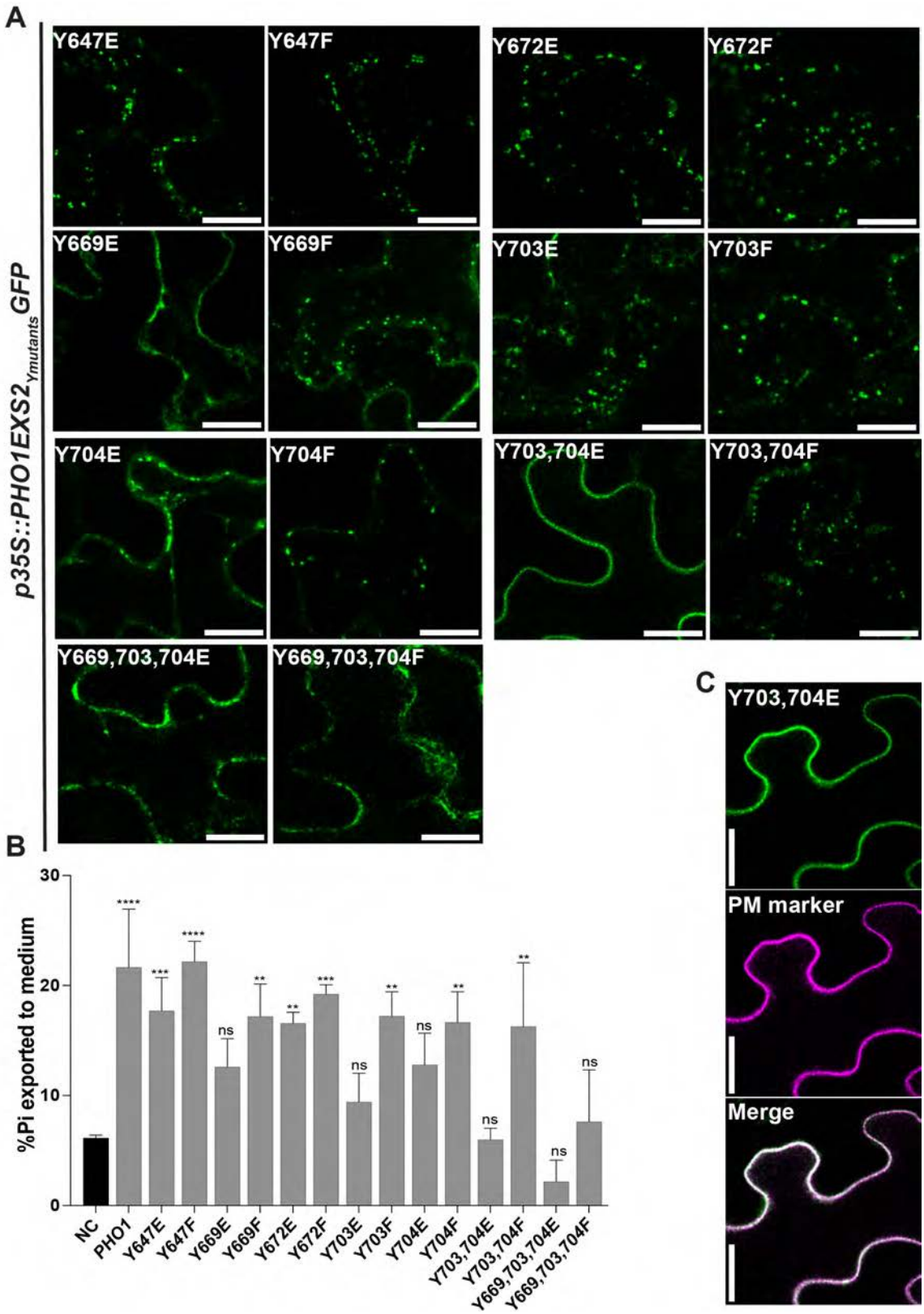

Figure 15. The phosphomimic of *Y703, 704* double mutant localizes to the PM in *N. benthamiana*. Subcellular localization (A) and Pi export (B) mediated by GFP fused single, double, and triple phospho- and non-phosphomimic tyrosine mutants from the EXS2 region of PHO1 when transiently expressed in *N. benthamiana*. Non-infiltrated (NC) leaves were used as controls for determination of Pi export activity. (C) Co-

localization of GFP fluorescence from the expression of *PHO1 EXS2 Y703,704E-GFP* with PM marker *CBL1-OFP* to the PM in the epidermal cells of *N. benthamiana.* Error bars represent SD (*n = 3*, 5-6 discs were pooled for each biological replicate). Asterisks represent statistically significant differences compared with NC (ANOVA; ****P < 0.0001; ***P < 0.001; **P <0.01). Scale, 20 μm.

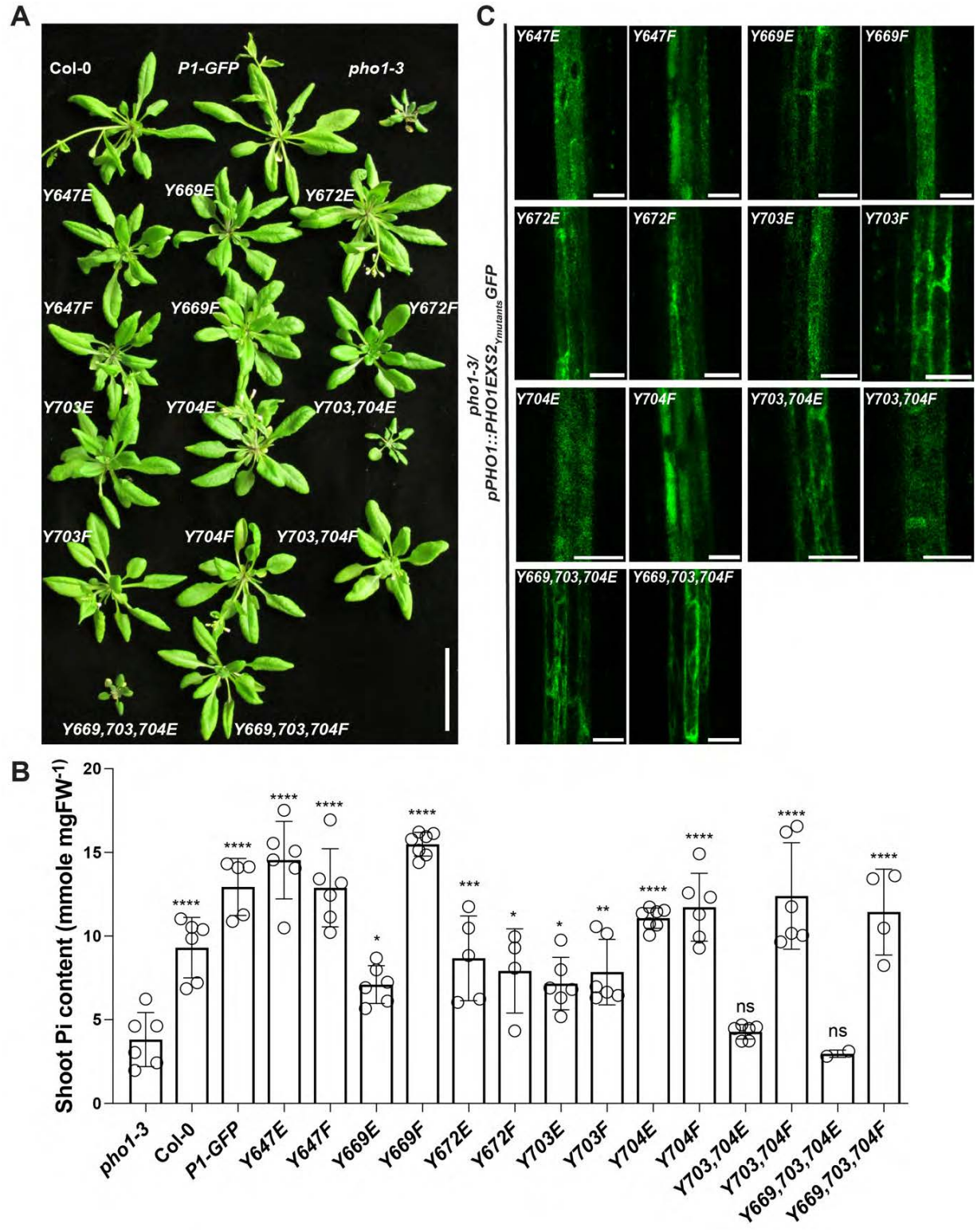

Figure 16. The phosphomimic of *Y703, 704* double mutant is not functional in *A. thaliana*. (A) Phenotypic characterization of *pho1-3* stably transformed with constructs bearing phospho- and non-phosphomimic of tyrosine residue in EXS2 region compared to Col-0, *P1-GFP*, and *pho1-3.* Scale, 5 cm. (B) Shoot Pi content of 3-week-old plants mentioned in (A) compared with *pho1-3* mutant. (C) Localization of above-mentioned mutants in the root vasculature. Error bars represent SD (*n = 2-8).* Asterisks represent statistically significant differences compared with NC (ANOVA; ****P < 0.0001; ***P < 0.001; **P <0.01; *P <0.05). Scale, 20 μm.

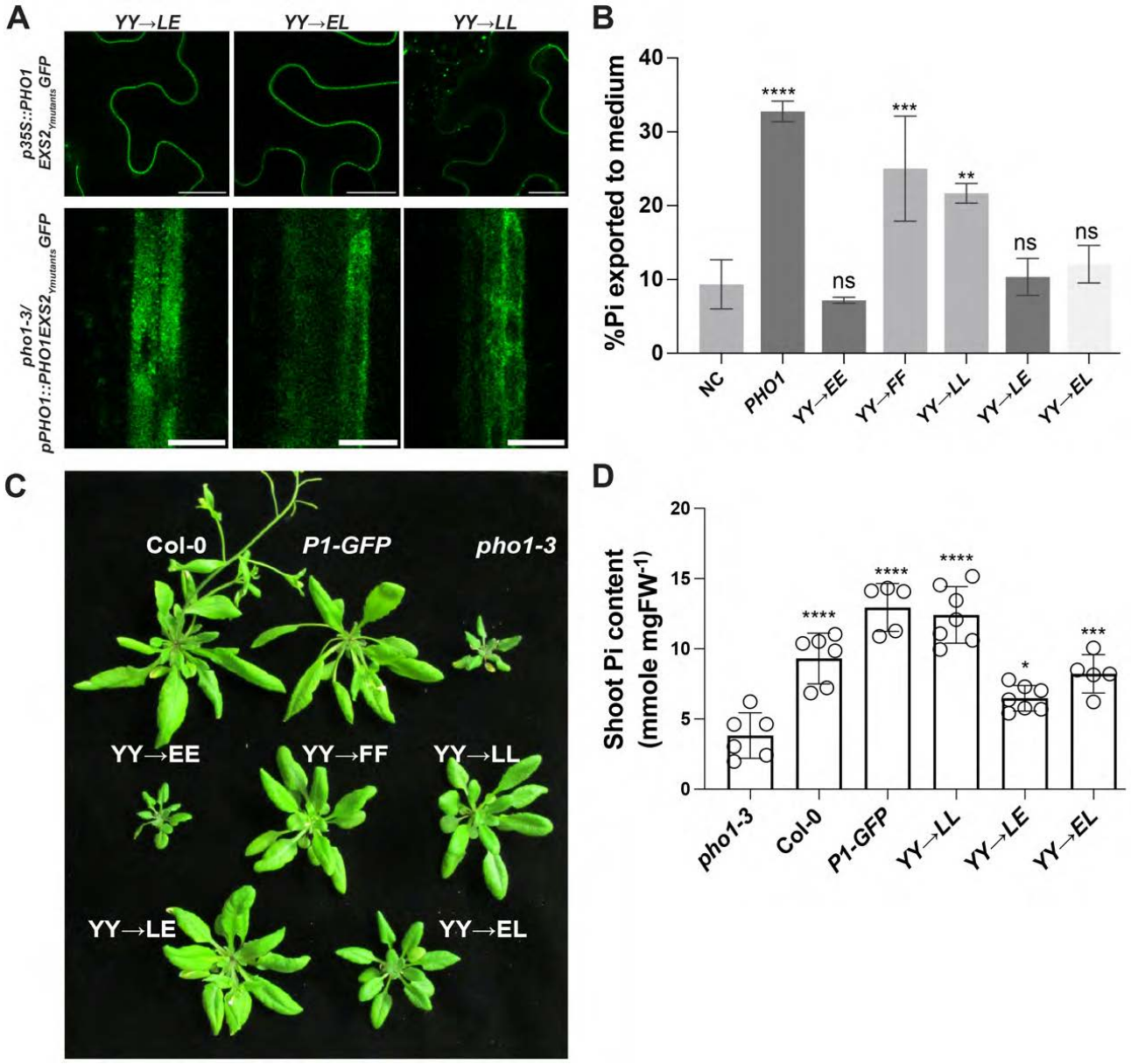

Figure 17. The non-phosphomimic of *Y703, 704* double mutants complement *pho1-3* mutant. (A) Subcellular localization of *Y703,704* double mutants in the epidermal cells of *N. benthamiana* and the vasculature of *A. thaliana*. (B) Pi export mediated by *Y703,704* double mutants of PHO1 when transiently expressed in *N. benthamiana*. Non-infiltrated (NC) leaves were used as controls for determination of Pi export activity. *n=3.* (C) Phenotypic characterization and shoot Pi content (D) of *pho1-3* stably transformed with constructs bearing *Y703,704* double mutants in EXS2

region compared to Col-0, *P1-GFP*, and *pho1-3. n=5-7.* Error bars represent SD. Asterisks represent statistically significant differences. (ANOVA; ****P < 0.0001; ***P < 0.001; **P <0.01; *P <0.05). Scale, 20 μm.

In addition to the abundance of expressed PHO1 protein, its localization to Golgi/TGN is crucial for its proper targeting to the PM and determining the transport activity. In this mutagenesis screen, we observed punctate-like structures in a few variants. Some variants exhibited ER-like localization with or without punctate. And the GFP fluorescence in some variants was more like diffused signal in the vasculature. As many of the tyrosine residue variants functionally complemented *pho1* mutant despite the distinct expression patterns of their GFP fusions in the vasculature, it will be safe to assume that at least a portion of the expressed protein is localized and targeted properly. And perhaps, the reason for the absence or less fraction of punctuates in these mutants is the rapid internalization and degradation of the mutated *PHO1* variants.

We think that PHO1 structure could be more important for its activity and localization rather than a signal sequence/motif because Y703,704E mutant with two negatively charged glutamic acid substitutions could not functionally complement the *pho1* mutant whereas the plants with uncharged amino acid substitutions (phenylalanine and leucine) behaved like WT. Fontenot et al., 2015 has shown that Arabidopsis AtPHT1;1 and AtPHT1;4 can form both homomerics and heteromerics, and the mutation of AtPHT1;1 Tyr312 (Y312) to aspartate (phosphomimic) but not alanine or phenylalanine (non-phosphomimic) leads to increased Pi transport, which might be attributed to the disruption of the homomeric interactions upon Y312D mutation. It is reasoned that the interactions between AtPHT1;1 and AtPHT1;4 monomers may modify the structure to control substrate access and/or transport through the pore. In case of PHO1, the non-functionality of the Y703,704E mutant prevents further investigations but suggests an essential structural role of these residues. Moreover, we cannot rule out the possibility of PHO1 forming homomer to export Pi.

Although we could not establish a role for phosphorylation in PHO1 trafficking across the PM, our data suggest that the strictly conserved tyrosine residues at 703 and 704 positions and the EXS domain, in general, might have a structural role for PHO1 function and hence, its localization. However, these speculations need experimental validation. Future experiments aimed at deciphering the structure, specificities and

biochemical properties of PHO1 will contribute to our understanding regarding its affinity, stability and very important, its mode of action.

List of Primers

- **List of primers used to generate mutations in *AtPHO1*.**

No	Primer name	Sequence (5'→3')
1	EXS1_AtPHO1_FP EXS1_AtPHO1_RP	GTCGATAATTAACCCATTAATCGTGTTC GGTTAATTATCGACTAAATTAGATGTCG
2	EXS2_AtPHO1_FP EXS2_AtPHO1_RP	CACTATGAACATTAATTTACAG TTAATGTTCATAGTGTCTTAGAAG
3	EXS3_AtPHO1_FP EXS3_AtPHO1_RP	TGTTTCACAATTTATGATCTTCGAC CATAAATTGTGAAACACGCTATAG
4	EXS_Y647E_FP EXS_Y647E_RP	CATAACCGAAGCGAGAGAAAACAACGACTTGTG CTCGCTTCGGTTATGCGGACTCCGGCTG
5	EXS_Y647F_FP EXS_Y647F_RP	CATAACCTTCGCGAGAGAAAACAACGACTTGTG CTCGCGAAGGTTATGCGGACTCCGGCTG
6	EXS_Y669E_FP EXS_Y669E_RP	CTATTGAACAATTATACTGGGACTTTGTCAAG TAATTGTTCAATAGTTGCCACAACGGAG
7	EXS_Y669F_FP EXS_Y669F_RP	CTATTTTCCAATTATACTGGGACTTTGTCAAG TAATTGGAAAATAGTTGCCACAACGGAG
8	EXS_Y672E_FP EXS_Y672E_RP	CAATTAGAATGGGACTTTGTCAAGG GTCCCATTCTAATTGGTAAATAGTTGCCAC
9	EXS_Y672F_FP EXS_Y672F_RP	CAATTATTCTGGGACTTTGTCAAGG GTCCCAGAATAATTGGTAAATAGTTGCCAC
10	EXS_Y703E_FP EXS_Y703E_RP	CTTCGAATACCTCTCCATTGTAAGCCAATTACATAAC GAGAGGTATTCGAAGTTCTTGTTCCGGAGAAC
11	EXS_Y703F_FP EXS_Y703F_RP	CTTCTTCTACCTCTCCATTGTAAGCCAATTACATAAC GAGAGGTAGAAGAAGTTCTTGTTCCGGAGAAC
12	EXS_Y704E_FP EXS_Y704E_RP	CTTCTACGAACTCTCCATTGTAAGCCAATTACATAAC GAGAGTTCGTAGAAGTTCTTGTTCCGGAGAAC
13	EXS_Y704F_FP EXS_Y704F_RP	CTTCTACTTCCTCTCCATTGTAAGCCAATTACATAAC GAGAGGAAGTAGAAGTTCTTGTTCCGGAGAAC
14	EXS_Y703,704E_FP EXS_Y703,704E_RP	CTTCGAAGAACTCTCCATTGTAAGCCAATTAC GAGAGTTCTTCGAAGTTCTTGTTCCGGAGAAC
15	EXS_Y703,704F_FP EXS_Y703,704F_RP	CTTCTTCTTCCTCTCCATTGTAAGCCAATTAC GAGAGGAAGAAGAAGTTCTTGTTCCGGAGAAC
16	EXS_Y703L704E_FP EXS_Y703L704E_RP	CTTCTTAGAACTCTCCATTGTAAGCCAATTAC GAGAGTTCTAAGAAGTTCTTGTTCCGGAGAAC
17	EXS_Y703E704L_FP EXS_Y703E704L_RP	CTTCGAATTACTCTCCATTGTAAGCCAATTAC GAGAGTAATTCGAAGTTCTTGTTCCGGAGAAC
18	EXS_Y703L704L_FP EXS_Y703L704L_RP	CTTCTTATTACTCTCCATTGTAAGCCAATTAC GAGAGTAATAAGAAGTTCTTGTTCCGGAGAAC

Chapter 3

Chapter 3

Comparative analysis of *Arabidopsis thaliana* PHO1 localization and its orthologs in *Medicago truncatula*

Aim

Recently, Nguyen et al., 2020 identified three closely related members of the *Medicago truncatula PHO1* gene family, namely *MtPHO1.1*, *MtPHO1.2*, and *MtPHO1.3. MtPHO1.1* and *MtPHO1.2* are expressed in the root vascular cylinder and nodules, however, *MtPHO1.3* is expressed only in the vasculature (Figure 18A). Using a transient transformation assay in *N. benthamiana* leaves, Ngyuen et al. were able to confirm that MtPHO1.1 and MtPHO1.2 act as Pi exporters similar to their closest relative in *A. thaliana*. Nodule-specific downregulation of both *MtPHO1.1* and *MtPHO1.2* led to reduced ^{33}P transfer from nodule cells into bacteroids and a three-fold reduction in symbiotic nitrogen fixation (SNF), establishing the role of *MtPHO1* genes as Pi transporters in bacteroid Pi homeostasis and SNF (Figure 18B). The PM localization of MtPHO1.1 and Golgi localization of MtPHO1.2 observed in *N. benthamiana* was particularly intriguing for us. The study of the subcellular localizations of the chimeras of the different domains of the two *MtPHO1* genes provided us with a tool to explore the gene region that could drive MtPHO1.1 to the PM. Moreover, studying the signal responsible for MtPHO1.1's PM localization in *N. benthamiana* was compelling because it could answer the main question of the mechanism that regulates PHO1 dynamics from endo-membranes to the PM and *vice-versa* in the Arabidopsis root vascular cells. Moreover, this approach could provide a comparative analysis of PHO1 localization in two different plant species and help to identify conserved molecular mechanisms that regulate Pi homeostasis in plants.

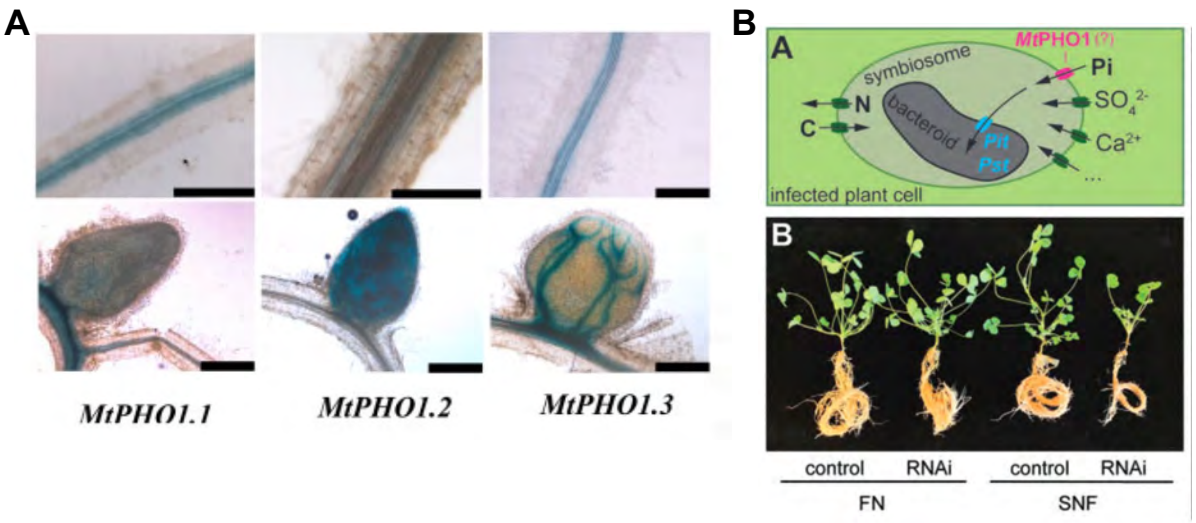

Figure 18. *Medicago truncatula PHO1* family of transporters is involved in Pi supply of rhizobia by the host plant. (A) GUS staining in *M. truncatula* roots (upper panels) and nodules (lower panels) transformed with *promoter:cDNA-GUS* fusions for genes *MtPHO1.1, MtPHO1.2*, and *MtPHO1.3*. Scale, 200 μm. (B) Schematic representation of a plant cell infected with rhizobium (upper panel). The symbiosome membrane where differentiated bacteroid is harbored contains different transporters critical for nutrient and ion exchange between the symbiotic partners. MtPHO1 transporters are suggested to be important for Pi transport across the symbiosome membrane. *Medicago truncatula* RNAi plants (downregulation of both, *MtPHO1.1* and *MtPHO1.2)* show reduced biomass relative to control plants when grown under symbiotic nitrogen fixation (SNF) conditions but not when grown under full nitrogen (FN) (lower panel). (Panel A is adapted from Nguyen et al., 2020 and Panel B is adapted from Muller, 2021).

Material and Methods

Plant material and Cloning

M. truncatula ecotype A17 was used for hairy root transformations (Nguyen et al., 2020). The EXS fragments of *MtPHO1.1* and *MtPHO1.2* to generate chimeras were synthesized from GeneScript. Wild-type and chimeric *PHO1*s from Medicago were first cloned in pENTR2B (Invitrogen) entry vector either by infusion or Golden gateway strategy and then transferred into pMDC32 (with original 2X35S promoter) and pK7FW2,0 (for *M. truncatula* hairy root transformation) binary plant expression vectors by LR reactions (Curtis and Grossniklaus, 2003; Engler et al., 2008).

M. truncatula hairy root transformation

First, seeds were scarified for 10 min in H_2SO_4 and washed 5 times with sterile water, followed by surface sterilization for 10 min with 33% (v/v) commercial bleach. Sterilized seeds were again rinsed 5 times with sterile water and left in the dark for 1 h to imbibe. This was followed by placing them on 0.7% agarose plates and incubation of plates in an inverted position in dark for 3 d at 4 °C and 1 d at 20 °C. Germinated seedlings were transferred to agar-solidified Fahräeus medium (0.132 g/L $CaCl_2$, 0.12 g/L $MgSO_4.7H_2O$, 0.1 g/L KH_2PO_4, 0.075 g/L $Na_2HPO_4.2H_2O$, 5 mg/L Fe-citrate, and 0.07 mg/L each of $MnCl_2.4H_2O$, $CuSO_4.5H_2O$, $ZnCl_2$, H_3BO_3, and $Na_2MO_4.2H_2O$, adjusted to pH 7.5 before autoclaving). Seedlings were grown for 10 days for *Agrobacterium rhizogenes* ARqua1-mediated hairy root transformation as described previously (Boisson-Dernier et al., 2001). Following hairy root transformation, seedlings were grown vertically on Fahräeus medium supplemented with 25 µg/mL kanamycin in a growth chamber at 21 °C (16 h light/8 h dark cycles) for 14 days before analyzing their roots under the confocal microscope.

Protoplast transformation

Plants were grown on plates as mentioned above. Protoplasts were isolated from *M. truncatula* by cutting the roots into small pieces of 2-5 mm in length. *MtPHO1.1* and *1.2* constructs were then transiently expressed in protoplasts using DNA-PEG-calcium transfection as described previously (Jia et al., 2018), and images were taken by laser scanning confocal microscopy.

Phosphate efflux assay

For the Pi export assay, *N. benthamiana* leaves were infiltrated with *Agrobacterium tumefaciens* carrying the WT or mutated PHO1 constructs. *Agrobacterium*-carrying constructs were grown at 28 ^{0}C incubator to OD= 1, and bacterial pellet was resuspended in infiltration buffer containing 10 mM $MgCl_2$, 10 mM MES, and 150 µM acetosyringone to OD = 0.6 to 0.8. The cultures were incubated further for 1-2 h at 28 ^{0}C on a shaker incubator. P19 was used to inhibit the silencing of transgenes. For co-infiltration, the *Agrobacterium* strain carrying two constructs was mixed in an equal amount along with P19. Experiments (Pi export or confocal imaging) were done two days post-infiltration.

Confocal microscopy

Subcellular localization of GFP/YFP and RFP/m-cherry/mScarlet fusion constructs in Arabidopsis roots and *N. benthamiana* epidermal cells was performed either by Zeiss LSM 700 or Zeiss LSM 880 confocal microscope.

Results

MtPHO1.1 and *MtPHO1.2* are Pi transporters

In silico analysis showed that *M. truncatula* homologs of Arabidopsis *PHO1*, such as *MtPHO1.1* and *MtPHO1.2* consisting of SPX and EXS domains had ~75% similarity with *AtPHO1* (Figure 19A; Nguyen et al., 2020). Phylogenetic analysis grouped *MtPHO1.1* and *MtPHO1.2* in the same clade as *AtPHO1* (Figure 19B). The subcellular

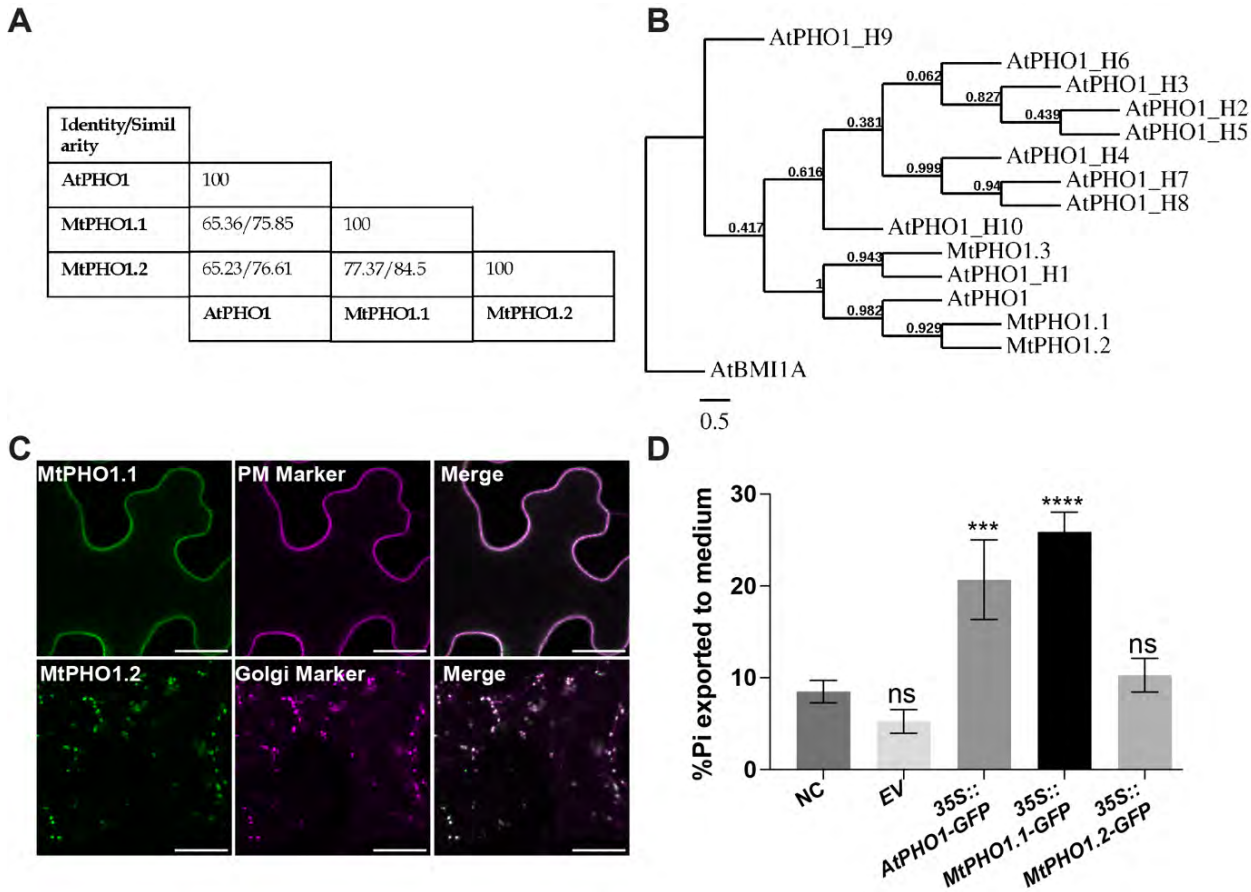

Figure 19. Phylogeny of *PHO1* family in *M. truncatula* and activity in *N. benthamiana*. (A) Identity and similarity matrix of MtPHO1.1 and MtPHO1.2 with AtPHO1. (B) Phylogenetic tree of PHO1 from Arabidopsis and *M. truncatula* with two clades. Tree was rooted using AtBMI1A (a non-PHO1 related protein). The branch length is proportional to the number of substitutions per site (TreeDyn). (C) Co-localization of MtPHO1.1 and MtPHO1.2 GFP-fusions with CBL1-OFP (PM marker)

and ManI-mCherry (Golgi marker). (D) Measurement of Pi export mediated by MtPHO1s when transiently expressed in *N. benthamiana* leaf discs, and the amount of Pi exported to the apoplast was measured after 5h. As controls, Pi export was measured in leaf discs expressing either GFP (EV) or non-infiltrated (NC). Errors bars represent SD (*n = 3*, 5-6 discs were pooled for each biological replicate). Asterisks represent statistically significant differences compared with non-infiltrated control (ANOVA; ****P < 0.0001; ***P < 0.001). Scale, 20 μm.

localization of MtPHO1.1 and MtPHO1.2 GFP fusions in *N. benthamiana* was determined by co-infiltration with either the Golgi marker, ManI-mCherry, or the PM marker, CBL1-OFP. MtPHO1.1 co-localized primarily with the PM marker and MtPHO1.2 co-localized with the Golgi marker when transiently expressed (Figure 19C). The transient expression of MtPHO1.1-GFP resulted in the export of Pi to the extracellular medium compared to free GFP (empty vector) and non-infiltrated controls and was comparable to AtPHO1-GFP, whereas MtPHO1.2-GFP fusion exported less Pi compared to MtPHO1.1 and AtPHO1, but slightly higher than GFP and non-infiltrated controls (Figure 19D).

MtPHO1.1 and MtPHO1.2 exhibit punctate-like patterns in *M. truncatula* root protoplast

Expression of MtPHO1.1-GFP and MtPHO1.2-GFP fusion proteins in *M. truncatula* hairy root transformants (Boisson-Dernier et al., 2001) using the gene's endogenous promoters did not show reliable GFP expression above the autofluorescence background in root vascular cylinder (data not shown). Previous attempts to express MtPHOs under the CaMV 35S promoter also failed due to its strong silencing effect. Thus, we transiently expressed MtPHO1.1-GFP and MtPHO1.2-GFP in protoplasts isolated from the roots of *M. truncatula* (Jia et al., 2018). The protoplasts expressing MtPHO1.1 and MtPHO1.2 showed a punctate-like pattern (Figure 20).

EXS domain contributes to the PM localization of MtPHO1.1 in *N. benthamiana*

Because of the high sequence similarity between MtPHO1.1 and MtPHO1.2, but their different subcellular localizations, it was interesting to know what drives MtPHO1.1 at the PM in *N. benthamiana*. To study this, we generated three chimeric GFP fusion constructs of *MtPHO1.1* and *MtPHO1.2* each by swapping their SPX, TM, and EXS domains as shown in the schematic (Figure 21A). The chimeras were transiently

expressed in *N. benthamiana* to check their subcellular localization and Pi export activity.

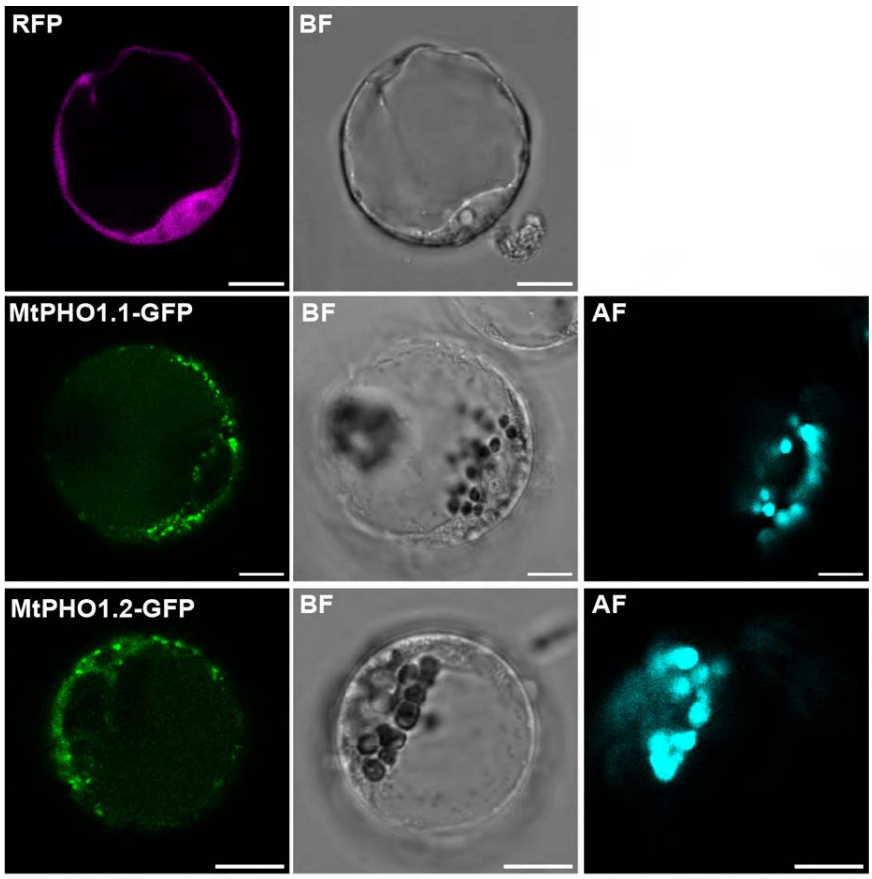

Figure 20. Subcellular localization of *MtPHO1* genes in *M. truncatula* root protoplasts. (A) The root protoplasts of *M. truncatula* transformed with *RFP* (control), *MtPHO1.1-GFP* and *MtPHO1.2-GFP*. The protoplasts expressing *MtPHO1.1-GFP* and *MtPHO1.2-GFP* exhibited punctate pattern shown in left panel. Bright field images are shown in middle panel and right panel demonstrates the autofluorescence. Scale, 10 μm.

The subscript numbers and letters in the following text denote the domain of the gene that was cloned in the mentioned *MtPHO1* gene to generate chimeras. Transient expression of *cMtPHO1.1*$_{SPX1.2}$, *cMtPHO1.1*$_{TM1.2}$, and *cMtPHO1.2*$_{EXS1.1}$ resulted in PM localization similar to WT *MtPHO1.1* (Figure 21B), while the expression of *cMtPHO1.1*$_{EXS1.2}$, *cMtPHO1.2*$_{SPX1.1}$, and *cMtPHO1.2*$_{TM1.1}$ resulted in Golgi localization like WT *MtPHO1.2* (Figure 21C). Thus, swapping of EXS domain between MtPHO1.1 and MtPHO1.2, changed the localization of chimeric proteins in epidermal cells. cMtPHO1.1$_{EXS1.2}$ colocalized with Golgi marker, whereas cMtPHO1.2$_{EXS1.1}$ showed PM localization (Figures 21B-C).

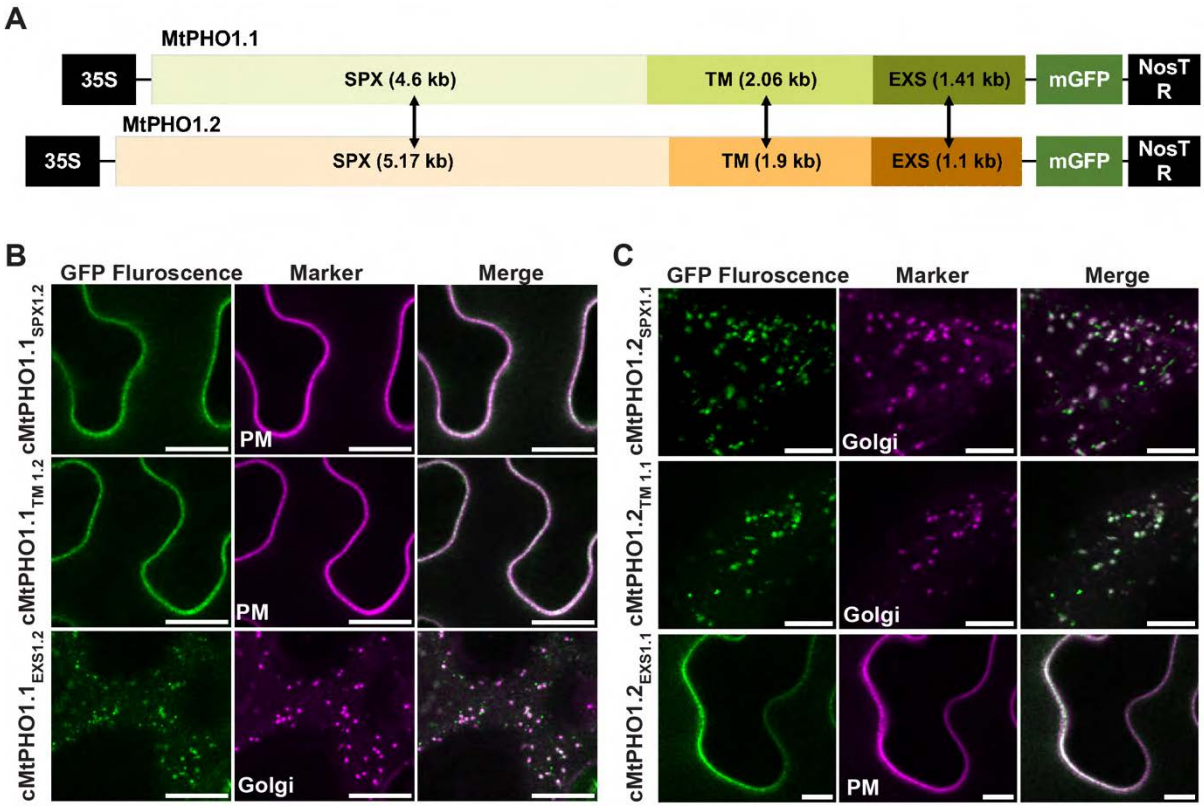

Figure 21. Subcellular localization of *MtPHO1.1* and *MtPHO1.2* chimeras *N. benthamiana*. (A) Schematic representation of the chimeras generated by swapping individual domain of *MtPHO1.1* and *MtPHO1.2* separately with each other. (B) Subcellular localization of chimeric MtPHO1.1-GFP and (C) MtPHO1.2-GFP fusion proteins transiently expressed in *N. benthamiana*. cMtPHO1.1$_{SPX1.2}$, cMtPHO1.1$_{TM1.2}$ and cMtPHO1.2$_{EXS1.1}$ were co-expressed with the plasma membrane marker, CBL1-OFP while cMtPHO1.1$_{SPX1.2}$, cMtPHO1.2$_{SPX1.1}$ and cMtPHO1.2$_{TM1.1}$ were co-expressed with the Golgi marker, ManI-mCherry. Scale, 10 μm.

We identified that a change in the localization of cMtPHO1.1$_{EXS1.2}$ and cMtPHO1.2$_{EXS1.1}$ did not alter their Pi export activity compared to WT protein controls (Figure 22). However, swapping of the SPX domain led to less Pi export from *N. benthamiana* leaves infiltrated with cMtPHO1.1$_{SPX1.2}$ and more in cMtPHO1.2$_{SPX1.1}$ (Figure 22). Chimeras with swapped TM domain neither had any effect on their function nor subcellular localization. Subsequently, we replaced the EXS domain of *AtPHO1* with the EXS of *MtPHO1.1*. We generated *cAtPHO1$_{EXS1.1}$ GFP* fusion construct under the control of CaMV 35S promoter and transiently expressed in epidermal cells of *N. benthamiana*. cAtPHO1$_{EXS1.1}$ GFP behaved like WT AtPHO1 because it co-localized with PHO1-mScarlet fusion (Figure 23A) along with the Pi export comparable to GFP and non-infiltrated controls (Figure 23B).

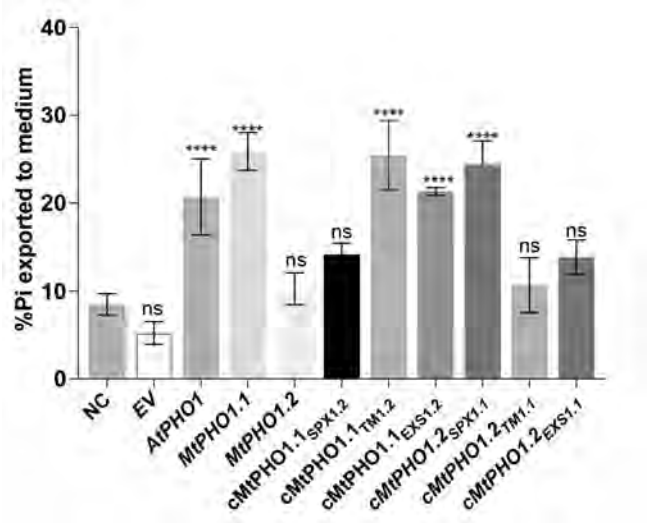

Figure 22. Activity of *MtPHO1.1* and *MtPHO1.2* chimeras *N. benthamiana*. Measurement of Pi export mediated by the transient expression of *chimeric MtPHO1.1s, chimeric MtPHO1.2s and AtPHO1* in *N. benthamiana* leaf discs. As controls, Pi export was measured in leaf discs expressing either free GFP or not infiltrated (NC). Error bars represent SD (*n=3*). Asterisks represent statistically significant differences compared to non-infiltrated control. (ANOVA; ****P < 0.0001).

The region of MtPHO1.1 from residue number 669 to 773 controls its PM localization in *N. benthamiana*

To understand the region/motif in the EXS domain responsible for PM localization of MtPHO1.1, we generated six constructs where the EXS domain of both MtPHO1.1 and MtPHO1.2 was divided in fragments EXS1 (E1), EXS2 (E2) and EXS3 (E3) and was swapped with one another (Figure 24A). The fragments generated were at the same locations as AtPHO1 EXS fragments (Figure 12A; Chapter 2) since both proteins share high sequence similarity in the EXS domain (Figure 14). E1 fragment started from residue 555 to 624, E2 from 625 to 698, and E3 covered a region from 699 to 773 in MtPHO1.1 (Figure 14), and similar fragments were generated in MtPHO1.2. Out of six chimeric constructs, *cMtPHO1.1_E3$_{1.2}$* and *cMtPHO1.2_E3$_{1.1}$*, where the third fragment of EXS was swapped changed their respective localization. *cMtPHO1.1_E3$_{1.2}$* changed the localization from PM to Golgi and *cMtPHO1.2_E3$_{1.1}$* changed from Golgi to PM when transiently expressed (Figure 24B). To narrow the region further, we generated three constructs where three fragments of MtPHO1.1 EXS3 region (EXS3_1, EXS3_2, and EXS3_3) were swapped with that of MtPHO1.2 one by one (Figure 24C). However, all three constructs showed both PM localization as well as punctate-like structures indicative of Golgi localization in *N. benthamiana* (Figure 24D).

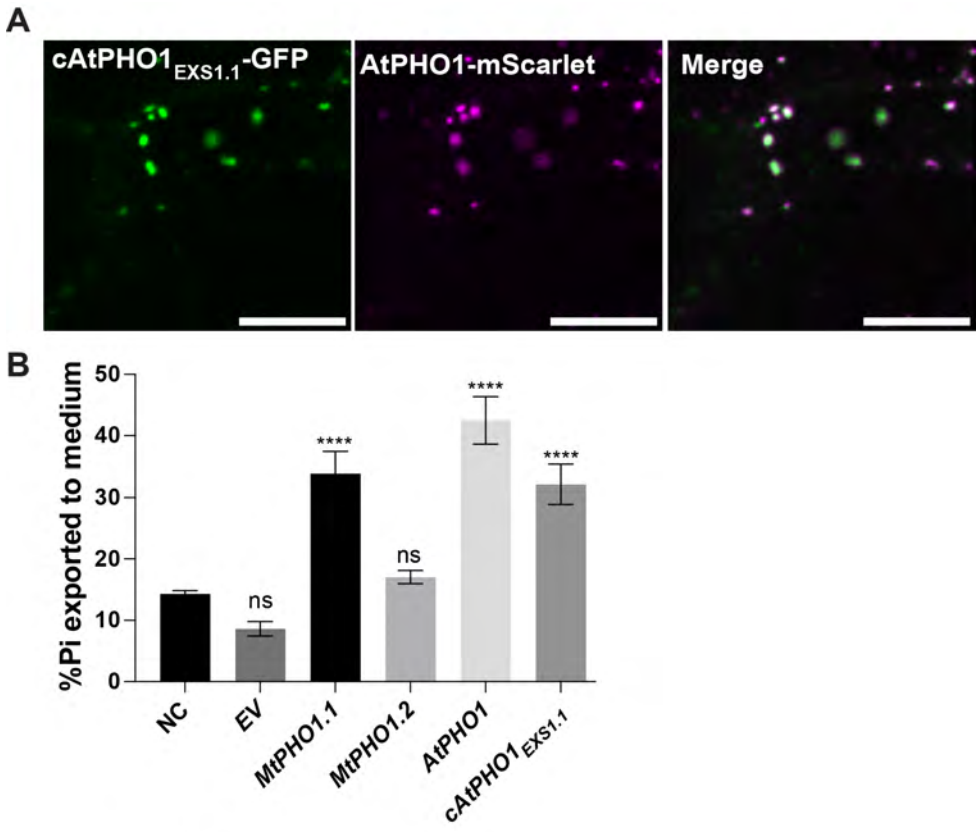

Figure 23. Swapping EXS domain of MtPHO1.1 does not affect the activity and localization of AtPHO1 in *N. benthamiana*. (A) Co-localization of cAtPHO1$_{EXS1.1}$-GFP with AtPHO1-mScarlet fusion proteins to punctate-like structures when transiently expressed in *N. benthamiana*. (B) Measurement of Pi export mediated by the transient expression in *N. benthamiana* leaf discs. Error bars represent SD (*n*=*3*). Asterisks represent statistically significant differences compared to non-infiltrated control. (ANOVA; ****P < 0.0001). Scale, 10 μm.

Discussion

The *MtPHO1* homologs, *MtPHO1.1* and *MtPHO1.2* contain SPX and EXS domains and share ~75% similarity in their protein sequence, with the majority of similarity coming from TM and EXS domains. Functional expression of MtPHO1.1-GFP and MtPHO1.2-GFP in *N. benthamiana* showed Pi export activity and subcellular localization to PM and Golgi, respectively. AtPHO1 has previously been shown to co-localize with the Golgi marker (Arpat et al., 2012), and a similar localization occurred with the *MtPHO1.2-GFP* construct (Figure 19C). Similar to the Pi exporters AtPHO1 and AtPHO1; H1 in Arabidopsis and OsPHO1.2 in rice (Hamburger, 2002; Stefanovic et al., 2007; Jabnoune et al., 2013), these *M. truncatula* genes are also expressed in

the root vascular cylinder (Figure 18A; Nguyen et al., 2020). These data, along with the Pi export activity of *MtPHO1.1* and *MtPHO1.2* in *N. benthamiana*, suggested the probable role of these genes as Pi transporters. Their subcellular localizations in *N. benthamiana* provided us with an opportunity to explore the site/region that might control the PM localization of AtPHO1.

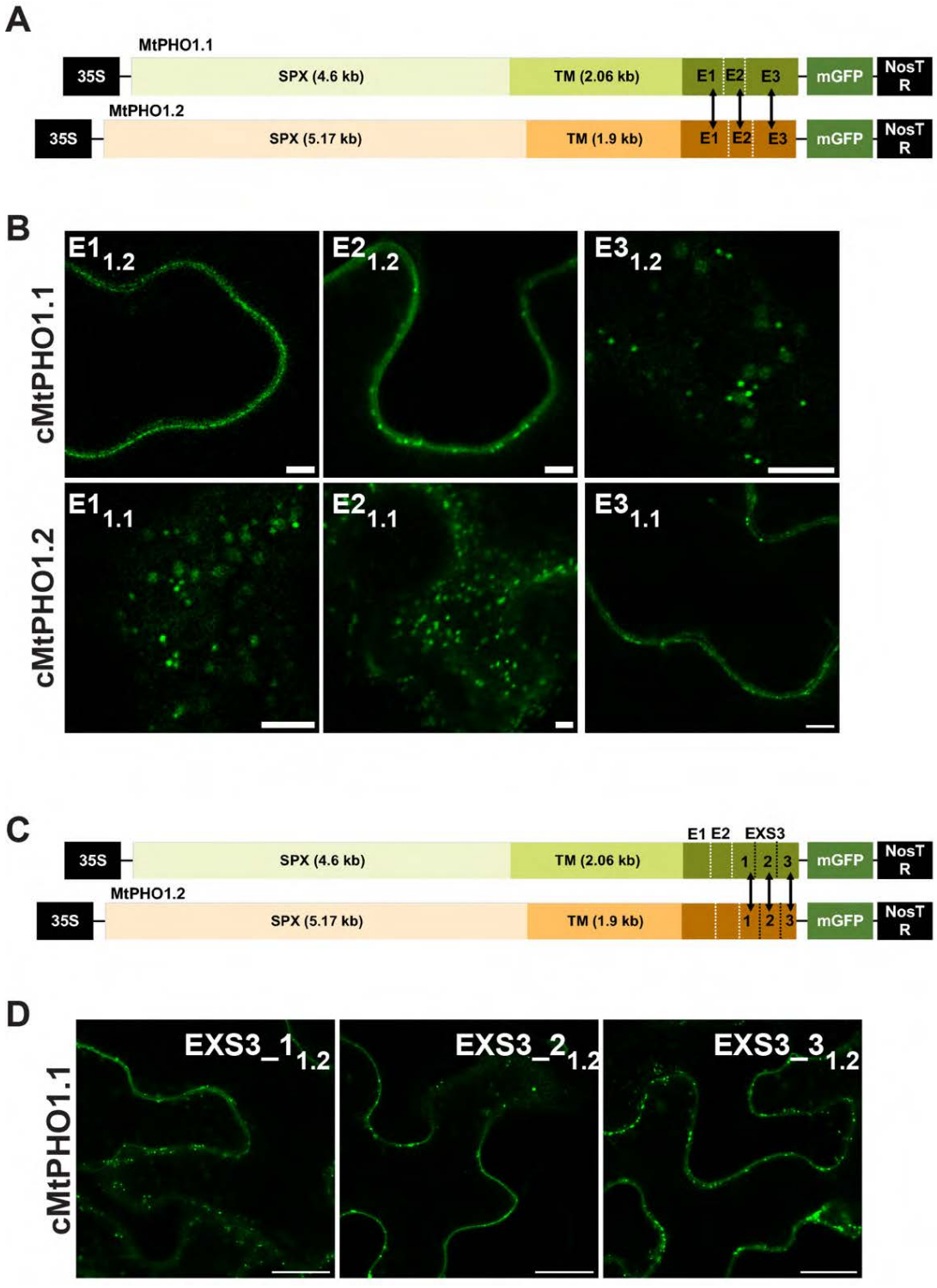

Figure 24. EXS3 region of *MtPHO1.1* controls its PM localization in *N. benthamiana*. (A) Schematic representation of the chimeras generated by swapping three different regions, EXS1, EXS2 and EXS3 of EXS domain of *MtPHO1.1* and *MtPHO1.2* separately with each other. (B) Subcellular localization of fusion proteins mentioned in (A) transiently expressed in *N. benthamiana*. Scale, 5 μm. (C) Schematic representation of the chimeras generated by swapping three different regions 1, 2 and 3 of EXS3 domain of *MtPHO1.1* with that of *MtPHO1.2* separately with each other. (D) Subcellular localization of fusion proteins generated as (C) in *N. benthamiana*. Scale, 20 μm.

Co-localization and Pi export study of chimeric MtPHO1.1 and MtPHO1.2 protein fusions revealed the role of the EXS domain in MtPHO1.1's PM localization (Figure 21). A similar role has been demonstrated for the EXS domain in the regulation of PHO1 localization at the PM in Arabidopsis (Figure 2A; Chapter 1). However, the EXS3 region of MtPHO1.1 seemed to control its PM localization (Figure 24B), whereas the EXS2 region of the EXS domain was important for PM localization of AtPHO1 in *N. benthamiana* (Figures 13A, 15C; Chapter 2). Moreover, the swapping of the AtPHO1 EXS domain with MtPHO1.1 did not result in PM localization when transiently expressed (Figure 23A). The transformation of GFP fusion constructs of *MtPHO1* genes under the control of Arabidopsis *PHO1* promoter was unable to functionally complement Arabidopsis *pho1* mutants (data not shown). Although the EXS domain is responsible for PM localization of both AtPHO1 and MtPHO1.1, we speculate that their underlying regulatory mechanism might be different.

Swapping the SPX domains affected the Pi export activity of MtPHO1.1 and MtPHO1.2 (Figure 22), however, it will be important to check their protein levels in transient assays to confirm this claim. In this study, our aim was to identify the signal that could control AtPHO1 localization by investigating the localizations of *MtPHO1* genes. Surprisingly, after many attempts of hairy root transformation to visualize the localization of *MtPHO1* genes, transient expression of MtPHO1.1-GFP and MtPHO1.2-GFP in root protoplast resulted in a punctate-like pattern contrary to our expectation (Figure 20). Although MtPHO1's localization and Pi export data suggest their role as Pi exporters in *N. benthamiana*, we don't have such evidence in *M. truncatula* as we have in the case of AtPHO1. Nonetheless, our data establish the importance of the EXS domain in the localization and proper targeting of *PHO1* genes at least in *N. benthamiana* and *A. thaliana*.

List of Primers

- **List of primers used to generate chimeras in *MtPHO1s*.**

No	Primer name	Sequence (5'→3')
1	MtPHO1.1 SPX FP (A) MtPHO1.1 SPX RP	TTAGGTCTCACATTATGGTGAAATTTTCAAAGGAAC TAAGGTCTCTAAATAACTTGCAGAAGCTGTTTGG
2	MtPHO1.1 TM FP MtPHO1.1 TM RP	TTAGGTCTCAATTTGAAAACAGTGAAAAGATCAC TAAGGTCTCTGCCATAAAAAAGTCCACTAGAAGAAC
3	MtPHO1.1 EXS FP MtPHO1.1 EXS RP (B)	TTAGGTCTCATGGCTGATCAACTTACTAGCCA TAA GGTCTCT ATGT ATTATCCGAATCTGCATCACG
4	MtPHO1.2 SPX FP (A) MtPHO1.2 SPX RP	TTAGGTCTCACATTATGGTGAAATTCTCAAAGGAGC TAAGGTCTCTAAATAACTTGAAGAAGCTTTTTGGCA
5	MtPHO1.2 TM FP MtPHO1.2 TM RP	TTAGGTCTCAATTTAAAAGAAGTGAAGAAATCCCAT TAAGGTCTCTGCCATAAAAAAGTCTACTAGCAGA
6	MtPHO1.2 EXS FP MtPHO1.2 EXS RP (B)	TTAGGTCTCA TGGCTGATCAACTAACTAGCCAG TAAGGTCTCTATGTATAGTCAGAATCTGTCTCTCGAAA
7	MtPHO1.1 EXS1 RP MtPHO1.1 EXS2 FP	TAAGGTCTCTCATACTTCCCCATGTTAGCCAAATGTG TTAGGTCTCATATGTTTCTGCAATGGTTGCG
8	MtPHO1.1 EXS2 RP MtPHO1.1 EXS3 FP	TAAGGTCTCTACATGTAGTATATGCTTTTATTCTTC TTAGGTCTCAATGTCTATGGTAATTTCTATTTACCTC
9	MtPHO1.2 EXS1 RP MtPHO1.2 EXS2 FP	TAAGGTCTCTCATAAAAAAGTTTAATTAGCAATGTAAC TTAGGTCTCATATGTTACTGACTAATAGTACACATGC
10	MtPHO1.2 EXS2 RP MtPHO1.2 EXS3 FP	TAAGGTCTCTACATATAGTATATGCTTTTTTTCTTTAAC TTAGGTCTCAATGTCTATTGTAAGTTCTCTATCTCTTAATG

Concluding remarks and perspectives

Plants depend on different families of phosphate transporters to mediate Pi uptake from the soil, its distribution across different organelles, and for remobilization between the source and sink tissues. Once imported into the plants, the allocation of Pi across far-located tissues relies on the Pi efflux activity of the stele-localized PHO1 protein. The physiological role of PHO1 for root-to-shoot Pi allocation was demonstrated by the reduced Pi in the shoots and higher Pi accumulation in the roots of *pho1* mutants in Arabidopsis and rice (Poirier et al., 1991; Secco et al., 2010). Unexpectedly, PHO1 exhibited Golgi/TGN localization instead of PM in Arabidopsis as well as when transiently expressed in the epidermal cells of *N. benthamiana* (Arpat et al., 2012; Wege et al., 2016). Thus, how PHO1 mediates Pi export to the xylem apo-plastic space despite its localization to Golgi/TGN was a puzzle for a long time.

To get insights on these mechanisms, we carried out three approaches. By genetically interfering with CME, we were able to show that PHO1 localizes to the PM and is internalized from the PM via CME in AP2 independent manner. This indicated that PHO1 cycles between Golgi/TGN and PM. PHO1 localization was not affected by the availability of Pi in the medium further highlighted the role of endocytosis for its constitutive internalization, perhaps to maintain the low abundance of PHO1 at the PM. Surprisingly, PM-stabilized PHO1 showed reduced Pi export activity, which could be a regulatory mechanism exerted by plants to limit the Pi transfer to the aerial tissues for plant Pi homeostasis.

The second approach involved a reverse genetics strategy, where we mutated potential amino acids to decipher the post-translational modification that might control PHO1 localization. Though we did not find any signal/motif that could regulate PHO1 localization, we could eliminate the role of potential ubiquitination and phosphorylation sites in the C-terminal cytosolic region of PHO1. Moreover, our data on phosphomimic tyrosine mutants suggested the structural role of the EXS domain in the localization and activity of PHO1. Finally, we performed comparative analysis of the localization of *PHO1* gene family from Arabidopsis and *Medicago truncatula* to decipher the PHO1 localization. We found that the EXS domain of MtPHO1.1 had a role in its PM localization in *N. benthamiana*; however, it could not change the localization of AtPHO1. This implies that the EXS domain could be necessary for the localization in

both MtPHO1.1 and AtPHO1 but would have a different regulatory mechanism. However, the function of the EXS domain remains to be verified in *M. truncatula.* It would be interesting to see if the function of the EXS domain is conserved in all PHO1 homologs. Recently, AtPHO1 ortholog in Rice, OsPHO1;2 is found to be localized at the plasma membrane of rice sheath protoplasts and onion epidermal cells with occasional localization in intracellular compartments (Ma et al., 2021). Moreover, immunoelectron microscopy revealed the association of immunogold particles with the PM of cells from the nucellar epidermis and vascular tissues of developing seeds (Ma et al., 2021). The emerging investigations on the PHO1-type Pi transporters will likely resolve the mechanisms by which various Pi transporters work to precisely control Pi fluxes across different tissues.

Our study shows the implication of endocytosis as a crucial regulator for PHO1 dynamics; however, understanding the underlying molecular mechanisms involved in PHO1 localization remains an exciting challenge. One possibility for the absence of PHO1 at the PM, as suggested by Arpat et al., 2012, is that, at the steady-state level, only a minor fraction of PHO1 is localized at the PM to export Pi like iron transporter IRT1 (Figure 25A). IRT1 is also localized in the TGN/early endosomes of root hair cells and functions in the uptake of reduced iron from extracellular space into roots (Barberon et al., 2011). IRT1 was observed at the PM only when its recycling from the PM to endosomes was inhibited by the drug tyrophostin A23 or blocking mono-ubiquitination which led to severe growth defects and oxidative stress due to metal toxicity (Barberon et al., 2011). In a similar manner, constitutive internalization of PHO1 can be seen as a mechanism to prevent uncontrolled Pi export activity. In this context, it is surprising that the stabilization of PHO1 at the PM of the root pericycle via CME inhibition led to a decrease in PHO1-mediated Pi export activity instead of an expected increase, which would be anticipated if the Pi export activity of PHO1 was mediated by a PM-localized protein. This impaired export activity might be associated with the lack of a partner protein or a posttranslational modification that would be required for PHO1 to be functionally active. Alternatively, this lower Pi export activity could be due to the loss of lateral polarity of the PM-stabilized PHO1.

An alternate and our favorite hypothesis on PHO1 localization has suggested the model where its mode of action in mediating Pi export would be different from the

aforementioned PM-localized nutrient transporters. According to this hypothesis, PHO1 would mediate Pi export by loading Pi into secretory vesicles, followed by the release of Pi to the extracellular space through exocytosis and the rapid recycling of PHO1 from the PM by endocytosis and endosomal trafficking (Figure 25B; Arpat et al., 2012). This model would explain the presence of a large fraction of PHO1 in the Golgi/TGN. However, the decrease in Pi export is still puzzling because we would expect the vesicles to fuse to the PM and export more Pi *via* exocytosis irrespective of CME inhibition, unless this process is tightly controlled by its feedback mechanism. In that case, Pi export is anticipated only when the secretory vesicles release their content and recycle away from the PM. In other words, the observed decrease in Pi export activity of PM-stabilized PHO1 may be explained by a reduction in the number of recycled endosomes available to participate in further rounds of vesicular Pi loading and export. Such a secretory pathway-mediated mechanism has been previously indicated for the Golgi-localized manganese (Mn^{2+}) transporter MTP11. Arabidopsis *mtp11* mutants are hypersensitive, but plants that overexpress *MTP11* are more tolerant to elevated levels of Mn^{2+}. Due to the overaccumulation of Mn^{2+} in plant tissues in *mtp11* mutant, MTP11 was proposed to confer Mn^{2+} tolerance by excluding the metal through vesicular trafficking and exocytosis (Delhaize et al., 2007; Peiter et al., 2007).

A similar hypothesis has been suggested for the activity of ECA3 on Ca^{+2} and Mn^{+2} homeostasis (Li et al., 2008) as well as for the export of nicotianamine and iron in the vasculature by NAET and NPF transporters respectively (Chao et al., 2021; Chen et al., 2021). Surprisingly, these transporters were localized on a type of secretory endosomal vesicles in root vasculature with no apparent PM localization. This synaptic-like vesicle mediated exocytosis pathway to maintain ion homeostasis resembles the release of neurotransmitters in animals (Chao et al., 2021) and suggests that the secretory pathways in plants and animals may be more conserved than expected. While most of the mechanisms of membrane protein trafficking are heavily influenced by studies on the PM-localized auxin efflux carriers (PINs) and receptors, these transporters and PHO1 could represent very interesting and sophisticated models to study the regulatory mechanisms and membrane protein dynamics, particularly in the root vasculature.

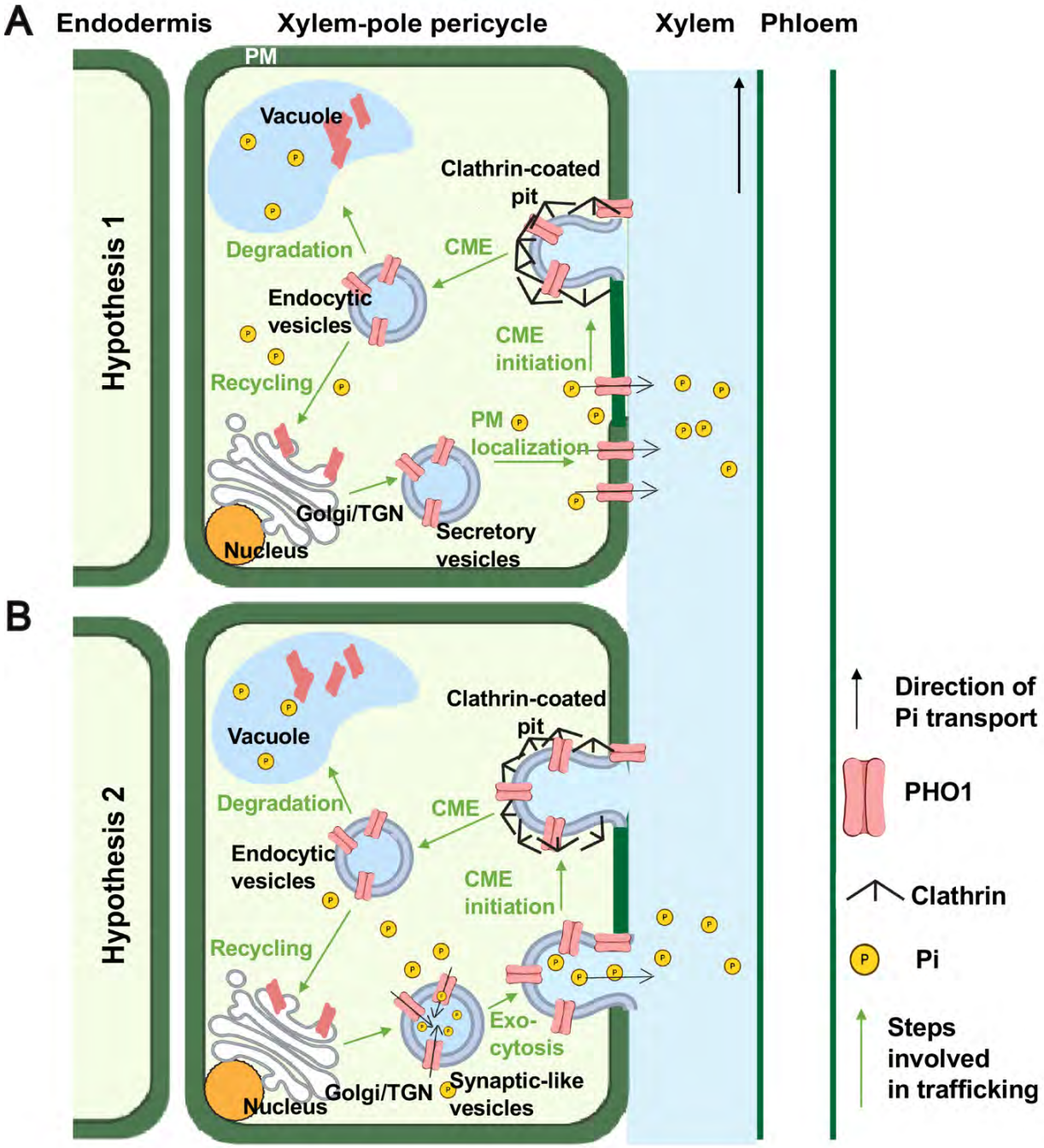

Figure 25. Schematic representation of hypotheses on PHO1's mechanism of Pi export. (A) Suggests the mode of action of PHO1 where Golgi/TGN localized PHO1 is secreted to the PM and exports Pi into the xylem apo-plastic space followed by its internalization *via* CME. (B) Represents second hypothesis, where Golgi/TGN localized PHO1 loads Pi into the synaptic-like vesicles followed by release of Pi to the xylem via exocytosis and its internalization by CME. The last step involves recycling and/or degradation of PHO1.

Apart from the roots, *PHO1* is also expressed in guard cells in *A. thaliana*. In guard cells, *PHO1* is upregulated following the treatment with abscisic acid (ABA) and is involved in the ABA-induced stomatal response (Zimmerli et al., 2012). A specific expression of *PHO1* in guard cells was required for ABA-triggered stomatal closure. However, the response of guard cells to other stimuli, such as light, high extracellular calcium, or auxin, was not affected in the absence of *PHO1* expression. Similarly, *PHO1* is also expressed in the chalazal seed coat, where it transfers Pi from maternal tissues to embryos in developing seeds in Arabidopsis (Vogiatzaki et al., 2017). Although the role of PHO1 in guard cells and the chalazal seed coat was clear, its subcellular localization and mode of action remained to be determined. Nonetheless, based on our data indicating constitutive internalization of PM-localized PHO1 in the root vascular tissues, it is possible that a small fraction of PHO1 also localizes to the PM of guard cells and chalazal seed coat to transfer Pi to the respective cells, except in these cases, the localization of PHO1 to the PM could be dependent on a particular cue and/or signal. For instance, ABA in the case of stomatal closure or Pi export in the embryo specifically at the mature green stage of seed development, probably to regulate the ion fluxes associated with these specific processes.

Now, we have two pieces of evidence that indicate that PHO1-type transporters (AtPHO1 and OsPHO1;2) can be localized at the PM (Ma et al., 2021; Vetal et al., unpublished). In the future, it will be very interesting to investigate the molecular mechanism that controls this localization. Although we have shown that ubiquitination of selected lysines and phosphorylation of selected serine/threonine/tyrosine residues is not involved in this regulation, we can not rule out the possible ubiquitination of other documented non-lysine residues such as cysteine, serine, and threonine (Cadwell and Coscoy, 2005; Wang et al., 2007; Gilkerson et al., 2015). Nonetheless, our data from serine and threonine residue mutations indirectly eliminates their role as potential sites for ubiquitination.

PHO1 represents a promising target gene for breeding crops with high yield under low Pi availability. In cereals (Rice and Maize), *PHO1*s are expressed in the root vasculature and the vasculature of the uppermost node connecting to the panicle and in developing seed tissues, where they are involved in the allocation of Pi during grain filling (Che et al., 2020; Ma et al., 2021). Pi efflux activity and its localization to the

plasma membrane of seed tissues have implicated a specific role for rice OsPHO1;2 in Pi reallocation during grain filling (Ma et al., 2021). Moreover, the ectopic overexpression of *OsPHO1;2* enhanced grain yield, especially under low-Pi conditions. Thus, understanding the regulatory mechanisms controlling PHO1 abundance and localization may provide a useful tool for improving PUE in agriculture.

References

(for Introduction, Chapter 2 and Chapter 3)

Akiyama K, Matsuzaki K, Hayashi H (2005) Plant sesquiterpenes induce hyphal branching in arbuscular mycorrhizal fungi. Nature **435**: 824–827

Ames BN (1966) Assay of inorganic phosphate, total phosphate and phosphatases. Methods Enzymol **8**: 115-118.

Aniento F, Sánchez de Medina Hernández V, Dagdas Y, Rojas-Pierce M, Russinova E (2022) Molecular mechanisms of endomembrane trafficking in plants. Plant Cell **34**: 146–173

Arpat AB, Magliano P, Wege S, Rouached H, Stefanovic A, Poirier Y (2012) Functional expression of PHO1 to the Golgi and trans-Golgi network and its role in export of inorganic phosphate. Plant J **71**: 479-491

Aung K, Lin S-I, Wu C-C, Huang Y-T, Su C, Chiou T-J (2006) *pho2*, a phosphate overaccumulator, is caused by a nonsense mutation in a MicroRNA399 target gene. Plant Physiol **141**: 1000–1011

Ayadi A, David P, Arrighi J-F, Chiarenza S, Thibaud M-C, Nussaume L, Marin E (2015) Reducing the genetic redundancy of Arabidopsis PHOSPHATE TRANSPORTER1 transporters to study phosphate uptake and signaling. Plant Physiol **167**: 1511–1526

Bar M, Avni A (2009) EHD2 inhibits ligand-induced endocytosis and signaling of the leucine-rich repeat receptor-like protein LeEix2. Plant J **59**: 600–611

Barberon M, Dubeaux G, Kolb C, Isono E, Zelazny E, Vert G (2014) Polarization of IRON-REGULATED TRANSPORTER 1 (IRT1) to the plant-soil interface plays crucial role in metal homeostasis. Proc Natl Acad Sci USA **111**: 8293–8298

Barberon M, Geldner N (2014) Radial transport of nutrients: The plant root as a polarized epithelium. Plant Physiol **166**: 528–537

Barberon M, Zelazny E, Robert S, Conéjéro G, Curie C, Friml J, Vert G (2011) Monoubiquitin-dependent endocytosis of the IRON-REGULATED TRANSPORTER 1 (IRT1) transporter controls iron uptake in plants. Proc Natl Acad Sci USA **108**: E450–E458

Bari R, Datt Pant B, Stitt M, Scheible W-R (2006) PHO2, MicroRNA399, and PHR1 define a phosphate-signaling pathway in plants. Plant Physiol **141**: 988–999

Bashline L, Li S, Anderson CT, Lei L, Gu Y (2013) The endocytosis of cellulose synthase in Arabidopsis is dependent on μ2, a clathrin-mediated endocytosis adaptin. Plant Physiol **163**: 150–160

Bates TR, Lynch JP (1996) Stimulation of root hair elongation in *Arabidopsis thaliana* by low phosphorus availability. Plant Cell Environ **19**: 529–538

Bayle V, Arrighi J-F, Creff A, Nespoulous C, Vialaret J, Rossignol M, Gonzalez E, Paz-Ares J, Nussaume L (2011) *Arabidopsis thaliana* high-affinity phosphate transporters exhibit multiple levels of posttranslational regulation. Plant Cell **23**: 1523–1535

Besserer A, Puech-Pagès V, Kiefer P, Gomez-Roldan V, Jauneau A, Roy S, Portais J-C, Roux C, Bécard G, Séjalon-Delmas N (2006) Strigolactones stimulate arbuscular mycorrhizal fungi by activating mitochondria. PLoS Biol **4**: e226

Boisson-Dernier A, Chabaud M, Garcia F, Bécard G, Rosenberg C, Barker DG (2001) *Agrobacterium rhizogenes* -transformed roots of *Medicago truncatula* for the study of nitrogen-fixing and endomycorrhizal symbiotic associations. Mol Plant-Microbe Interact **14**: 695–700

Burch-Smith TM, Zambryski PC (2012) Plasmodesmata paradigm shift: Regulation from without versus within. Annu Rev Plant Biol **63**: 239–260

Cadwell K, Coscoy L (2005) Ubiquitination on nonlysine residues by a viral E3 ubiquitin ligase. Science **309**: 127–130

Castaings L, Alcon C, Kosuth T, Correia D, Curie C (2021) Manganese triggers phosphorylation-mediated endocytosis of the Arabidopsis metal transporter NRAMP1. Plant J **106**: 1328–1337

Chao Z-F, Wang Y-L, Chen Y-Y, Zhang C-Y, Wang P-Y, Song T, Liu C-B, Lv Q-Y, Han M-L, Wang S-S, et al (2021) NPF transporters in synaptic-like vesicles control delivery of iron and copper to seeds. Sci Adv **7**: eabh2450

Che J, Yamaji N, Miyaji T, Mitani-Ueno N, Kato Y, Shen RF, Ma JF (2020) Node-localized transporters of phosphorus essential for seed development in Rice. Plant Cell Physiol **61**: 1387–1398

Chen S-Y, Gu T-Y, Qi Z-A, Yan J, Fang Z-J, Lu Y-T, Li H, Gong J-M (2021) Two NPF transporters mediate iron long-distance transport and homeostasis in Arabidopsis. Plant Commun **2**: 100244

Chen Y-F, Li L-Q, Xu Q, Kong Y-H, Wang H, Wu W-H (2009) The WRKY6 transcription factor modulates *PHOSPHATE1* expression in response to low Pi stress in *Arabidopsis*. Plant Cell **21**: 3554–3566

Chiou T-J, Liu H, Harrison MJ (2001) The spatial expression patterns of a phosphate transporter (MtPT1) from *Medicago truncatula* indicate a role in phosphate transport at the root/soil interface. Plant J **25**: 281–293

Clough SJ, Bent AF (1998) Floral dip: a simplified method for Agrobacterium-mediated transformation of *Arabidopsis thaliana*. Plant J **16**: 735–743

Collins BM, McCoy AJ, Kent HM, Evans PR, Owen DJ (2002) Molecular architecture and functional model of the endocytic AP2 complex. Cell **109**: 523–535

Cruz-Ramírez A, Oropeza-Aburto A, Razo-Hernández F, Ramírez-Chávez E, Herrera-Estrella L (2006) Phospholipase DZ2 plays an important role in extraplastidic galactolipid biosynthesis and phosphate recycling in *Arabidopsis* roots. Proc Natl Acad Sci USA **103**: 6765–6770

Curtis MD, Grossniklaus U (2003) A gateway cloning vector set for high-throughput functional analysis of genes in planta. Plant Physiol **133**: 462–469

Dahhan DA, Bednarek SY (2022) Advances in structural, spatial, and temporal mechanics of plant endocytosis. FEBS Lett **596**: 2269-2287

Delhaize E, Gruber BD, Pittman JK, White RG, Leung H, Miao Y, Jiang L, Ryan PR, Richardson AE (2007) A role for the *AtMTP11* gene of *Arabidopsis* in manganese transport and tolerance. Plant J **51**: 198–210

Delhaize E, Randall PJ (1995) Characterization of a phosphate-accumulator mutant of Arabidopsis thaliana. Plant Physiol **107**: 207–213

Dettmer J, Hong-Hermesdorf A, Stierhof Y-D, Schumacher K (2006) Vacuolar H+-ATPase activity is required for endocytic and secretory trafficking in *Arabidopsis*. Plant Cell **18**: 715–730

Dhonukshe P, Aniento F, Hwang I, Robinson DG, Mravec J, Stierhof Y-D, Friml J (2007) Clathrin-mediated constitutive endocytosis of PIN auxin efflux carriers in Arabidopsis. Curr Biol **17**: 520–527

Di Rubbo S, Irani NG, Kim SY, Xu Z-Y, Gadeyne A, Dejonghe W, Vanhoutte I, Persiau G, Eeckhout D, Simon S, et al (2013) The clathrin adaptor complex AP-2 mediates endocytosis of BRASSINOSTEROID INSENSITIVE1 in *Arabidopsis*. Plant Cell **25**: 2986–2997

Diril MK, Schmidt S, Krauß M, Gawlik V, Joost H-G, Schürmann A, Haucke V, Augustin R (2009) Lysosomal localization of GLUT8 in the testis - the EXXXLL motif of GLUT8 is sufficient for its intracellular sorting via AP1- and AP2-mediated interaction. FEBS J **276**: 3729–3743

Dubeaux G, Vert G (2017) Zooming into plant ubiquitin-mediated endocytosis. Curr Opin Plant Biol **40**: 56–62

Engler C, Kandzia R, Marillonnet S (2008) A one pot, one step, precision cloning method with high throughput capability. PLoS ONE **3**: e3647

Essigmann B, Güler S, Narang RA, Linke D, Benning C (1998) Phosphate availability affects the thylakoid lipid composition and the expression of *SQD1* , a gene required for sulfolipid biosynthesis in *Arabidopsis thaliana*. Proc Natl Acad Sci USA **95**: 1950–1955

Fan L, Hao H, Xue Y, Zhang L, Song K, Ding Z, Botella MA, Wang H, Lin J (2013) Dynamic analysis of *Arabidopsis* AP2 σ subunit reveals a key role in clathrin-mediated endocytosis and plant development. Development **140**: 3826–3837

Fink JR, Inda AV, Tiecher T, Barrón V (2016) Iron oxides and organic matter on soil phosphorus availability. Ciênc agrotec **40**: 369–379

Fontenot EB, Ditusa SF, Kato N, Olivier DM, Dale R, Lin W-Y, Chiou T-J, Macnaughtan MA, Smith AP (2015) Increased phosphate transport of *Arabidopsis thaliana* Pht1;1 by site-directed mutagenesis of tyrosine 312 may be attributed to the disruption of homomeric interactions. Plant Cell Environ **38**: 2012–2022

Gao J, Chaudhary A, Vaddepalli P, Nagel M-K, Isono E, Schneitz K The Arabidopsis receptor kinase STRUBBELIG undergoes clathrin-dependent endocytosis. J Exp Bot **70**: 3881-3894

Gao Y, Chao D (2022) Localization and circulation: vesicle trafficking in regulating plant nutrient homeostasis. Plant J **112**: 1350–1363

Gadeyne A, Sánchez-Rodríguez C, Vanneste S, Di Rubbo S, Zauber H, Vanneste K, Van Leene J, De Winne N, Eeckhout D, Persiau G, et al (2014) The TPLATE adaptor complex drives clathrin-mediated endocytosis in plants. Cell **156**: 691–704

Gaymard F, Pilot G, Lacombe B, Bouchez D, Bruneau D, Boucherez J, Michaux-Ferrière N, Thibaud J-B, Sentenac H (1998) Identification and disruption of a plant shaker-like outward channel involved in K+ release into the xylem sap. Cell **94**: 647–655

Giehl RFH, Laginha AM, Duan F, Rentsch D, Yuan L, von Wirén N (2017) A critical role of AMT2;1 in root-to-shoot translocation of ammonium in Arabidopsis. Mol Plant **10**: 1449–1460

Gilkerson J, Kelley DR, Tam R, Estelle M, Callis J (2015) Lysine residues are not required for proteasome-mediated proteolysis of the auxin/indole acidic acid protein IAA1. Plant Physiol **168**: 708–720

González E, Solano R, Rubio V, Leyva A, Paz-Ares J (2005) PHOSPHATE TRANSPORTER TRAFFIC FACILITATOR1 is a plant-specific SEC12-related protein that enables the endoplasmic reticulum exit of a high-affinity phosphate transporter in *Arabidopsis*. Plant Cell **17**: 3500–3512

Gu M, Chen A, Sun S, Xu G (2016) Complex regulation of plant phosphate transporters and the gap between molecular mechanisms and practical application: what is missing? Mol Plant **9**: 396–416

Guo B, Jin Y, Wussler C, Blancaflor EB, Motes CM, Versaw WK (2008) Functional analysis of the Arabidopsis PHT4 family of intracellular phosphate transporters. New Phytol **177**: 889–898

Gutiérrez-Alanís D, Ojeda-Rivera JO, Yong-Villalobos L, Cárdenas-Torres L, Herrera-Estrella L (2018) Adaptation to phosphate scarcity: tips from Arabidopsis roots. Trends Plant Sci **23**: 721–730

Haglund K, Dikic I (2012) The role of ubiquitylation in receptor endocytosis and endosomal sorting. J Cell Sci **125**: 265–275

Hamburger D (2002) Identification and characterization of the Arabidopsis PHO1 gene involved in phosphate loading to the xylem. Plant Cell **14**: 889–902

Holford ICR (1997) Soil phosphorus: its measurement, and its uptake by plants. Soil Res **35**: 227

Höning S, Ricotta D, Krauss M, Späte K, Spolaore B, Motley A, Robinson M, Robinson C, Haucke V, Owen DJ (2005) Phosphatidylinositol-(4,5)-bisphosphate regulates sorting signal recognition by the clathrin-associated adaptor complex AP2. Mol Cell **18**: 519–531

Huang T-K, Han C-L, Lin S-I, Chen Y-J, Tsai Y-C, Chen Y-R, Chen J-W, Lin W-Y, Chen P-M, Liu T-Y, et al (2013) Identification of downstream components of ubiquitin-conjugating enzyme PHOSPHATE2 by quantitative membrane proteomics in *Arabidopsis* roots. Plant Cell **25**: 4044–4060

Ivanov R, Vert G (2021) Endocytosis in plants: Peculiarities and roles in the regulated trafficking of plant metal transporters. Biol Cell **113**: 1–13

Jabnoune M, Secco D, Lecampion C, Robaglia C, Shu Q, Poirier Y (2013) A Rice *cis* -natural antisense RNA acts as a translational enhancer for its cognate mrna and contributes to phosphate homeostasis and plant fitness. Plant Cell **25**: 4166–4182

Jia N, Zhu Y, Xie F (2018) An efficient protocol for model legume root protoplast isolation and transformation. Front Plant Sci **9**: 670

Jung J-Y, Ried MK, Hothorn M, Poirier Y (2018) Control of plant phosphate homeostasis by inositol pyrophosphates and the SPX domain. Curr Opin Biotechnol **49**: 156–162

Karthikeyan AS, Varadarajan DK, Mukatira UT, D'Urzo MP, Damsz B, Raghothama KG (2002) Regulated expression of Arabidopsis phosphate transporters. Plant Physiol **130**: 221–233

Kim SY, Xu Z-Y, Song K, Kim DH, Kang H, Reichardt I, Sohn EJ, Friml J, Juergens G, Hwang I (2013) Adaptor protein complex 2–mediated endocytosis is crucial for male reproductive organ development in *Arabidopsis*. Plant Cell **25**: 2970–2985

Lauwers E, Erpapazoglou Z, Haguenauer-Tsapis R, André B (2010) The ubiquitin code of yeast permease trafficking. Trends Cell Biol **20**: 196–204

Li B, Byrt C, Qiu J, Baumann U, Hrmova M, Evrard A, Johnson AAT, Birnbaum KD, Mayo GM, Jha D, et al (2016) Identification of a stelar-localized transport

protein that facilitates root-to-shoot transfer of chloride in Arabidopsis. Plant Physiol **170**: 1014–1029

Li X, Chanroj S, Wu Z, Romanowsky SM, Harper JF, Sze H (2008) A distinct endosomal Ca2+/Mn2+ pump affects root growth through the secretory process. Plant Physiol **147**: 1675–1689

Li X, Wang X, Yang Y, Li R, He Q, Fang X, Luu D-T, Maurel C, Lin J (2011) Single-molecule analysis of PIP2;1 dynamics and partitioning reveals multiple modes of *Arabidopsis* plasma membrane aquaporin regulation. Plant Cell **23**: 3780–3797

Lin S-H, Kuo H-F, Canivenc G, Lin C-S, Lepetit M, Hsu P-K, Tillard P, Lin H-L, Wang Y-Y, Tsai C-B, et al (2008) Mutation of the *Arabidopsis NRT1.5* nitrate transporter causes defective root-to-shoot nitrate transport. Plant Cell **20**: 2514–2528

Lin W-Y, Huang T-K, Chiou T-J (2013) NITROGEN LIMITATION ADAPTATION, a target of MicroRNA827, mediates degradation of plasma membrane–localized phosphate transporters to maintain phosphate homeostasis in *Arabidopsis*. Plant Cell **25**: 4061–4074

Liu D, Kumar R, Claus LAN, Johnson AJ, Siao W, Vanhoutte I, Wang P, Bender KW, Yperman K, Martins S, et al (2020) Endocytosis of BRASSINOSTEROID INSENSITIVE1 is partly driven by a canonical Tyr-based motif. Plant Cell **32**: 3598–3612

Liu J, Yang L, Luan M, Wang Y, Zhang C, Zhang B, Shi J, Zhao F-G, Lan W, Luan S (2015) A vacuolar phosphate transporter essential for phosphate homeostasis in *Arabidopsis*. Proc Natl Acad Sci USA. **112**: E6571-E6578

Liu T-Y, Huang T-K, Tseng C-Y, Lai Y-S, Lin S-I, Lin W-Y, Chen J-W, Chiou T-J (2012) PHO2-dependent degradation of PHO1 modulates phosphate homeostasis in Arabidopsis. Plant Cell **24**: 2168–2183

Liu T-Y, Huang T-K, Yang S-Y, Hong Y-T, Huang S-M, Wang F-N, Chiang S-F, Tsai S-Y, Lu W-C, Chiou T-J (2016) Identification of plant vacuolar transporters mediating phosphate storage. Nat Commun **7**: 11095

Löfke C, Luschnig C, Kleine-Vehn J (2013) Posttranslational modification and trafficking of PIN auxin efflux carriers. Mech Dev **130**: 82–94

Ma B, Zhang L, Gao Q, Wang J, Li X, Wang H, Liu Y, Lin H, Liu J, Wang X, et al (2021) A plasma membrane transporter coordinates phosphate reallocation and grain filling in cereals. Nat Genet **53**: 906–915

Ma Z, Bielenberg DG, Brown KM, Lynch JP (2001) Regulation of root hair density by phosphorus availability in *Arabidopsis thaliana*: Phosphorus regulates root hair density. Plant Cell Environ **24**: 459–467

Marger, M. D., & Saier, M. H., Jr. (1993). A major superfamily of transmembrane

facilitators that catalyse uniport, symport and antiport. Trends Biochem Sci **18**: 13-20

Martín Y, Navarro FJ, Siverio JM (2008) Functional characterization of the *Arabidopsis thaliana* nitrate transporter CHL1 in the yeast Hansenula polymorpha. Plant Mol Biol **68**: 215–224

Martins S, Dohmann EMN, Cayrel A, Johnson A, Fischer W, Pojer F, Satiat-Jeunemaître B, Jaillais Y, Chory J, Geldner N, et al (2015) Internalization and vacuolar targeting of the brassinosteroid hormone receptor BRI1 are regulated by ubiquitination. Nat Commun **6**: 6151

McMahon HT, Boucrot E (2011) Molecular mechanism and physiological functions of clathrin-mediated endocytosis. Nat Rev Mol Cell Biol **12**: 517–533

Misson J, Raghothama KG, Jain A, Jouhet J, Block MA, Bligny R, Ortet P, Creff A, Somerville S, Rolland N, et al (2005) A genome-wide transcriptional analysis using *Arabidopsis thaliana* Affymetrix gene chips determined plant responses to phosphate deprivation. Proc Natl Acad Sci USA **102**: 11934–11939

Misson J, Thibaud M-C, Bechtold N, Raghothama K, Nussaume L (2004) Transcriptional regulation and functional properties of Arabidopsis Pht1;4, a high affinity transporter contributing greatly to phosphate uptake in phosphate deprived plants. Plant Mol Biol **55**: 727–741

Morcuende R, Bari R, Gibon Y, Zheng W, Pant BD, Bläsing O, Usadel B, Czechowski T, Udvardi MK, Stitt M, et al (2007) Genome-wide reprogramming of metabolism and regulatory networks of Arabidopsis in response to phosphorus. Plant Cell Environ **30**: 85–112

Muchhal US, Pardo JM, Raghothama KG (1996) Phosphate transporters from the higher plant *Arabidopsis thaliana*. Proc Natl Acad Sci USA **93**: 10519–10523

Mudge SR, Rae AL, Diatloff E, Smith FW (2002) Expression analysis suggests novel roles for members of the Pht1 family of phosphate transporters in Arabidopsis: Putative roles of Arabidopsis Pht1 genes. Plant J **31**: 341–353

Müller LM (2021) PHO1 proteins mediate phosphate transport in the legume-rhizobium symbiosis. Plant Physiol **185**: 26–28

Müller R, Morant M, Jarmer H, Nilsson L, Nielsen TH (2007) Genome-wide analysis of the Arabidopsis leaf transcriptome reveals interaction of phosphate and sugar metabolism. Plant Physiol **143**: 156–171

Nguyen NNT, Clua J, Vetal PV, Vuarambon DJ, De Bellis D, Pervent M, Lepetit M, Udvardi M, Valentine AJ, Poirier Y (2020) PHO1 family members transport phosphate from infected nodule cells to bacteroids in *Medicago truncatula*. Plant Physiol **185:** 196-209

Nussaume L, Kanno S, Javot H, Marin E, Pochon N, Ayadi A, Nakanishi TM, Thibaud MC (2011) Phosphate import in plants: focus on the PHT1 transporters. Front Plant Sci **2**: 83

Otegui MS, Mastronarde DN, Kang B-H, Bednarek SY, Staehelin LA (2001) Three-dimensional analysis of syncytial-type cell plates during endosperm cellularization visualized by high resolution electron tomography. Plant Cell **13**: 2033

Paez Valencia J, Goodman K, Otegui MS (2016) Endocytosis and endosomal trafficking in plants. Annu Rev Plant Biol **67**: 309–335

Pan W, Wu Y, Xie Q (2019) Regulation of ubiquitination is central to the phosphate starvation response. Trends Plant Sci **24**: 755–769

Peiter E, Montanini B, Gobert A, Pedas P, Husted S, Maathuis FJM, Blaudez D, Chalot M, Sanders D (2007) A secretory pathway-localized cation diffusion facilitator confers plant manganese tolerance. Proc Natl Acad Sci USA **104**: 8532–8537

Plaxton WC, Tran HT (2011) Metabolic adaptations of phosphate-starved plants. Plant Physiol **156**: 1006–1015

Poirier Y, Bucher M (2002) Phosphate transport and homeostasis in Arabidopsis. The Arabidopsis Book **1**: e0024

Poirier Y, Jaskolowski A, Clúa J (2022) Phosphate acquisition and metabolism in plants. Curr Biol **32**: R623–R629

Poirier Y, Thoma S, Somerville C, Schiefelbein J (1991) A mutant of Arabidopsis deficient in xylem loading of phosphate. Plant Physiol **97**: 1087–1093

del Pozo JC, Allona I, Rubio V, Leyva A, de la Pena A, Aragoncillo C, Paz-Ares J (1999) A type 5 acid phosphatase gene from *Arabidopsis thaliana* is induced by phosphate starvation and by some other types of phosphate mobilising/oxidative stress conditions. Plant J **19**: 579–589

Prak S, Hem S, Boudet J, Viennois G, Sommerer N, Rossignol M, Maurel C, Santoni V (2008) Multiple phosphorylations in the C-terminal tail of plant plasma membrane aquaporins: role in subcellular trafficking of *At*PIP2;1 in response to salt stress. Mol Cellular Proteomics **7**: 1019–1030

Puga MI, Mateos I, Charukesi R, Wang Z, Franco-Zorrilla JM, de Lorenzo L, Irigoyen ML, Masiero S, Bustos R, Rodriguez J, et al (2014) SPX1 is a phosphate-dependent inhibitor of PHOSPHATE STARVATION RESPONSE 1 in Arabidopsis. Proc Natl Acad Sci USA **111**: 14947–14952

Raghothama K (2000) Phosphate transport and signaling. Curr Opin Plant Biol **3**: 182-187

Remy E, Cabrito TR, Batista RA, Teixeira MC, Sá-Correia I, Duque P (2012) The Pht1;9 and Pht1;8 transporters mediate inorganic phosphate acquisition by the *Arabidopsis thaliana* root during phosphorus starvation. New Phytol **195**: 356–371

Robinson DG, Neuhaus J-M (2016) Receptor-mediated sorting of soluble vacuolar proteins: myths, facts, and a new model. J Exp Bot **67**: 4435–4449

Rodriguez-Furlan C, Minina EA, Hicks GR (2019) Remove, recycle, degrade: regulating plasma membrane protein accumulation. Plant Cell **31**: 2833–2854

Roth TF, Porter KR (1964) yolk protein uptake in the oocyte of the mosquito *Aedes aegypti L*. J Cell Biol **20**: 313–332

Rouached H, Arpat AB, Poirier Y (2010) Regulation of phosphate starvation responses in plants: signaling players and cross-talks. Mol Plant **3**: 288–299

Rouached H, Stefanovic A, Secco D, Bulak Arpat A, Gout E, Bligny R, Poirier Y (2011) Uncoupling phosphate deficiency from its major effects on growth and transcriptome via PHO1 expression in Arabidopsis. Plant J **65**: 557–570

Saeed B, Deligne F, Brillada C, Dünser K, Ditengou FA, Turek I, Allahham A, Grujic N, Dagdas Y, Ott T, et al (2023) K63-linked ubiquitin chains are a global signal for endocytosis and contribute to selective autophagy in plants. Curr Biol **33**: 1337-1345

Sakano K (1990) Proton/Phosphate stoichiometry in uptake of inorganic phosphate by cultured cells of *Catharanthus roseus* (L.) G. Don. Plant Physiol **93**: 479–483

Sancho-Andrés G, Soriano-Ortega E, Gao C, Bernabé-Orts JM, Narasimhan M, Müller AO, Tejos R, Jiang L, Friml J, Aniento F, et al (2016) Sorting motifs involved in the trafficking and localization of the PIN1 auxin efflux carrier. Plant Physiol **171**: 1965–1982

Sattari SZ, Bouwman AF, Martinez Rodríguez R, Beusen AHW, van Ittersum MK (2016) Negative global phosphorus budgets challenge sustainable intensification of grasslands. Nat Commun **7**: 10696

Schachtman DP, Reid RJ, Ayling SM (1998) Phosphorus uptake by plants: From soil to cell. Plant Physiol **116**: 447–453

Secco D, Baumann A, Poirier Y (2010) Characterization of the Rice *PHO1* gene family reveals a key role for *OsPHO1;2* in phosphate homeostasis and the evolution of a distinct clade in dicotyledons. Plant Physiol **152**: 1693–1704

Shin H, Shin H-S, Dewbre GR, Harrison MJ (2004) Phosphate transport in *Arabidopsis* : Pht1;1 and Pht1;4 play a major role in phosphate acquisition from both low- and high-phosphate environments. Plant J **39**: 629–642

Stefanovic A, Arpat AB, Bligny R, Gout E, Vidoudez C, Bensimon M, Poirier Y (2011) Over-expression of PHO1 in Arabidopsis leaves reveals its role in mediating phosphate efflux. Plant J **66**: 689–699

Stefanovic A, Ribot C, Rouached H, Wang Y, Chong J, Belbahri L, Delessert S, Poirier Y (2007) Members of the PHO1 gene family show limited functional redundancy in phosphate transfer to the shoot and are regulated by phosphate deficiency via distinct pathways. Plant J **50**: 982–994

Su T, Xu Q, Zhang F-C, Chen Y, Li L-Q, Wu W-H, Chen Y-F (2015) WRKY42 modulates phosphate homeostasis through regulating phosphate translocation and acquisition in Arabidopsis. Plant Physiol **167**: 1579–1591

Takano J, Miwa K, Yuan L, von Wiren N, Fujiwara T (2005) Endocytosis and degradation of BOR1, a boron transporter of *Arabidopsis thaliana*, regulated by boron availability. Proc Natl Acad Sci USA **102**: 12276–12281

Takano J, Noguchi K, Yasumori M, Kobayashi M, Gajdos Z, Miwa K, Hayashi H, Yoneyama T, Fujiwara T (2002) Arabidopsis boron transporter for xylem loading. Nature **420**: 337–340

Takano J, Tanaka M, Toyoda A, Miwa K, Kasai K, Fuji K, Onouchi H, Naito S, Fujiwara T (2010) Polar localization and degradation of Arabidopsis boron transporters through distinct trafficking pathways. Proc Natl Acad Sci USA **107**: 5220–5225

Tanno H, Komada M (2013) The ubiquitin code and its decoding machinery in the endocytic pathway. J Biochem **153**: 497–504

Tian J, Ge F, Zhang D, Deng S, Liu X (2021) Roles of phosphate solubilizing microorganisms from managing soil phosphorus deficiency to mediating biogeochemical P cycle. Biology **10**: 158

Traub LM (2009) Tickets to ride: selecting cargo for clathrin-regulated internalization. Nat Rev Mol Cell Biol **10**: 583–596

Trull MC, Deikman J (1998) An Arabidopsis mutant missing one acid phosphatase isoform. Planta **206**: 544–550

Ullrich-Eberius CI, van AJE (1984) Phosphate uptake in *Lemna gibba* GI: energetics and kinetics. Planta **161**: 46-52

Versaw WK, Harrison MJ (2002) A chloroplast phosphate transporter, PHT2;1, influences allocation of phosphate within the plant and phosphate-starvation responses. Plant Cell **14**: 1751–1766

Vogiatzaki E, Baroux C, Jung J-Y, Poirier Y (2017) PHO1 exports phosphate from the chalazal seed coat to the embryo in developing Arabidopsis seeds. Curr Biol **27**: 2893-2900

Wang Q, Zhao Y, Luo W, Li R, He Q, Fang X, Michele RD, Ast C, von Wirén N, Lin J (2013) Single-particle analysis reveals shutoff control of the *Arabidopsis*

ammonium transporter AMT1;3 by clustering and internalization. Proc Natl Acad Sci USA **110**: 13204–13209

Wang X, Herr RA, Chua W-J, Lybarger L, Wiertz EJHJ, Hansen TH (2007) Ubiquitination of serine, threonine, or lysine residues on the cytoplasmic tail can induce ERAD of MHC-I by viral E3 ligase mK3. J Cell Biol **177**: 613–624

Wang Y (2004) Structure and expression profile of the Arabidopsis PHO1 gene family indicates a broad role in inorganic phosphate homeostasis. Plant Physiol **135**: 400–411

Wege S, Khan GA, Jung J-Y, Vogiatzaki E, Pradervand S, Aller I, Meyer AJ, Poirier Y (2016) The EXS domain of PHO1 participates in the response of shoots to phosphate deficiency via a root-to-shoot signal. Plant Physiol **170**: 385–400

Wild R, Gerasimaite R, Jung J-Y, Truffault V, Pavlovic I, Schmidt A, Saiardi A, Jessen HJ, Poirier Y, Hothorn M, et al (2016) Control of eukaryotic phosphate homeostasis by inositol polyphosphate sensor domains. Science **352**: 986–990

Williamson LC, Ribrioux SPCP, Fitter AH, Leyser HMO (2001) Phosphate availability regulates root system architecture in Arabidopsis. Plant Physiol **126**: 875–882

Xiao X, Zhang J, Satheesh V, Meng F, Gao W, Dong J, Zheng Z, An G-Y, Nussaume L, Liu D, et al (2022) SHORT-ROOT stabilizes PHOSPHATE1 to regulate phosphate allocation in Arabidopsis. Nat Plants **8**: 1074–1081

Xu L, Zhao H, Wan R, Liu Y, Xu Z, Tian W, Ruan W, Wang F, Deng M, Wang J, et al (2019) Identification of vacuolar phosphate efflux transporters in land plants. Nat Plants **5**: 84–94

Yamaoka S, Shimono Y, Shirakawa M, Fukao Y, Kawase T, Hatsugai N, Tamura K, Shimada T, Hara-Nishimura I (2013) Identification and dynamics of *Arabidopsis* adaptor protein-2 complex and its involvement in floral organ development. Plant Cell **25**: 2958–2969

Ye Q, Wang H, Su T, Wu W-H, Chen Y-F (2018) The ubiquitin E3 ligase PRU1 regulates WRKY6 degradation to modulate phosphate homeostasis in response to low-pi stress in Arabidopsis. Plant Cell **30**: 1062–1076

Yoshinari A, Hosokawa T, Amano T, Beier MP, Kunieda T, Shimada T, Hara-Nishimura I, Naito S, Takano J (2019) Polar localization of the borate exporter BOR1 requires AP2-dependent endocytosis. Plant Physiol **179**: 1569–1580

Yu B, Xu C, Benning C (2002) *Arabidopsis* disrupted in *SQD2* encoding sulfolipid synthase is impaired in phosphate-limited growth. Proc Natl Acad Sci USA **99**: 5732–5737

Zhang Z, Liao H, Lucas WJ (2014) Molecular mechanisms underlying phosphate sensing, signaling, and adaptation in plants. J Integr Plant Biol **56**: 192–220

Zhu W, Miao Q, Sun D, Yang G, Wu C, Huang J, Zheng C (2012) The mitochondrial phosphate transporters modulate plant responses to salt stress via affecting atp and gibberellin metabolism in *Arabidopsis thaliana*. PLoS ONE **7**: e43530

Zimmerli C, Ribot C, Vavasseur A, Bauer H, Hedrich R, Poirier Y (2012) *PHO1* expression in guard cells mediates the stomatal response to abscisic acid in Arabidopsis. Plant J **72**: 199–211